THESIS APPROVAL

GRADUATE SCHOOL, KASETSART UNIVERSITY

Master of Engineering (Chemical Engineering)

DEGREE

Chemical Engineering | Chemical Engineering

FIELD | **DEPARTMENT**

TITLE: Differential Geometric Controller Design with Stability Constraint for Uncertain Chemical Processes

NAME: Miss Solada Naksiri

THIS THESIS HAS BEEN ACCEPTED BY

THESIS ADVISOR

(Mr. Chanin Panjapornpon, Ph.D.)

THESIS CO-ADVISOR

(Assistant Professor Attasak Jaree, Ph.D.)

DEPARTMENT HEAD

(Associate Professor Phungphai Phanawadee, Ph.D.)

APPROVED BY THE GRADUATE SCHOOL ON _____

DEAN

(Associate Professor Gunjana Theeragool, D.Agr.)

THESIS

DIFFERENTIAL GEOMETRIC CONTROLLER DESIGN WITH STABILITY CONSTRAINT FOR UNCERTAIN CHEMICAL PROCESSES

SOLADA NAKSIRI

A Thesis Submitted in Partial Fulfillment of
the Requirements for the Degree of
Master of Engineering (Chemical Engineering)
Graduate School, Kasetsart University
2009

Solada Naksiri 2009: Differential Geometric Controller Design with Stability Constraint for Uncertain Chemical Processes. Master of Engineering (Chemical Engineering), Major Field: Chemical Engineering, Department of Chemical Engineering. Thesis Advisor: Mr. Chanin Panjapornpon, Ph.D. 156 pages.

The control of chemical and biological processes frequently encounters the problem of robustness achievement caused by inaccuracy of kinetic models and unmeasured disturbances. The traditional linear controller such as PI/PID does not perform satisfactorily in the presences of severe uncertainties resulted in the degradation of the controller performance. To overcome such problem, this work presented a control technique for uncertain chemical processes by using input/output (I/O) linearization integrating with Lyapunov stability constraint. The I/O linearization is enhanced the setpoint tracking while Lyapunov stability constraint is ensured asymptotic closed-loop stability. The unmeasured uncertainty estimated through the optimizer and then feed back to the compensator to eliminate the output offset. The domain of stability is investigated with bifurcation analysis to determine the tuning parameters. The performance of the proposed method was illustrated through the examples of chemical/biological reactors with multiple steady states, in which the uncertainties are appeared in the kinetic parameters and the feed. The simulation results showed that the proposed method was successfully handle the process at the desired setpoints whether stable or unstable processes.

_____ _____ ___ /___ /___

Student's signature Thesis Advisor's signature

ACKNOWLEDGEMENTS

This thesis is an account of the two years devoted work in the area of process and control system, at Chemical Engineering department, Kasetsart University. I cannot go through many hardships along this journey without help and support of many people around me.

First of all, I wish to express my deep appreciation to my advisor, Dr. Chanin Panjapornpon for all the guidance, discussion, great student understanding, and the lessons, which he had given me on a great detail to become success in chemical engineering. Even though there were times that I did not understand his teaching, he still shown the keenness to explain me the lesson of advanced process control in a simpler and clearer manner. I wish to thank my committee member, Assistant Professor Attasak Jaree for all the guidance and comments that helped me to improve the quality of this thesis.

I would like to thank Postgraduate Education and Research Development Office (PERDO) and Department of Chemical Engineering at Kasetsart University for financial support to this work. I wish to thank all my colleagues in Dr. Chanin's research group for many useful discussions as well as providing me a warm and friendly working environment. I will always cherish the great memory we had shared during working together in this group. I wish to thank my best friends who stood beside me and encouraged me constantly during my difficult times.

Finally, and most importantly, I wish to thank my parents and sister for their continuous love and support in many aspects of life. They are always my strength when I am down.

Solada Naksiri

April 2009

TABLE O F CONTENTS

Page

LIST OF TABLES

LIST OF FIGURES

LIST OF FIGURES (Continued)

LIST OF FIGURES (Continued)

LIST OF FIGURES (Continued)

LIST OF FIGURES (Continued)

LIST OF FIGURES (Continued)

LIST OF FIGURES (Continued)

LIST OF FIGURES (Continued)

Appendix Figure **Page**

LIST OF ABBREVIATIONS

A	=	Heat transfer area (m^2)
$\tilde{A}$	=	Jacobian matrix
β	=	Adjustable controlled parameters
ε	=	Adjustable controlled parameters
$\tilde{B}$	=	Input Jacobian matrix
C_A	=	Concentration of A (kmol m^{-3})
C_{Ai}	=	Initial concentration (mol l^{-1})
C_{if}	=	Initiator feed concentration (mol l^{-1})
C_{mf}	=	Monomer feed concentration (mol l^{-1})
C_{gp}	=	Growing polymer concentration (mol l^{-1})
C_p	=	Heat capacity of the reaction mixture (J g^{-1} K^{-1})
C_{pc}	=	Heat capacity of the cooling jacket mixture (J g^{-1} K^{-1})
CLF	=	Control Lyapunov function
D	=	Vector of disturbances
$\mathcal{D}$	=	Differential operator
Đ	=	Open subset of $\mathbb{R}^n$
DGC	=	Differential geometric control
ρ	=	Density of the reaction mixture (g l^{-1})
ρ_c	=	Density of the cooling jacket mixture (g l^{-1})
γ	=	Activation energy (m^3 K $kmol^{-1}$)
E_a	=	Activation energy for rate constant (kJ $kmol^{-1}$)
f	=	Initiator efficiency
$f(x)$	=	Nonlinear vector function
F	=	Feed flowrate (m^3 hr^{-1})
G	=	Scalar function
GPMN	=	Generalized pointwise min-norm

LIST OF ABBREVIATIONS (Continued)

μ	=	Growth rate (min^{-1})
$h(x)$	=	Scalar function
ΔH_r	=	Heat of reaction (J mol^{-1})
I	=	Initiator
I/O	=	Input/output
ψ	=	Input function
J	=	Objective function
K	=	Robust controller block
K_1	=	Saturation parameter (m^3 kg^{-1})
K_m	=	Inhibition parameter (kg m^{-3})
k_{d0}	=	Rate constant for initiator decomposition (s^{-1})
k_{t0}	=	Rate constant for termination (l mol^{-1} s^{-1})
k_0	=	Rate constant (s^{-1})
k_{p0}	=	Rate constant for propagation (l mol^{-1} s^{-1})
LBC	=	Lyapunov-based control
LMI	=	Linear matrix inequality
μ_{max}	=	Maximum growth rate (min^{-1})
m	=	Number of manipulated inputs
M	=	Monomer species
MPC	=	Model predictive control
n	=	Number of state variables
NMBC	=	Nonlinear model-based control
Δ	=	Nonlinear perturbation
Φ	=	Nonlinear vector function
P	=	Positive definite matrix
δ	=	Positive constants
α	=	Positive constants

LIST OF ABBREVIATIONS (Continued)

Q_i	=	Initiator flowrate (s^{-1})
Q_s	=	Solvent flowrate ($l\ s^{-1}$)
Q_m	=	Monomer flowrate ($l\ s^{-1}$)
Q_c	=	Cooling jacket flowrate ($l\ s^{-1}$)
q	=	Heat of reaction ($K\ s^{-1}$)
Q	=	Positive semidefinite real symmetric matrix
r	=	Relative degree of the output
R	=	Radical
R	=	Universal gas constant ($kJ\ kmol^{-1}\ K^{-1}$)
$\mathbb{R}$	=	Set of real number
S	=	Substrate concentration ($kg\ m^{-3}$)
S_F	=	Substrate-feed concentration ($kg\ m^{-3}$)
ζ	=	States of zero dynamics
t	=	Time (min)
$t(x)$	=	Scalar function
T_f	=	Reactor feed temperature (K)
T_{cf}	=	Cooling jacket feed temperature (K)
T	=	Temperature (K)
T_i	=	Initial temperature (K)
u	=	Manipulated input vector
$\mathbb{U}$	=	Constrained subspace for manipulated input vector
U	=	Overall heat transfer coefficient ($J\ m^{-2}\ K^{-1}\ s^{-1}$)
θ	=	Updated setpoint
ν	=	Updated steady state
V	=	Lyapunov function
V_c	=	Cooling jacket volume (l)
X_B	=	Biomass concentration ($kg\ m^{-3}$)

LIST OF ABBREVIATIONS (Continued)

χ	=	Vector of the estimates of the uncertainty-free State variables
x_i	=	Vector of state variables
x_{is}	=	Steady state values
$\mathbb{X}$	=	Constrained subspace for manipulated state variables vector
y	=	Vector of controlled variables
Y	=	Yield coefficient
Z_2	=	H_2 objective to be minimized
Z_∞	=	H_∞ objective to be minimized

DIFFERENTIAL GEOMETRIC CONTROLLER DESIGN WITH STABILITY CONSTRAINT FOR UNCERTAIN CHEMICAL PROCESSES

INTRODUCTION

Many chemical processes, including high purity distillation columns, highly exothermic chemical reactor and batch reactor frequently present multiple steady states or called multiplicity behaviors due to the complexity of the relationships between the operating conditions of reactor and the product properties. For example, the polymerization reactor of methyl methacrylate (Fuente *et al.*, 2006) exhibits the multiplicity behaviors that occur from very complex kinetics, heat and mass transfer limitations. From multiplicity behaviors, the processing phase has an effect on quality of the product. In case of operating system near lower condition, the monomers are produced with low conversion. In case of operating system near upper condition, the gel effect may occur in the polymerization reactor, which is the sudden increase of the rate of a free radical polymerization and the viscosity of the reacting medium. Because free radical polymerizations are highly exothermic, it induces a sudden increase of the temperature, which may result in runaway effects, low quality products, instabilities and even explosions in industrial applications. Thus, the operation of the polymerization of methyl methacrylate is not recommended near this steady state. To achieve the high yield and high product quality, the optimal operating point should be necessary to choose near an unstable or middle steady state at intermediate conversion. However, it is very difficult task to design the control system for the practicing control engineer due to the limitation of the stability region. The traditional controller used in the industries such PI/PID linearization must be tuned very particularly to achieve the closed-loop stability at unstable steady state. If the controller cannot maintain the closed-loop stability to obtain the desired output, it may result in reactor thermal runaway resulting in off-spec production or hazardous plant operation.

Although some researchers proposed the control techniques for chemical processes with multiplicity behavior (Gerhard *et al*., 2004; Ramaswamy *et al*., 2005) they have still the limitation of robustness and closed-loop stability of the control for chemical processes with uncertainty. The kinetic parameters and heat transfer coefficients estimated from laboratory-scale experiments may not be appropriate when is used in the large-scale reactor due to changes in volume ratio, mixing, and wall catalyst. The uncertainty of parameter may result the oscillation of measurement signal lead to the degradation of control performance. Moreover, the uncertainty generally found during the process operation that is the process uncertainty due to the sensor and the measured devices. In practice, the range of measured device may mismatch the actual value of process parameter. Furthermore, the sensor is very sensitive when the external disturbances occur in the process. To convert digital signal to analog signal, the sampling time may not be appropriate to keep the values. The process uncertainty can affect the accuracy value of variables lead to difficult in the operation.

During the past two decades, many efforts to encounter the control problem of uncertain chemical processes have focused in the area of nonlinear model-based control (NMBC) techniques, which can be categorized into 3 main techniques: differential geometric control (DGC), Lyapunov-based control (LBC), and model predictive control (MPC). The details of each technique will be referred to again in the literature review of nonlinear model-based control. Although many research works of NMBC development presented several techniques to account for uncertainties, they still have some disadvantages. The differential geometric control is generally not ensured stability when the nonlinear system is non-minimum phase. Moreover, input constraints are not considered. Lyapunov-based control is difficult to find the Lyapunov function and to design the domain attraction that affects to feasibility of control action. MPC have many tuning parameter and not applicable to unstable, non-minimum-phase processes directly.

Motivated by this limitation, this research work proposes a controller design within framework of I/O linearization, a class of differential geometric control, and

Lyapunov stability constraint for uncertain chemical processes. The advantages of the proposed control technique are easy implementation due to less tuning parameter than other techniques and guarantee the closed-loop stability. The I/O linearization is used to enhance the setpoint tracking while Lyapunov stability constraint is used to ensures asymptotic closed-loop stability region. The state feedback is formulated by minimizing the difference between controlled output and its setpoint under the Lyapunov stability constraint. Bifurcation analysis is applied to controller tuning to determine the optimal tuning parameter under the proposed control technique. To illustrate controller performance, the proposed control method will be applied through process simulation of chemical processes with steady state multiplicity.

OBJECTIVE

The objective of this research is to develop the control system for uncertain chemical processes with multiplicity behavior by using the framework of I/O linearization integrated with Lyapunov stability constraint.

Scope of Thesis

The control system is developed for uncertain chemical processes with multiplicity behavior which includes the feedback controller, target calculation, state observer and compensator. The feedback controller will use the combination of I/O linearization and Lyapunov stability constraint that can reduce the effect of the uncertainties within the desired stability region. Furthermore, the tuning parameters are determined by analyzing the domain of stability with bifurcation analysis. The target calculation and compensator should cooperate with the feedback controller to achieve closed-loop stability although the process and model are mismatched. The effectiveness of control system will be tested through applications of uncertain chemical processes with multiple steady states. The proposed technique will be compared with the well-mentioned I/O linearization used for uncertain chemical processes presented by Kolevennu (2000).

Impact of Results

The developed control system can effectively maintain the closed-loop stability and easy to implement due to less tuning parameters. The controller can force the output to the desired setpoint with less operation time whether the chemical, the biochemical, and the polymerization reactor. With the result of a controller design, the uncertain chemical processes will be operated with safe operation, meeting environmental regulations, and maintaining desired product quality specifications.

LITERATURE REVIEW

1. Uncertainty in chemical processes

The uncertainty is a challenging problem of the controller design for chemical processes. If the controller cannot efficiently control, this uncertain may cause performance deterioration and even closed-loop instability. Generally, the uncertainty can be classified into two categories: parametric uncertainty and unmeasured disturbance.

1.1 Parametric uncertainty

The parametric uncertainty is uncertainty that directly related to the physical process parameters and model parameters due to imperfect knowledge. Examples of parametric uncertainty are uncertainty in heat transfer coefficients and uncertainty in kinetic parameters obtained from experimental and pilot-plant data (Palanki *et al.*, 2002). Uncertainty in heat transfer coefficients arises from imperfect mixing; the concentrations of the various reacting species will be non-uniform, especially near the reactor wall. It is not possible to precisely measure the value of the heat transfer coefficient online with sensor technology. It may only be estimated empirically. This uncertainty may lead to a loss of control performance. Uncertainty in kinetic parameters estimation arises from limited laboratory data. Due to changes in mass transfer characteristics in the production scale reactor, the apparent kinetic parameters may not match the values extracted from the bench scale reactor. These problems can degrade the controller performance.

1.2 Unmeasured disturbances

The unmeasured disturbances are uncertainty during process operation that cannot be measured directly. This uncertainty may occur from flowrate and temperature deviations, unknown internal or external disturbances, stream quality fluctuations, and so on fall into this category which is usually described by a

probability distributional form obtained from online measurements (Pistikopoulos, 1995). The errors of state estimation arise when output instead of state measurements is available and the estimated state is used in the controller formulation in place of the actual state. If the unmeasured disturbances occur frequently, the process identification is difficult. It can cause the control performance to be sluggish and loss of stability.

2. Nonlinear model-based control (NMBC)

From the control problem in chemical processes, the control for uncertain processes is very challenge and difficult for control engineers. During the past two decades, the advanced control technique such NMBC, that is integrated the mathematical model into the controller design receives more attention from both industries and researchers due to high performance. Generally, NMBC for uncertain processes can be categorized into 3 main techniques: differential geometric control (DGC), Lyapunov-based control (LBC), and model predictive control (MPC).

2.1 Differential geometric control

The DGC is a direct synthesis approach that transforms a system into a linear one by means of feedback and coordinates transformation. The simplified schematic diagram of general DGC is illustrated in Figure 1. The state feedback controller is derived by requesting a desired closed-loop response in the absence of input constraints.

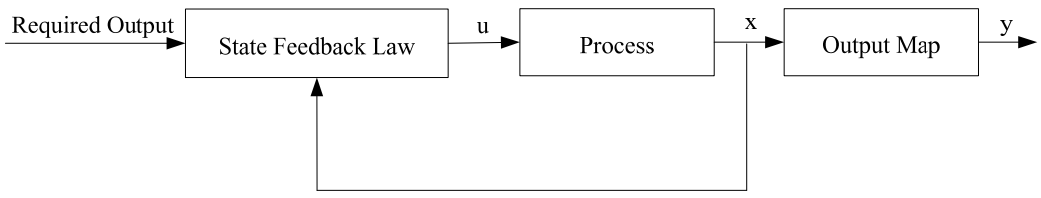

Figure 1 The schematic diagram of general DGC.

The DGC methods for uncertain processes were addressed by various techniques including I/O linearization (Sampath *et al*., 1998; Kolevennu, 1999, 2000, 2001, 2003). I/O linearization integrating with LBC (Kravaris *et al.*, 1988; Krothapally *et al.*, 1998), and approximate I/O linearization (Femat *et al.*, 1999; Sampath *et al.*, 2002; Palanki *et al.*, 2003).

2.1.1 Input/output linearization

I/O linearization requests the closed-loop response in the sense of linear input/output behavior. Consider a process, which has mathematical model in the form:

$$\begin{aligned} \dot{x} &= f(x) + g(x)u \\ y &= h(x) \end{aligned} \tag{1}$$

under the linearizing static state feedback

$$u = p(x) + q(x)v \tag{2}$$

where v is an external reference input, $p(x)$ and $q(x)$ are scalar valued functions of the state vector x, the resulting closed-loop structure is given by

$$\begin{aligned} \dot{x} &= \left[f(x) + g(x)p(x) \right] + \left[g(x)q(x) \right] v \\ y &= h(x) \end{aligned} \tag{3}$$

The I/O linearization technique has many advantages such as less tuning parameters than other techniques and guaranteed closed-loop stability. However, only I/O linearization technique cannot effectively control for the uncertain process because it does not guarantee robustness in the presence of uncertainty. When

an inaccurate model is used, the nonlinearities are not cancelled exactly leading to deterioration in controller performance. Furthermore, I/O linearization technique can only be applied to process with stable zero dynamics or minimum phase. In order to control uncertain processes, I/O linearization needs to use special design technique, for example, the control method proposed by Kolavennu (Kolavennu *et al.*, 1999, 2000, 2001, 2003), in which it was developed based on I/O linearization and multi-objective H_2/H_∞ synthesis. This technique is to find the linear state feedback gain that stabilizes all bounded uncertainties by satisfying the infinity-norm constraint. A controller is solved by the use of multi-objective optimization techniques such as mixed H_2/H_∞ synthesis with pole placement constraints. The simplified schematic diagram of general multi-model H_2/H_∞ synthesis is illustrated in Figure 2. w contains all the external disturbances. Z_2 and Z_∞ contains the relevant errors signals that want to maintain small with respect to the 2-norm (average) and ∞-norm (worst case), respectively. P is the process model together with performance and normalization weights and perturbations.

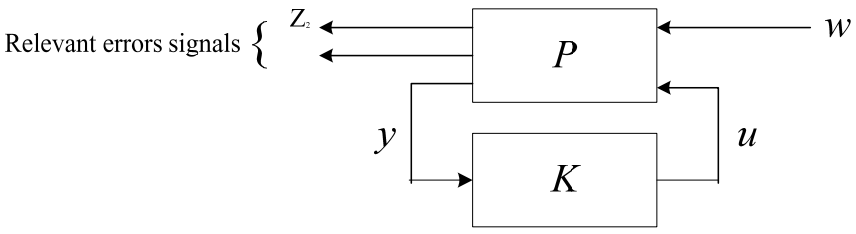

Figure 2 Multi-model H_2/H_∞ synthesis problem.

The objective is to find a stabilizing controller K such that

$$\alpha \left\| T_{z_\infty w} \right\|_\infty + \sigma \left\| T_{z_2 w} \right\|_2 \tag{4}$$

is minimized. $T_{z_\infty w}$ and $T_{z_2 w}$ are linear operators mapping Z_∞ to w and w to Z_∞ respectively. α, σ are positive numbers representing the trade-off between the H_2/H_∞ objective. The advantage of H_2/H_∞ synthesis is readily applicable to problems

involving multivariable systems with decoupling. However, the practical applicability of mixed H_2/H_∞ synthesis is still questionable because the hard input and output constraints cannot be added to the controller design procedure in a straightforward manner. Furthermore, another special design technique of I/O linearization for uncertain processes is the structured singular values (μ -synthesis) (Sampath *et al*., 1998). In this technique, the I/O linearizing state feedback is used to cancel the nominal nonlinearities. The μ -synthesis is used to find a controller *K* such that the uncertain process is internally stable. The simplified schematic diagram of general μ -synthesis is illustrated in Figure 3. The perturbation block Δ considers in structure the interconnections between the uncertain parameters and the generalized process, *P*. The generalized process is the process model together with the weights, *w*, which contains all external disturbances. The relevant errors signals, *z* represent the output errors which typically includes weighted error signals to be minimized.

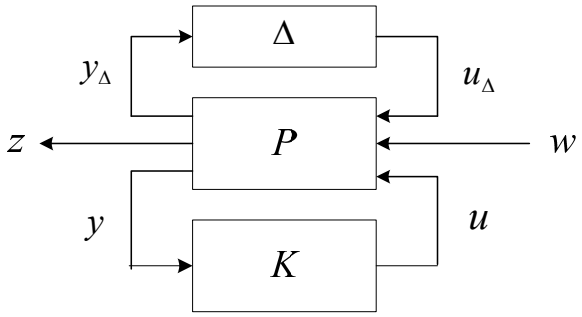

Figure 3 General interconnection structure for μ-synthesis.

A stabilizing controller *K* described by:

$$\underset{\Delta}{sub}\left\|T_{wz}\right\|_\infty \tag{5}$$

where T_{wz} is the linear operator from *w* to *z*. An appropriate controller can be found by solving a standard optimization problem online to minimize (5). However, the disadvantages of μ -synthesis is the computation of the structured singular value is not an easy task. Moreover, the order of resultant μ -controllers is usually very high,

and hence controller-order reduction must be applied. Although I/O linearization can handle the uncertain process, it cannot ensure stability when the nonlinear system has unstable zero dynamics or the nonlinear system is non-minimum phase (inverse response) because the designed controller will include an inverse of the process model, causing closed-loop instability in the case of non-minimum phase processes.

2.1.2 Input/output linearization integrating with Lyapunov-based control

In order to guarantee the stability region of controller for uncertain processes, I/O linearization integrating with LBC were proposed. The controller proposed by Kravaris *et al.* (Kravaris *et al.*, 1988) used a LBC approach to guarantee uniform ultimate bound of the states and the output. Another LBC technique that was applied to I/O linearization for uncertain processes was sliding mode control (SMC) (Krothapally *et al.*, 1998). The control method used state feedback together with a switching control law to force the state trajectories towards an invariant manifold. The states of system were confined to a selected subset of the state space so as to achieve some desirable dynamics. However, for systems with time delay in the feedback loop, it is observed that the performance of the SMC may deteriorate. In addition, the state feedback of I/O linearization integrating with LBC technique requires an exact description of the process and cannot be applied to non-minimum phase processes directly. Due to uncertainty, I/O linearity as well as decoupling may be lost resulting in serious degradation in controller performance as well as loss of stability.

2.1.3 Approximate input/output linearization

The approximate I/O linearization technique is possible to the avoidance of internal or zero dynamics. If the system is non-minimum phase, then the zero dynamics are unstable. This control method is to neglect terms in input derivatives until the required system order is reached (Tsourdos *et al.*, 1999). Although the approximate I/O linearization can handle the uncertain processes with non-minimum phase behavior (Femat *et al.*, 1999; Sampath *et al.*, 2002; Palanki *et*

al., 2003), it is only neglect the undesired response, which is inaccuracy in practical process.

2.2 Lyapunov-based control

One of the most important concepts in the study of control theory is the concept of stability. Stability theory concerns the behavior of the system trajectories of a dynamical system when the initial state of system is near an equilibrium state. The most complete stability analysis was developed by Aleksandr Lyapunov (Haddad and Chellaboina, 2008). Lyapunov's method is based on construction of a function of the system state coordinates that serves as a generalized norm of the solution of the dynamical system. Two dominant methods of Lyapunov stability are used to investigate the stability of nonlinear systems, called indirect and direct methods. The indirect method determines the stability of the nonlinear system by the evaluated eigenvalues of the Jacobian matrix of the linearized system around equilibrium. If the linearized system is asymptotically stable, we can always construct a quadratic Lyapunov function that guarantees local exponential stability of the nonlinear process. The direct method is to determine the stability properties of a nonlinear process by constructing a Lyapunov function or energy-like function formulated as real positive definite for a process and examining how this function develops in the time domain. The control method based on the Lyapunov's direct methods can be classified into two categories (Panjapornpon, 2005; Dubljevic and Christofides, 2006; Haddad and Chellaboina, 2008).

a) To assume a suitable control law, then find a proper Lyapunov function to prove closed-loop stability.

b) To assume a Lyapunov function candidate, then find a control law to make this candidate a real Lyapunov function, usually called converse Lyapunov theorem.

Most Lyapunov-based control for uncertain chemical processes focused on converse Lyaponov theorem including inverse optimal control (El-Farra *et al.*,

1999, 2001), generalized pointwise min-norm (GPMN) (He *et al.*, 2007), hybrid predictive control (Mhaskar *et al.*, 2005), the feedback control with backstepping (Qing and Shurong, 2006) and adaptive stabilization technique (Fu and Cheng, 2008). El-Farra *et al.* (El-Farra *et al.*, 1999) proposed the inverse optimal control problem under the concept of control Lyapunov function (CLF). A feedback control, u is found that renders negative definite of $\dot{V}\left(x,u\left(x\right)\right)$. The existence of bounding functions captured the size of the uncertain variables. Although the input constraint is added to evaluate control performance, it is difficult to determine the proper parameters of performance cost and Lyapunov function. Another inverse optimal control based on CLF was the control method of GPMN (He *et al.*, 2007). The state feedback and uncertainty is obtained by solving the optimization problem with inequality constraint where the objective function is formulated in form of Lyapunov function. In hybrid predictive control (Mhaskar *et al.*, 2005), the key idea is to use a Lyapunov-based bounded robust controller. A set of switching laws are designed that exploit the performance of MPC whenever possible, while using the bounded controller to provide the stability guarantees. However, the drawback of the proposed hybrid method was that it has many tuning parameters. For the feedback control with backstepping (Qing and Shurong, 2006), a new CLF is constructed at every step by augmenting the CLF from the previous step by a penalty term of the difference between a state variable and its desired value. The backstepping algorithm can be divided into 3 parts: (i) introduce a virtual state and control, and rewrite the current state equation in terms of these, (ii) choose a CLF for the system, treating it as a final stage, and (iii) choose an equation for the virtual control that stabilizes the CLF. A advantage of backstepping is the construction of a Lyapunov function whose derivative can be made negative definite by a variety of control laws rather than by a specific control law. Furthermore, backstepping can be used for adaptive control of parametric pure-feedback systems in which unknown parameters enter into equations in an affine manner. However, the control based on backstepping neglects dynamic behaviors, which is very important in practical processes. The dynamic behaviors of the systems affect the quality of products and the economic benefit of plants. Another technique of Lyapunov-based control proposed adaptation of the feedback gains by

constructing the adaptive laws of the feedback gains (Fu and Cheng, 2008) that can stabilize the closed-loop system without the knowledge of the system parameters. However, the Lyapunov analysis for adaptive control is difficult in chemical processes that uncertainty in process occurs frequently and has inappropriately magnitude of uncertainty.

Although a few control techniques of LBC can be effectively controlled in spite of many tuning parameters (El-Farra *et al.*, 2001; Mhaskar *et al.*, 2005), it is difficult to find Lyapunov functions that guarantee stability. Moreover, the domain attraction was designed for nonlinear systems that affect the feasibility of control action.

2.3 Model predictive control

The MPC is the popular control method for controlling the multivariable chemical processes with constraints due to its ability to handle the constraint problem. The control actions of MPC is computed by solving an optimization problem online in each sampling period, in which the objective function of the optimization problem is formulated by the difference between the predicted output and its reference. The general optimization problem in form of performance index can be written as Equation (6).

$$\min_{u} \sum_{j=1}^{N} y\left(t+j|t\right)^{T} Q_j y\left(t+j|t\right) + \sum_{j=1}^{N_u} u\left(t+j|t\right)^{T} R_j u\left(t+j|t\right) \tag{6}$$

where N is the cost horizon, N_u is the control horizon, $y\left(t+j|t\right)$ is the predicted output for $t+j$, $Q_j = Q_j^T \geq 0$ and $R_j = R_j^T > 0$ are used as weighting parameters.

The simplified schematic diagram of general MPC is presented in Figure 4 (Seborg *et al.*, 2004). The process model is used to predict the dynamic and static interactions between input, output, and disturbance variables. The constraints on

inputs and outputs are considered in a systematic manner. Furthermore, the control calculations can be coordinated with the calculation of optimum set points. Although MPC is an efficient technique it still has some disadvantages. The MPC require many efforts in computational load to solve the optimization problem online especially nonlinear problem. In addition, MPC obtains to face the problem of unconvergence in solution due to the complexity of objective function that is possible to have many local minimums.

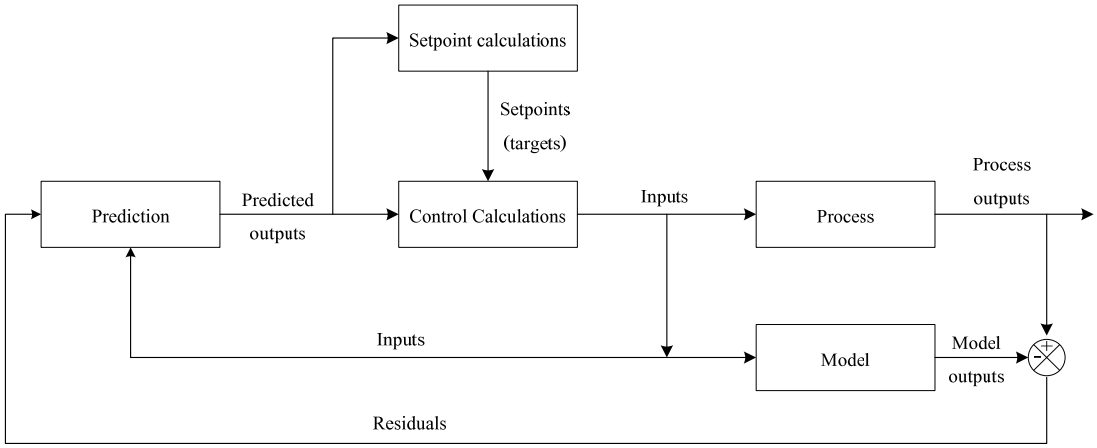

Figure 4 The schematic diagram of general MPC.

For the control problem of uncertain processes, the MPC methods such linear matrix inequality (LMI)-based robust MPC methods (Rodrigues and Odloak, 2000; Cheng and Jia, 2002; Wan and Kothare, 2003; Sandoval, 2008) and min-max robust MPC methods were proposed.

2.3.1 LMI-based robust MPC methods

The important factors of LMI are computing the several matrix variables of many complex control systems and finding a solution with multiple constraints and numerical difficulty (Sandoval, 2008). The LMI has the form described by Equation (7).

$$F(x) = F_0 + \sum_{i=1}^{m} x_i F_i > 0 \tag{7}$$

where $x \in \mathbb{R}^m$ are the decision variables and $F_i = F_i^T \in \mathbb{R}^{n \times n}$ are symmetric matrix that are given. The inequality symbol in Equation (7) mean that $F(x)$ is positive definite such as $u^T F(x) u > 0$ for all nonzero $u \in \mathbb{R}^n$. The objective of this control problem is to minimize some objective function, while guaranteeing a set of LMI feasibility constraints to be satisfied for all possible uncertainty. Several researchers (Rodrigues and Odloak, 2000; Cheng and Jia, 2002; Wan and Kothare, 2003) considered the uncertainty through a polytopic system of process model described by Figure (5). It usually arises when the uncertain process is modeled as linear time-varying system with state space matrix:

$$x(k+1) = Ax(k) + Bu(k) \tag{8}$$

where $A \in \mathbb{R}^{n \times n}$ and $B \in \mathbb{R}^{n \times m}$ are the model matrix of appropriate dimensions. A polytopic domain is given by (Rodrigues and Odloak, 2000):

$$\Omega = \left\{ \begin{bmatrix} A_1 & B_1 \end{bmatrix}, \begin{bmatrix} A_2 & B_2 \end{bmatrix}, \ldots, \begin{bmatrix} A_L & B_L \end{bmatrix} \right\} \tag{9}$$

where L is the number of vertices of the polytope.

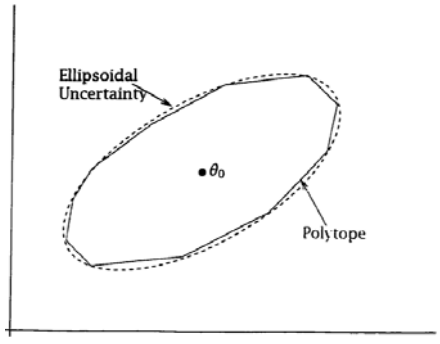

Figure 5 Polytopic domain description.

Most method of LMI feasibility constraints used the Lyapunov's direct method to guarantees asymptotic stability of the closed-loop system. For example, the quadratic matrix inequality is considered in Equation (10):

$$A^T P + PA + PBR^{-1}B^T P + Q < 0 \tag{10}$$

where A, B, $Q = Q^T$, $R = R^T > 0$ are given matrices of appropriate sizes, and $P = P^T$ is the variable. It can be expressed as the linear matrix inequality in Equation (11).

$$\begin{bmatrix} -A^T P + PA - Q & PB \\ B^T P & R \end{bmatrix} > 0 \tag{11}$$

If the objective function as the eigenvalue problem (EVP) is considered to minimize the maximum eigenvalue of a matrix subject to an LMI constraint, it can be described by

$$\min \ \gamma$$

subject to

$$\begin{bmatrix} -A^T P + PA - Q & PB \\ B^T P & \gamma I \end{bmatrix} > 0, \quad P > 0 \tag{12}$$

where P and γ are the optimization variables.

The applications of LMI technique to uncertain processes addressed by the following various techniques. Rodrigues and Odloak (2000) proposed the performance objective of the deviation between the setpoint and the controlled output. Lyapunov stability constraint is determined with Schur's complement to inequality constraint. Cheng and Jia (2002); Wan and Kothare (2003) proposed the performance objective under Lyapunov stability constraint to find robustly stabilizing state feedback gain that

minimized the worst performance objective for the given uncertainty. The uncertainty was incorporated by state feedback and recalculation of the feedback gain at each time instant. Casavola *et al.*, (2004) extended the concept of Wan and Kothare (2003) to uncertain chemical processes with input constraint described by norm bounded uncertainties. However, LMI is difficult to determine the proper tuning parameter. Furthermore, this control technique just an approximation of the original nonlinear process and tend to be in large error when the operating conditions are far from the steady state, which affect significantly the Lyapunov stability constraint.

2.3.2 Min-max robust MPC methods

This method was originally proposed in Witsenhausen (1968). A min-max MPC problem can typically be written as Equation (13).

$$\min_{u} \max_{D} \sum_{j=1}^{N} y\left(t+j|t\right)^{T} Q_j y\left(t+j|t\right) + \sum_{j=1}^{N_u} u\left(t+j|t\right)^{T} R_j u\left(t+j|t\right) \tag{13}$$

subject to

$$u\left(t+j|t\right) \in \mathbb{U}$$

$$x\left(t+j|t\right) \in \mathbb{X}$$

$$D\left(t+j|t\right) \in \mathbb{D}$$

The objective function is used to determine the optimal control action that minimizes the worst performance objective for the uncertainty. The effect of the uncertainty can be easily taken into account in the output constraints. Thus, it is ensured that for all uncertainty values within the bounds, the constraints would be satisfied. The min-max robust MPC controller, which successfully controls systems with time varying uncertainties in process gain, time constant and time delay was presented by Wang *et al.* (2004a, 2004b). This controller guarantees stability and offset-free set point tracking in the presence of model uncertainty. The robust regulator uses a tree

trajectory to forecast the time varying model uncertainty and the controller design procedure uses integrators to reject nonzero disturbances and maintain the process at the optimal setpoints. Another approach of min-max robust MPC methods presented by Munoz *et al.* (2005). The min-max robust MPC method was applied to a scaled laboratory process and showed how to move most computations offline obtaining the explicit from of this control law by means of a heuristic algorithm. The result shown that min-max MPC is less sensitive to system dynamic changes. However, this formulation dramatically increases the computational cost of the online control problem (Wang, 2002). Moreover, the issue of offset free tracking needs to be addressed.

From literature review, although many research works were presented to account in the presence of uncertainties it still have some above mentioned disadvantages. The differential geometric control is generally not ensured stability when the nonlinear system is non-minimum phase. Moreover, input constraints are not considered. Lyapunov-based control is difficult to find the Lyapunov function and to design the domain attraction that affects to feasibility of control action. MPC require many efforts in computational load to solve the optimization problem online . In addition, MPC have many tuning parameter and not applicable to unstable, non-minimum-phase processes directly. From the surveyed control technique of NMBC, there is no research work focusing on the controller design of uncertain chemical process with steady state multiplicity behavior, which is often found natural behavior in chemical processes.

To overcome limitations of existing control methods that cannot handle the uncertain chemical processes with steady state multiplicity behavior, this research work proposed a new control technique by the integration of I/O linearization and Lyapunov stability constraint. The I/O linearization is enhanced the setpoint tracking which leads to asymptotic linearization of the closed-loop I/O behavior while LBC is guaranteed asymptotic closed-loop stability region in order to ensure the desired dynamic characteristics. The key feature of the proposed control technique is ability in the determination of proper tuning parameters using bifurcation analysis based on

controller tuning due to the demonstration of domain of solution and flexible Lyapunov stability constraint that support the amount of uncertainty. With the result of developed control method, the uncertain chemical process will be operated effectively at multiple steady states.

MATERIALS AND METHODS

To have a better understanding in the development of proposed control method, the brief reviews of relative order, zero dynamics, I/O linearization, and stability analysis are described in following sections.

1. Mathematical preliminaries

Consider general class of multivariable processes with uncertainty described by the continuous-time, mathematical model of the form:

$$\begin{aligned} \dot{x} &= \Phi(x, u, D) \\ y &= h(x) \end{aligned} \tag{14}$$

where $x \in \mathbb{R}^n$, $u \in \mathbb{R}^m$, $y \in \mathbb{R}^m$ and $D \in \mathbb{R}^n$ denote the vector of the state variables, the manipulated inputs, the controlled outputs and the unmeasured disturbances, respectively. It will be implied that the values of the higher derivatives of disturbances, $D^{(0)}, \ldots, D^{(n-1)}$ are set to zero.

1.1 Relative order

For the process in the form of Equation (14), the relative order of the controlled output y_i with respect to the manipulated inputs is denoted by r_i, where r_i is the smallest integer for which a change in the manipulated input u_i can affect the output, $\partial[d^{r_i} y_i / dt^{r_i}] / \partial u \neq 0$. The following notation will be used:

$$
\begin{aligned}
h_i^0(x) &= h_i(x) \\
h_i^1(x, D) &= \frac{dy_i}{dt} \\
&\vdots \\
h_i^{r_i-1}(x, D) &= \frac{d^{r_i-1} y_i}{dt^{r_i-1}} \\
h_i^{r_i}(x, u, D) &= \frac{d^{r_i} y_i}{dt^{r_i}}
\end{aligned}
\tag{15}
$$

Assumptions (Panjapornpon and Soroush, 2007)

The following assumptions are made:

1) the relative orders $r_1, \ldots, r_m$ are finite.

2) the characteristic matrix of the process, $\frac{\partial}{\partial u} h_i^{r_i}(x, u) \neq [0 \cdots 0]$, is non-singular on $\mathbb{X} \times \mathbb{U}$.

3) the process is controllable and observable locally (around the nominal steady state).

4) the matrice $\partial f / \partial x$ and $[\partial h / \partial x][\partial f / \partial x]^{-1}[\partial f / \partial u]$ evaluate at nominal steady state pair, $\left(x_{ss}^N, u_{ss}^N\right)$, are non-singular.

Under the assumptions above, the function describing the dependence of the nominal steady state pair (x_{ss}^N, u_{ss}^N) on the piece-wise constant, output setpoint, y_{sp}, can be calculated from $0 = h\left(x_{ss}^N, u_{ss}^N\right)$ and $y_{sp} = h\left(x_{ss}^N\right)$ that is, $x_{ss}^N = G\left(y_{sp}\right)$.

In case of the controlled output y does not have a finite relative order ($r = \infty$), it means that the manipulated input u does not affects the controlled output, y.

1.2 Zero dynamics

The zero dynamics is analyzed to investigate the influence on control system design. The process with unstable mode in the zero dynamics exhibits the non-minimum phase behavior, which is one of the limitations of inherent process on the achievable control performance. The controlled output initially responds in the opposite of the desired direction (inverse response) leading to the degradation in control performance (Panjapornpon, 2005).

Referring to the inverse process, the nonlinear dialog of the minimum-phase property is related to the stability of the dynamic process:

$$\begin{aligned} \dot{\zeta}_1 &= F_1\left(y, \dot{y}, \ldots, \frac{d^{r-1}y}{dt^{r-1}}, \zeta_1, \ldots, \zeta_{n-r}\right) \\ &\vdots \\ \dot{\zeta}_{n-r} &= F_{n-r}\left(y, \dot{y}, \ldots, \frac{d^{r-1}y}{dt^{r-1}}, \zeta_1, \ldots, \zeta_{n-r}\right) \end{aligned} \tag{16}$$

In the case where the output is constrained to a constant value (setpoint, y_{sp}), it can be assumed to be zero without loss of generality. The zero dynamics is analyzed to determine the stability of the inverse process:

$$\begin{aligned} \dot{\zeta}_1 &= F_1\left(0, 0, \ldots, 0, \zeta_1, \ldots, \zeta_{n-r}\right) \\ &\vdots \\ \dot{\zeta}_{n-r} &= F_{n-r}\left(0, 0, \ldots, 0, \zeta_1, \ldots, \zeta_{n-r}\right) \end{aligned} \tag{17}$$

To determine the stability of the inverse process, we consider the nonlinear processes in the form of Equation (18):

$$\begin{aligned} \dot{x} &= f\left(x, u\right) \\ y &= h\left(x\right) \end{aligned} \tag{18}$$

where $x \in \mathbb{R}^n$, $u \in \mathbb{R}^m$ and $y \in \mathbb{R}^m$ denote the state variables, manipulated inputs, and controlled outputs, respectively. The equilibrium points of this process are the set of solutions obtained from the dynamic equations at steady state. The defining function is therefore:

$$f\left(x_{ss}, u_{ss}\right) = 0 \tag{19}$$

The approximated linearization of process model defined by Equation (18) is

$$\dot{x} = \tilde{A}x + \tilde{B}u \tag{20}$$

where x is an $n \times 1$ vector of state deviations from an operating point defined by the state vector, x, and the input vector, u,

u is an $m \times 1$ vector of input deviations from the input vector, u,

$\tilde{A}$ is the $n \times n$ Jacobian matrix, defined as:

$$\tilde{A} = \frac{\partial \mathrm{f}}{\partial \mathrm{x}} = \begin{bmatrix} \frac{\partial f_1}{\partial x_1} & \frac{\partial f_1}{\partial x_2} & \cdots & \frac{\partial f_1}{\partial x_n} \\ \frac{\partial f_2}{\partial x_1} & \frac{\partial f_2}{\partial x_2} & \cdots & \frac{\partial f_2}{\partial x_n} \\ \vdots & \vdots & \cdots & \vdots \\ \frac{\partial f_n}{\partial x_1} & \frac{\partial f_n}{\partial x_2} & \cdots & \frac{\partial f_n}{\partial x_n} \end{bmatrix}$$

$\tilde{B}$ is the $n \times m$ input-Jacobian matrix, defined as:

$$\tilde{B} = \frac{\partial \mathrm{f}}{\partial \mathrm{u}} = \begin{bmatrix} \frac{\partial f_1}{\partial u_1} & \frac{\partial f_1}{\partial u_2} & \cdots & \frac{\partial f_1}{\partial u_n} \\ \frac{\partial f_2}{\partial u_1} & \frac{\partial f_2}{\partial u_2} & \cdots & \frac{\partial f_2}{\partial u_n} \\ \vdots & \vdots & \cdots & \vdots \\ \frac{\partial f_n}{\partial u_1} & \frac{\partial f_n}{\partial u_2} & \cdots & \frac{\partial f_n}{\partial u_n} \end{bmatrix}$$

The stability of the zero dynamics is determined by evaluating the eigenvalues of the Jacobian matrix of (20) at a steady state (x_{ss}, u_{ss}). The eigenvalues are found by setting the determinant to zero:

$$\left| J - \lambda I \right| = 0 \tag{21}$$

The character of a steady state can be summarized as follows:

i) Stable node, if both eigenvalues are real and negative.

ii) Unstable node, if both eigenvalues are real and positive.

iii) Saddle node, if the eigenvalues are real with opposite signs.

iv) Stable focus, if the eigenvalues are complex conjugate with negative real parts.

v) Unstable focus, if the eigenvalues are complex conjugate with positive real parts.

If the zero dynamics of Equation (17) is asymptotically stable, then the original system is called non-minimum phase. Otherwise, it is called minimum phase.

To demonstrate the of zero dynamics analysis, the chemical reactor with the van de Vusse reaction is (Kuhlmann and Bogle, 1997):

$$A \xrightarrow{k_1} B \xrightarrow{k_2} C$$

$$2B \xrightarrow{k_3} D$$

The process model is given by

$$\begin{aligned}\frac{dC_A}{dT} &= -k_1 C_A - k_3 C_A^2 + D\left(C_{Ai} - C_A\right)\\ \frac{dC_B}{dT} &= k_1 C_A - k_2 C_B - D C_B\\ y &= C_B\end{aligned} \tag{22}$$

where C_A and C_B are the concentrations of A and B in the reactor, respectively. k_1 = 50 h $^{-1}$, k_2 = 1.5 h^{-1} and k_3 = 500 mol^{-1} h^{-1} are the reaction rate constants. C_{Ai} = 1 mol/l is the concentration of A in the feed stream. D = 3.91 h^{-1} is the dilution rate. The relative order of this process is one. The zero dynamics of the van de Vusse reaction model are

$$\frac{d\zeta}{dT} = -k_1\zeta - k_3\zeta^2 + \frac{\left(C_{Ai} - C_A\right)\left(k_1 C_A - k_2 y_{sp}\right)}{y_{sp}} \tag{23}$$

The stability of the zero dynamics is investigated with the eigenvalue of the linearization of Equation (22) at the steady states of this process. The steady states for the process model in Equation 22 are

$$\begin{aligned}C_{A,ss} &= \frac{\left(-k_1 - D\right)}{2k_3^2} + \frac{\sqrt{k_1^2 + 2k_1 D + 4C_{Ai}k_3 D + D^2}}{2k_3}\\ C_{B,ss} &= \frac{k_1\left(-k_1 - D + \sqrt{k_1^2 + 2k_1 D + 4C_{Ai}k_3 D + D^2}\right)}{2k_3\left(k_2 + D\right)}\end{aligned} \tag{24}$$

The eigenvalue of the zero dynamics is

$$\lambda = -k_1 + k_2 - 2k_3 C_{A,ss} + \frac{\left(C_{Ai}k_1 - 2k_1 C_{A,ss}\right)}{C_{B,ss}} \tag{25}$$

This expression is equivalent to the process zero. The sign of Equation 25 shows that the van de Vusse reaction is non-minimum phase.

2. Analytical model predictive control of input/output (I/O) linearization

I/O linearization can be applied to a process if the process is minimum phase. Moreover, the process must have a well-defined relative degree (Kravaris and Kantor, 1990). The requested closed-loop responses of the linear form:

$$\begin{aligned} \left[\varepsilon_1 \mathcal{D}+1\right]^{r_1} y_1 &= y_{sp_1} \\ &\vdots \\ \left[\varepsilon_m \mathcal{D}+1\right]^{r_m} y_m &= y_{sp_m} \end{aligned} \tag{26}$$

where $\mathcal{D}$ is the differential operator (i.e. $\mathcal{D} \triangleq \frac{d}{dt}$) and $\varepsilon_1,\ldots,\varepsilon_m$ are positive constant that set the speed of the response of the closed-loop outputs $y_1,\ldots,y_m$ respectively. It can be induced to an unconstrained process of the form (26) by implementing the solution to the following unconstrained optimization problem at each time instant

$$\min_{u,D} \sum_{i=1}^{m} \left\| \hat{y}_i(\tau) - y_{d_i}(\tau) \right\|^2 \tag{27}$$

where $\left\|q(\tau)\right\|$ denotes the 2-norm of a scalar function $q(\tau)$, given by:

$$\left\|q(\tau)\right\| \triangleq \sqrt{\int_{t}^{t+T_h} q(\tau)} \tag{28}$$

where $\hat{y}_i(\tau)$ is model-predicted future value of y_i at time τ, given by a Taylor series expansion of y_i around the present time, t:

$$\hat{y}_i(\tau) = h_i\,(x(t)) + \sum_{l=1}^{r_i-1} h_i^l\,(x(t), D(t))\frac{[\tau - t]^l}{l!} + h_i^{r_i}\,(x(t), u(t), D(t))\frac{[\tau - t]^{r_i}}{r_i!} + \text{h.o.t} \tag{29}$$

and $y_{d_i}(\tau)$ is the predicted future value of the reference trajectory of y_i at time τ, given by

$$\begin{aligned} [\varepsilon_1 \mathcal{D} + 1]^{r_1}\, y_{d_1}(\tau) &= y_{sp_1} \\ &\vdots \\ [\varepsilon_m \mathcal{D} + 1]^{r_m}\, y_{d_m}(\tau) &= y_{sp_m} \end{aligned} \tag{30}$$

initialized at

$$\frac{d^l y_i(t)}{dt^l} = h_i^l\,(x(t)), \quad l = 0, \ldots, r_i - 1, \qquad i = 1, \ldots, m$$

Taylor series expansion of y_{d_i} around the present time, *t,* yields:

$$y_{d_i}(\tau) = h_i\,(x(t)) + \sum_{l=1}^{r_i-1} h_i^l\,(x(t), D(t))\frac{[\tau - t]^l}{l!} + \frac{y_{sp_i}(t) - h_i\,(x(t)) - \sum_{l=1}^{r_i-1} \varepsilon_i^l \binom{r_i}{l} h_i^l\,(x(t), D(t))}{\varepsilon_i^{r_i}} \frac{[\tau - t]^{r_i}}{r_i!} + \text{h.o.t} \tag{31}$$

After substituting for $\hat{y}_i(\tau)$ and y_{d_i} for a very small prediction horizon T_h, the minimization problem of (31) takes the simplified form:

$$\min_{u,D}\sum_{i=1}^{m}\left[\frac{h_i\left(x\right)+\sum_{l=1}^{r_i-1}\varepsilon_i^l\binom{r_i}{l}h_i^l\left(x,D\right)}{\varepsilon_i^{r_i}}+\frac{\varepsilon_i^{r_i}h_i^{r_i}\left(x,u,D\right)-y_{sp_i}}{\varepsilon_i^{r_i}}\right]^2 \tag{32}$$

The static state feedback control law in Equation (32) is described by

$$\begin{aligned} u &= \psi\left(x, y_{sp}\right) \\ D &= \check{D}\left(x, y_{sp}\right) \end{aligned} \tag{33}$$

3. Stability theory

Stability analysis of time-varying systems considers the stability of the equilibrium states of the forced system which tracks a reference trajectory of the systems. For a nonlinear process (14) with initial condition $x(0) = x_0$ and $D = 0$, stability analysis of the equilibrium states in the Lyapunov stability is based on the following definition (Haddad and Chellaboina, 2008):

(i) The equilibrium point $x_e = 0$ is Lyapunov stable if, for all $\tilde{\varepsilon} > 0$, there exist $\tilde{\delta} = \tilde{\delta}(\tilde{\varepsilon}) > 0$ such that if $\|x(0)\| < \tilde{\delta}$, then $\|x(t)\| < \tilde{\varepsilon}$ for every $t \geq 0$. Lyapunov stability of an equilibrium point is shown in Figure 6, where $\tilde{\varepsilon}$ and $\tilde{\delta}$ are radius of sphere. The solution starts close enough to the equilibrium point within a distance $\tilde{\delta}$ and remain close enough forever within a distance $\tilde{\varepsilon}$.

(ii) The equilibrium point $x_e = 0$ is asymptotically stable if it is Lyapunov stable and there exist $\tilde{\delta} > 0$ such that if $\|x(0)\| < \tilde{\delta}$, then $\lim_{t\to\infty} x(t) = 0$. Asymptotic stability of an equilibrium point is shown in Figure 7. It is more rigorous than the Lyapunov stable, since the solution converges to the equilibrium point from which it was disturbed at t_0 when observation of the unforced system starts.

(iii) The equilibrium point $x_e = 0$ is exponentially stable if there exist positive constants $\tilde{\alpha}$, $\tilde{\beta}$, and $\tilde{\delta}$ such that if $\|x(0)\| < \tilde{\delta}$, then $\|x(t)\| \le \tilde{\alpha}\|x(0)\|e^{-\tilde{\beta}t}$, $t \ge 0$. The solution converges to equilibrium point with rate $\tilde{\alpha}\|x(0)\|e^{-\tilde{\beta}t}$.

(iv) The equilibrium point $x_e = 0$ is unstable if it is not Lyapunov stable as shown in Figure 8.

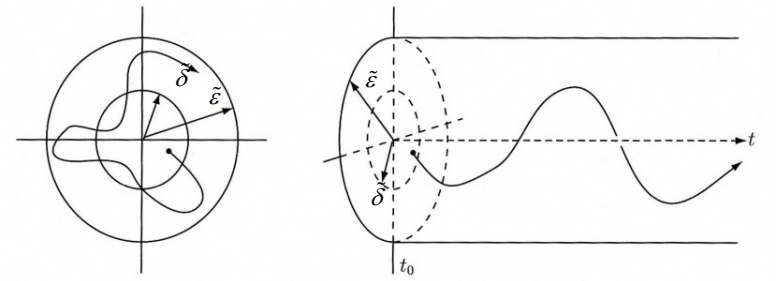

Figure 6 Lyapunov stability of an equilibrium point.

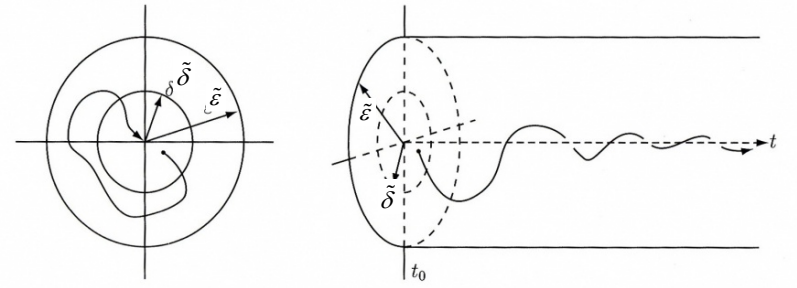

Figure 7 Asymptotic stability of an equilibrium point

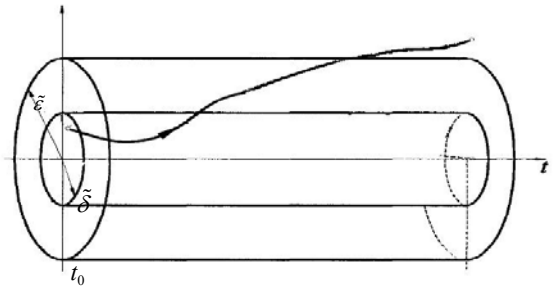

Figure 8 Unstable of an equilibrium point

Lyapunov's direct method

From stability analysis, the following result gives sufficient conditions for Lyapunov stable, asymptotic stable exponential stable and unstable. In Lyapunov's direct method, the stability properties of a nonlinear process are determined by constructing a Lyapunov function or energy-like function formulated as real positive definite. Consider the general nonlinear process in Equation (14) and assume that there exists a continuously differentiable function $V:Đ\to\mathbb{R}$ such that

$$V(0)=0, \tag{34}$$

$$V(x)>0, \qquad x\in Đ, \quad x\neq 0, \tag{35}$$

$$V'(x)f(x)\leq 0, \qquad x\in Đ. \tag{36}$$

where $Đ$ is open set with $0\in Đ$. Then the equilibrium point to (14) is Lyapunov stable. Moreover,

$$V'(x)f(x)<0, \qquad x\in Đ, \quad x\neq 0, \tag{37}$$

then the equilibrium point $x_e=0$ to (14) is asymptotically stable.

If $x_e\neq 0$ is an equilibrium point of (14), then Lyapunov's direct method holds with $V(0)=0$ and $x\neq 0$ replaced by $V(x_e)=0$ and $x\neq x_e$. A continuously differentiable function $V(\cdot)$ satisfying (35) and (36) is called a Lyapunov function candidate (Figure 9(a)) for a nonlinear process (14). If additionally, $V(\cdot)$ satisfies (37), $V(\cdot)$ is called a Lyapunov function for a nonlinear process (14).

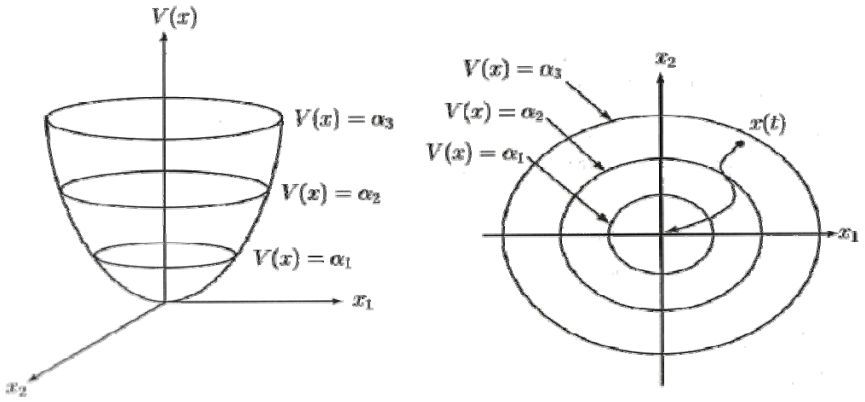

Figure 9 (a) Typical Lyapunov candidate and (b) constant Lyapunov energy surface ($\alpha_1 < \alpha_2 < \alpha_3$).

For condition (34)-(37), $V(\cdot)$ can be regarded as a generalized energy function for a nonlinear process (14). In particular, viewing the Lyapunov level surface $V(x) = \alpha$, for sufficiently small constants $\alpha > 0$, as constant energy surfaces covering the region, it follows from Lyapunov's direct method that requiring the Lyapunov derivative $\dot{V}(x) \triangleq V'(x) f(x)$ to be negative, the system trajectory of (14) move from one energy surface to an inner or lower energy surface. The trajectories of system will approach to the origin and remain within a ball, which is a constant energy surface, if condition in Equation (36) is satisfied. The system's energy surfaces shrink to zero so that the system trajectory approached zero asymptotically, if condition in Equation (37) is satisfied.

RESULTS AND DISCUSSION

1. Nonlinear controller design for uncertain chemical processes with multiplicity behavior

Consider the general class of multivariable processes, in which the continuous-time model in the form of Equation (14) is approximated into the discrete-time model described by

$$\begin{aligned} x(k+1) &= \Phi[x(k), u(k), D(k)], \\ y(k) &= h[x(k)] \end{aligned} \tag{38}$$

where $x(k) \in \mathbb{R}^n$, $u(k) \in \mathbb{R}^m$, $y(k) \in \mathbb{R}^m$ and $D(k) \in \mathbb{R}^n$ denote the state variables, manipulated inputs, controlled outputs vectors and unmeasured disturbances, respectively. The disturbances, $D(k)$, are assumed to be the piecewise constants during each time instant *k*. It will be implied that the values of the higher derivatives of disturbances, $D^{(1)}(k), \ldots, D^{(r_i-1)}$ are set to zero.

For nonlinear processes in the form of (38), the $r_1, \ldots, r_m$ denote the relative orders of the controlled output $y_1(k), \ldots, y_m(k)$ with respect to the manipulated inputs, where r_i is the smallest number of sampling periods that a change in the manipulated input $u_i(k)$ can affect the output. The following notation will be used:

$$\begin{aligned} y_i(k) &= h_i^0[x(k)] && i = 1, \ldots, m \\ y_i(k+l) &= h_i^l[x(k), D(k)] && l = 1, \ldots, r_i - 1 \\ &\vdots \\ y_i(k+r_i) &= h_i^{r_i}[x(k), u(k), D(k)] \end{aligned} \tag{39}$$

where

$$h_i^0[x(k)] \triangleq h_i[x(k)]$$
$$h_i^l[x(k), D(k)] \triangleq h_i^{l-1}\Phi[x(k), D(k), u(k)]$$
$$\vdots$$
$$h_i^{r_i}[x(k), u(k), D(k)] \triangleq h_i^{r_i-1}\Phi[x(k), u(k), D(k)]$$

Assumptions (Panjapornpon and Soroush, 2007)

The following assumptions are made:

1) the relative orders $r_1, \ldots, r_m$ are finite.

2) the characteristic matrix of the process, $\frac{\partial}{\partial u} h_i^{r_i}(x,u) \neq [0 \cdots 0]$, is non-singular on $\mathbb{X} \times \mathbb{U}$.

3) the process is controllable and observable locally (around the nominal steady state).

4) the matrice $\partial f / \partial x$ and $[\partial h / \partial x][\partial f / \partial x]^{-1}[\partial f / \partial u]$ evaluate at nominal steady state pair, $\left(x_{ss}^N, u_{ss}^N\right)$, are non-singular.

If the controlled output $y(k)$ does not have a finite relative order ($r = \infty$), it means that the manipulated input $u(k)$ never affects the controlled output $y(k)$. In every well formulated control problem, the output *y* must possess a finite relative order r_i. The system is steady state at time *t*, if

$$y_{sp} = y(k+1) = y(k) \tag{40}$$

in which $y_{sp} \in \mathbb{R}^m$ denote the desired output setpoint.

In assumption 1) - 4), the function describing the dependence of the nominal steady state pair $\left(x_{ss}^{N},u_{ss}^{N}\right)$ on the piecewise constant, output setpoint, y_{sp}, and steady state equilibrium pair, x_{ss}, can be calculated from $0=f\left(x_{ss}^{N},u_{ss}^{N}\right)$ and $y_{sp}=h\left(x_{ss}^{N}\right)$ that is $x_{ss}^{N}=G\left(y_{sp}\right)$.

1.1 Linearizating feedback controller design with Lyapunov stability constraint

1.1.1 Analytical model predictive control of input/output linearization

For a process in the form of (38) with input constraint

$$u_{\mathrm{i,l}}\le u_{i}\left(k\right)\le\ u_{\mathrm{i,h}},\ \ i=1,\ldots,m \tag{41}$$

where $u_{i,l}$ and $u_{i,h}$ denote lower bound and upper bound of input constraint. The closed-loop process output response of the linear form is requested by:

$$\begin{aligned}\left[\varepsilon_{1}D+1\right]^{r_1}\ y_{1}\left(k\right)&=y_{sp_1}\left(k\right)\\&\vdots\\\left[\varepsilon_{m}D+1\right]^{r_m}\ y_{m}\left(k\right)&=y_{sp_m}\left(k\right)\end{aligned} \tag{42}$$

where $\mathcal{D}$ is the differential operator in discrete-time defined by $(\mathcal{D}^{l}y_{i}(k)\triangleq\left[y_{i}(k+l+1)-y_{i}(k+l)\right]/\Delta t)$, $y_{sp_1}\left(k\right),\ldots y_{sp_m}\left(k\right)$ are the desired setpoints of the outputs $y_{1}\left(k\right),\ldots y_{m}\left(k\right)$ and $\varepsilon_{1},\ldots,\varepsilon_{m}$ are positive constants that set the speed of the responses of the process outputs, $y_{1}\left(k\right),\ldots y_{m}\left(k\right)$, respectively. It can be induced to an unconstrained process of the form (42) by implementing the solution to the following unconstrained optimization problem at each time instant.

$$\min_{u(k),D(k)} \sum_{i=1}^{m} \left\| \hat{y}_i\left(k+r_i\right) - y_{d_i}\left(k+r_i\right) \right\|^2 \tag{43}$$

where $\hat{y}_i\left(k+r_i\right)$ is model-predicted future value of $y_i(k)$ at $k+r_i$, given by a Taylor series expansion of $y_i(k)$ around the present time, *k*:

$$\begin{aligned} \hat{y}_i(k+r_i) = h_i\left[x(k)\right] + \sum_{l=1}^{r_i-1} \varepsilon_i^l \binom{r_i}{l} h_i^l\left[x(k), D(k)\right] \frac{\left[k+l\right]^l}{l!} \\ + h_i^{r_i}\left[x(k), u(k), D(k)\right] \frac{\left[k+r_i\right]^{r_i}}{r_i!} + \text{high order terms (h.o.t)} \end{aligned} \tag{44}$$

and $y_{d_i}\left(k+r_i\right)$ is the predicted future value of the reference trajectory of $y_i(k)$ at $k+r_i$, given by

$$\begin{aligned} \left[\varepsilon_1 D + 1\right]^{r_1} y_1(k+r_i) &= y_{sp_1}(k+r_i) \\ &\vdots \\ \left[\varepsilon_m D + 1\right]^{r_m} y_m(k+r_i) &= y_{sp_m}(k+r_i) \end{aligned} \tag{45}$$

initialized at

$$y_i(k+l) = h_i^l\left[x(k), D(k)\right], \quad l = 0,\ldots,r_i-1, \; i = 1,\ldots,m$$

Taylor series expansion of $y_{d_i}(k)$ around the present time, *k,* yields:

$$\begin{aligned} y_{d_i}(k+r_i) = h_i\left[x(k)\right] + \sum_{l=1}^{r_i-1} \varepsilon_i^l \binom{r_i}{l} h_i^l\left[x(k), D(k)\right] \frac{\left[k+r_i\right]^l}{l!} + \\ \frac{y_{sp_i}(t) - h_i\left[x(k)\right] - \sum_{l=1}^{r_i-1} \varepsilon_i^l \binom{r_i}{l} h_i^l\left[x(k), D(k)\right]}{\varepsilon_i^{r_i}} \frac{\left[k+r\right]^{r_i}}{r_i!} + \text{h.o.t} \end{aligned} \tag{46}$$

To formulate the analytical model predictive control after substituting for $y_i(k)$ and $y_{d_i}(k)$ that integrates the reference trajectories of input/output response in (42), the analytical model predictive method is modified as follows:

$$\min_{u(k),D(k)} \sum_{i=1}^{m} \left[\left[\varepsilon_i \mathcal{D} + 1 \right]^{r_i} y_i(k) - y_{sp_i}(k) \right]^2 \tag{47}$$

subject to

$$u_{\mathrm{i,l}} \le u_i(k) \le u_{\mathrm{i,h}}, \quad i = 1, \ldots, m$$

The recast form of the optimization problem is

$$\min_{u(k),D(k)} J\left[x(k), y_{sp}, u(k), D(k) \right] \tag{48}$$

subject to

$$u_{\mathrm{i,l}} \le u_i(k) \le u_{\mathrm{i,h}}, \quad i = 1, \ldots, m$$

where

$$J\left[x(k), y_{sp}(k), u(k), D(k) \right]$$
$$= \sum_{i=1}^{m} \left[\frac{h_i\left[x(k) \right] + \sum_{l=1}^{r_i - 1} \varepsilon_i^l \binom{r_i}{l} h_i^l \left[x(k), D(k) \right]}{\varepsilon_i^{r_i}} + \frac{\varepsilon_i^{r_i} h_i^{r_i} \left[x(k), u(k), D(k) \right] - y_{sp_i}(k)}{\varepsilon_i^{r_i}} \right]^2$$

Solving the constrained minimization problem of (48) leads to the static state feedback:

$$\begin{aligned} u(k) &= \psi\left[x(k), y_{sp}\right] \\ D(k) &= \check{D}\left[x(k), y_{sp}\right] \end{aligned} \tag{49}$$

1.1.2 Lyapunov stability constraint

The Lyapunov function in discrete-time, $V[x(k)]$, can be chosen to be quadratic form, that is

$$V[x(k)] = \left(x - x_{ss}^{N}\right)^{T} P \left(x - x_{ss}^{N}\right) \tag{50}$$

where $V[x(k)]$ is a positive definite function and x_{ss}^{N} is a nominal state equilibrium pair at given output y_{sp} , if $V[x(k)] = 0$ and $V[x(k)] > 0$ for all $x(k) \neq x(0)$.

$$\Delta V[x(k)] = V[x(k+1)] - V[x(k)], \qquad \Delta V[x(k)] \leq 0 \tag{51}$$

where the positive definite matrix P is chosen to satisfy the following Riccati equation:

$$\tilde{A}^{T} P + P\tilde{A} - P\tilde{B}\tilde{B}^{T} P = -Q, \qquad Q \geq 0 \tag{52}$$

where

$$\tilde{A} = \left.\frac{\partial f(x,u)}{\partial x}\right|_{(x_{ss}, u_{ss})}, \; \tilde{B} = \left.\frac{\partial f(x,u)}{\partial u}\right|_{(x_{ss}, u_{ss})}$$

Q is a positive semidefinite real symmetric matrix and $Q \geq 0$. If the Lyapunov function, $V[x(k)]$, satisfies the inequality constraint:

$$S\left[x(k), v(k), u(k), D(k)\right] \leq 0 \tag{53}$$

where

$$S\left[x(k), v(k), u(k), D(k)\right] = \beta\left(\frac{V[x(k+1)] - V[x(k)]}{\Delta t}\right) + V[x(k)]$$

$$-\left[\Phi\left[x(k), u(k), D(k)\right]\right]^T \times \Phi\left[x(k), u(k), D(k)\right]$$

$$V[x(k)] = \left(x(k) - x_{ss}^N\right)^T P\left(x(k) - x_{ss}^N\right)$$

$$v(k) = \hat{v}\left[x(k), y_{sp}(k), u(k), D(k)\right]$$

where β is a positive constant that set the rate of decay of $V[x(k)]$ and $v(k)$ is the target calculation that calculates the optimal steady state pair. Then the closed-loop system is asymptotically stable, because

$$\begin{aligned} \Delta V[x(k)] &< 0, \qquad x \neq x_{ss}^N \\ \Delta V[x(k)] &= 0, \qquad x = x_{ss}^N \end{aligned} \tag{54}$$

1.1.3 Reduced-order state observer

In many cases, the process is not complete state measurement. To estimate the state information, the reduced-order state observer (Soroush, 1997) is modified for uncertain chemical processes that are used to reconstruct the unmeasured state variables. Consider multivariable processes in the form of (38) with additional output measurements $Y_1, \ldots, Y_q$, that is,

$$\frac{dx}{dt} = \Phi[x, u, D], \quad x(0) = x_0$$

$$y = h(x) \tag{55}$$

$$Y = K(x)$$

The non-redundancy of the measured outputs ensures the existence of a locally-invertible state transformation of the form

$$\begin{bmatrix} \eta \\ y \\ Y \end{bmatrix} = T(x) = \begin{bmatrix} Qx \\ h(x) \\ K(x) \end{bmatrix} \tag{56}$$

where $\eta = [\eta_1, \ldots \eta_{n-m-l}]^T$ and Q is a constant (n-m−l)×n matrix which for the sake of simplicity, is chosen such that:

a) Each row of Q has only one nonzero term equal to one, and
b) Locally

$$\text{rank}\left\{ \frac{\partial}{\partial u} \begin{bmatrix} Qx \\ h(x) \\ K(x) \end{bmatrix} \right\} = n$$

Thus, the state transformation $[\eta \quad y \quad Y]^T = T(x)$ is locally invertible. The system of (38), in terms of the new state variables $\eta_1, \ldots \eta_{n-m-l}, y, Y$ takes the form

$$\begin{aligned} \dot{\eta} &= F_\eta[\eta, y, Y, u, D] \\ \dot{y} &= F_y[\eta, y, Y, u, D] \\ \dot{Y} &= F_Y[\eta, y, Y, u, D] \end{aligned} \tag{57}$$

where

$$F_\eta\left(\eta,y,Y,u,D\right)=Qf\left[H^{-1}\left(\eta,y,Y\right),u,D\right]$$

$$F_y\left(\eta,y,Y,u,D\right)=\left.\frac{\partial h\left(x\right)}{\partial x}\right|_{x=H^{-1}(\eta,y,Y)} f\left[H^{-1}\left(\eta,y,Y\right),u,D\right]$$

$$F_Y\left(\eta,y,Y,u,D\right)=\left.\frac{\partial K\left(x\right)}{\partial x}\right|_{x=H^{-1}(\eta,y,Y)} f\left[H^{-1}\left(\eta,y,Y\right),u,D\right]$$

A closed-loop, reduced-order observer is then designed in the form:

$$\begin{aligned}\dot{z}&=F_\eta\left(z+L_1y+L_2Y,y,Y,u,D\right)-L_1F_y\left(z+L_1y+L_2Y,y,Y,u,D\right)\\&\quad -L_2F_Y\left(z+L_1y+L_2Y,y,Y,u,D\right)\\\hat{x}&=H^{-1}\left[z+L_1y+L_2Y,y,Y\right]\end{aligned}\tag{58}$$

where $\hat{x}$ denotes the vector of the plant state estimates, L_1 and L_2 are the observer gains. The observer gains should be set such that the error dynamics are asymptotically stable, which means all eigenvalues of the [$(n-m-q)\times(n-m-q)$] matrix

$$\frac{\partial F_\eta\left[\eta,y,Y,u,D\right]}{\partial\eta}-L_1\frac{\partial F_y\left[\eta,y,Y,u,D\right]}{\partial\eta}-L_2\frac{\partial F_Y\left[\eta,y,Y,u,D\right]}{\partial\eta}\tag{59}$$

evaluated at the nominal steady-state pair to be in the left half of the complex plane.

When the state observer is approximated in the form of the discrete-time, a compact form of the state observer can describe by

$$\begin{aligned}z\left(k+1\right)&=F\left[z\left(k\right),y\left(k\right),u\left(k\right),D\left(k\right)\right]\\\hat{x}\left(k\right)&=H\left[z\left(k\right),y\left(k\right)\right]\end{aligned}\tag{60}$$

1.1.4 Integral action

To achieve offset-free set point tracking control, integral action has to be used in the controller to account in the presence of uncertainty. An estimate with disturbance process outputs is first calculated by using the closed-loop process model:

$$\begin{aligned} \chi(k+1) &= \Phi\left[\chi(k), \psi(\chi(k), \nu(k)), \check{D}(\chi(k), \nu(k))\right] \\ \xi(k) &= h[\chi(k)] \end{aligned} \tag{61}$$

where ξ is the estimate of controlled output with disturbance. The difference between this estimate and the measurement of the controlled output is added to the output setpoint in the form:

$$\begin{aligned} \chi(k+1) &= \Phi\left[\chi(k), \psi[\chi(k), \nu(k)], \check{D}[\chi(k), \nu(k)]\right] \\ \nu(k) &= \hat{v}[x(k), \theta(k), u(k), D(k)] \\ u(k) &= \psi[\chi(k), \nu(k)] \\ D(k) &= \check{D}[\chi(k), \nu(k)] \\ \theta(k) &= F[\nu(k) - y(k) + h[\chi(k)]] \end{aligned} \tag{62}$$

Then, integral action of the dynamic system of (61) is added to the state feedback of (49). If the closed-loop system is asymptotically stable under the state feedback of (49), it is asymptotically stable under (49), (61) and (62).

1.1.5 Developed controller system

The control system with state feedback that has integral action (62) in the optimization problem leads to the following control system in the form:

$$
\begin{aligned}
z(k+1) &= F\left[z(k), y(k), \psi\left[H\left[z(k), y(k)\right], \nu(k)\right],\right. \\
&\qquad \left. \check{D}\left[H\left[z(k), y(k)\right], \nu(k)\right]\right] \\
\chi(k+1) &= \Phi\left[\chi(k), \psi\left(\chi(k), \nu(k)\right), \check{D}\left[\chi(k), \nu(k)\right]\right] \\
u(k) &= \psi\left[H\left[z(k), y(k)\right], \nu(k)\right] \\
D(k) &= \check{D}\left[H\left[z(k), y(k)\right], \nu(k)\right]
\end{aligned}
\tag{63}
$$

To derive a state feedback of the form (49), the following constrained optimization problem is solved at each sampling period to obtain the value of $u(k)$ and $D(k)$:

$$
\min_{u(k), D(k)} J\left[x(k), \psi\left[H\left[z(k), y(k)\right], \nu(k)\right], \check{D}\left[H\left[z(k), y(k)\right], \nu(k)\right]\right] \tag{64}
$$

subject to

$$
\begin{aligned}
u_{\mathrm{i,l}} \le u_i(k) \le\ & u_{\mathrm{i,h}}, \quad i = 1, \ldots, m \\
S\left[\hat{x}(k), \nu(k), u(k), D(k)\right] \le\ & 0
\end{aligned}
$$

A block diagram of the control system is shown in Figure 10.

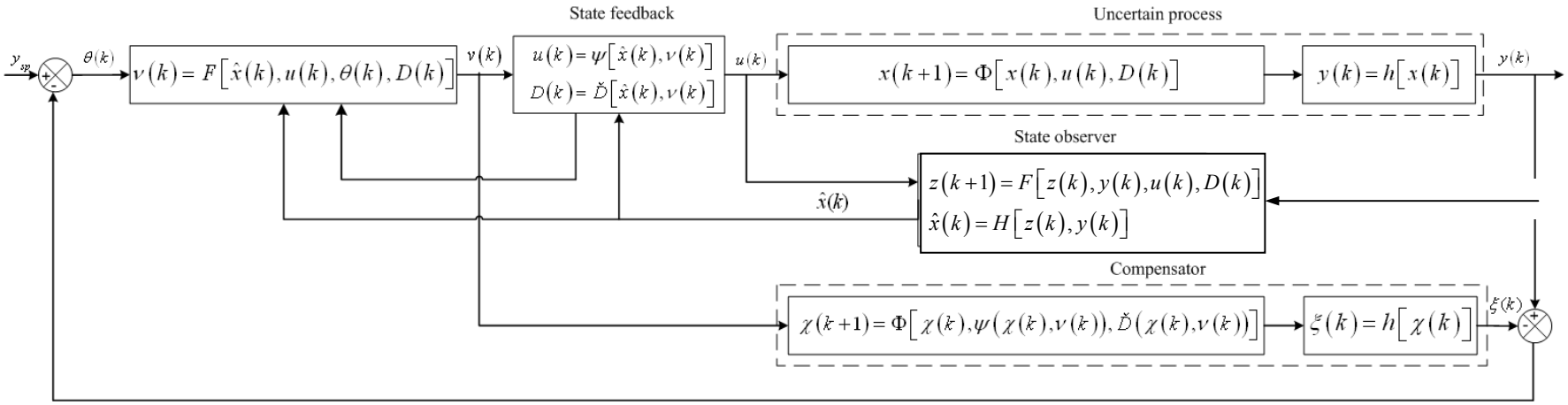

Figure 10 The control system with state feedback that has integral action.

1.2 Illustrative example for a control of uncertain chemical processes with multiplicity behavior

In this section, the application for the proposed control technique (63) is illustrated through various simulations of chemical processes: single-input single-output biochemical reactor, single-input single-output polymerization reactor and multi-input multi-output polymerization reactor. The objective is to maintain the controlled output with and without uncertainty at the desired setpoints. The generated uncertainties to chemical processes are both parametric uncertainty and unmeasured disturbance. MATLAB is used to solve the optimization problem with the fmincon command and to update the steady state pair with fsolve command. An integration of the differential equation for the closed-loop system is implemented into suitable time interval for each process with ODE45 command. Mathematica software is used to calculate the zero dynamics of the processes. To determine the optimal tuning parameters, MATCONT is used to generate the bifurcation diagram lead to analyze the domain of stability of the processes. The details of controller tuning with bifurcation analysis will be referred to again in section 2.

1.2.1 Single-input single-output biochemical reactor

To illustrate the control performance, a biochemical reactor of fermentation process with two components, a biomass and a substrate, is considered (Bequette 1998). The biochemical reactor exhibits several biological reactions occurring simultaneously in a liquid medium in which a biomass growth rate model is substrate inhibition kinetics. The process diagram for the biochemical reactor is shown in Figure 11, where the process is assumed no biomass in feed, a perfect mixing, constant volume, and constant physical and chemical properties.

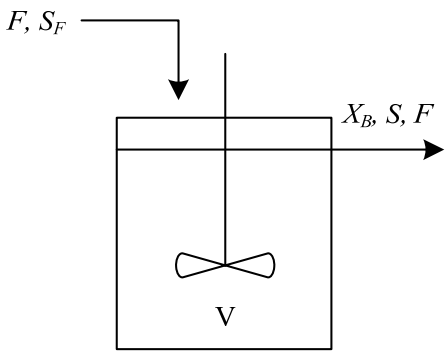

Figure 11 Process diagram for the biochemical reactor.

To describe the behavior of the biochemical reactor, the material balances on the biomass and the substrate are given in Equation (65).

$$\begin{aligned} \frac{dX_B}{dt} &= \mu(S)X_B - \frac{X_B F}{\mathrm{V}} \\ \frac{dS}{dt} &= -\frac{\mu(S)X_B}{Y} + \frac{(S_F - S)F}{\mathrm{V}} \\ \mu(S) &= \mu_{\max}\frac{S}{K_1 S^2 + S + K_m} \\ y &= S \end{aligned} \tag{65}$$

The biomass concentration X_B consists of cells that consume the substrate S. The substrate concentration S is controlled by manipulating the dilution rate $D = F/\mathrm{V}$. All state variables are assumed to be measured, $u = D = F/\mathrm{V}$, $x_1 = X_B$ and $y = x_2 = S$. A biochemical reactor is operated at the initial condition $\left[x_1(0), x_2(0)\right] = [1.75, 0.08]$ in stable minimum phase region. The controller implemented every sampling time of 2 seconds. The values of model parameters for process are listed in Table 1.

Table 1 The parameter values of SISO biochemical reactor

Parameter	Value
D	0.1 m^3
S_F	4 kg m^{-3}
Y	0.4
μ_{max}	8.82×10^{-3} min^{-1}
K_1	0.12 m^3 kg^{-1}
K_m	4.55×10^{-1} kg m^{-3}

Despite its apparent simplicity, the process exhibits multiplicity behavior. In the multiplicity analysis, a biochemical reactor has three steady states under the parameter values (Table 2) that is described in Figure 12.

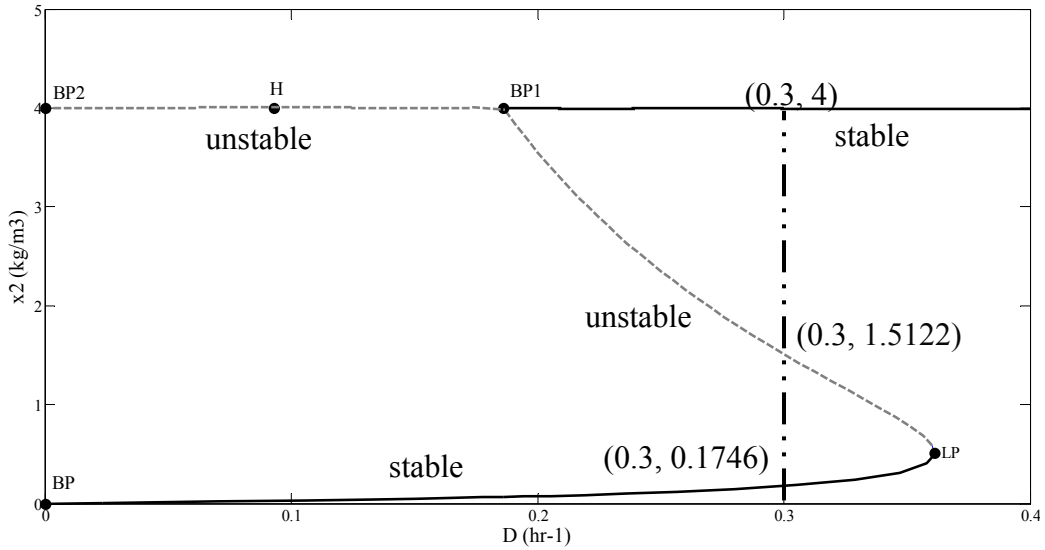

Figure 12 Bifurcation diagram for the biochemical reactor.

The steady state of manipulated input is evaluated at u_{ss} = 0.3. The opened-loop dynamic behaviors are analyzed by the eigenvalues of Jacobian matrix of both process and zero dynamics, which are shown in Table 2. The zero dynamics of this process are governed by:

$$\frac{d\zeta}{dt} = \zeta\left(-\frac{F}{V} + \frac{\mu_{max} y_{sp}}{K_m + y_{sp} + K_1 y_{sp}^2}\right) \tag{66}$$

Table 2 Values of steady state pair and the opened-loop dynamic behavior analysis of biochemical reactor.

Steady state pair	Eigenvalues of Jacobian matrix		Opened-loop dynamic
$[x_{1ss}, x_{2ss}]$	Process	Zero dynamics	behavior
[0, 4]	-0.3, -0.114	0.186	Stable, non-minimum phase
[0.995, 1.512]	-0.3, 0.170	-0.3	Unstable, minimum phase
[1.530, 0.176]	-2.262, -0.3	-0.3	Stable, minimum phase

When the biochemical reactor is operated at upper steady state, the biomass is not produced and the substrate concentration in the reactor is equal to the feed substrate concentration. All of the cells have been washed out of the reactor. Thus, an upper steady state with stable non-minimum phase is not considered. When the biochemical reactor is operated at lower steady state, the biomass is excess that may lead to not enough feed. From the steady state analysis, it is the difficult to control. The control performance of the proposed controller will be presented in the next section.

1.2.1.1 Controller system

The continuous-time biochemical reactor model in (65) is approximated into the discrete-time model with Euler's method. The resulting discrete-time model is

$$\begin{aligned}
x_1(k+1) &= x_1(k) + \Delta t\left(\frac{\mu_{\max} x_1(k) x_2(k)}{K_1 x_2(k)^2 + x_2(k) + K_m} - x_1(k) u(k)\right) \\
x_2(k+1) &= x_2(k) + \Delta t\left(-\frac{\mu_{\max} x_1(k) x_2(k)}{Y\left(K_1 x_2(k)^2 + x_2(k) + K_m\right)} + \left(S_F - x_2(k)\right) u(k)\right) \\
y(k) &= x_2(k)
\end{aligned} \tag{67}$$

The relative order of the process output with respect to the vector of manipulated input is $r=1$. The application of the controller system of (63) takes the form:

$$\begin{aligned}
\chi_1(k+1) &= \chi_1(k) + \Delta t\left[\frac{\mu_{\max}\chi_1(k)\chi_2(k)}{K_1\chi_2(k)^2+\chi_2(k)+K_m} - \chi_1(k)\psi\left(\chi(k),\nu(k)\right)\right] \\
&\quad + \check{D}_1\left(\chi(k),\nu(k)\right) \\
\chi_2(k+1) &= \chi_2(k) + \Delta t\left[-\frac{\mu_{\max}\chi_1(k)\chi_2(k)}{Y\left(K_1\chi_2(k)^2+\chi_2(k)+K_m\right)} + \left(S_F-\chi_2(k)\right)\psi\left(\chi(k),\nu(k)\right)\right] \\
&\quad + \check{D}_2\left(\chi(k),\nu(k)\right) \\
u(k) &= \psi\left(\hat{x}(k),\nu(k)\right) = \min_{u(k)}\left(\frac{\varepsilon\left(\hat{x}_2(k+2)\right)+\hat{x}_2(k)-\theta(k)}{\varepsilon}\right)^2 \\
D(k) &= \check{D}\left(\hat{x}(k),\nu(k)\right) = \min_{D(k)}\left(\frac{\varepsilon\left(\hat{x}_2(k+2)\right)+\hat{x}_2(k)-\theta(k)}{\varepsilon}\right)^2
\end{aligned} \tag{68}$$

subject to

$$0 < u(k) < 0.45$$

$$S(\hat{x}(k),\nu(k),u(k),D(k)) \le 0$$

where

$$S(\hat{x}(k),\nu(k),u(k),D(k)) = \beta\left(\frac{V[x(k+1)]-V[\hat{x}(k)]}{\Delta t}\right) - \begin{bmatrix}x_1(k+1)\\x_2(k+1)\end{bmatrix}\times\begin{bmatrix}x_1(k+1) & x_2(k+1)\end{bmatrix}$$

$$V[\hat{x}(k)] = \begin{bmatrix}\hat{x}_1(k)-\nu_1(k)\\\hat{x}_2(k)-\nu_2(k)\end{bmatrix}\begin{bmatrix}a_{11} & a_{12}\\a_{21} & a_{22}\end{bmatrix}\begin{bmatrix}\hat{x}_1(k)-\nu_1(k) & \hat{x}_2(k)-\nu_2(k)\end{bmatrix}$$

$$\theta(k) = y_{sp} - x_2(k) + \chi_2(k)$$

1.2.1.2 Selection of tuning parameters of biochemical reactor

To achieve the optimal response, the tuning parameters were determined by analyzing the stabilized domain of closed-loop system and bifurcation diagram. The details of controller tuning with bifurcation diagram will be referred to again in section 2. To test the effectiveness of the proposed controller, the substrate concentration S in biochemical reactor is controlled with multiple steady states. The process is initially at y_{sp}=1.5122 with unstable, minimum phase behavior, then at t = 1.5 min, it is adjusted to y_{sp}=0.1756 with stable, minimum phase behavior. The tuning parameter ε under I/O linearization technique is used to adjust the speed of the response of the closed-loop output. The tuning parameter β under Lyapunov stability constraint is used to set the rate of decay of Lyapunov function. The positive definite matrix P under Lyapunov stability constraint is chosen to satisfy the Riccati equation in Equation (52). In the tuning results under I/O linearization technique, although the output response with $\varepsilon = 0.8$ is fast it has still the oscillation leading to the degradation of control performance. In addition, the output response with $\varepsilon = 8.8$ is slow. In the tuning results under Lyapunov stability constraint, the output response with $\beta = 1$ is fast but it has the oscillation while the output response with $\beta = 100$ is slow. Thus, the optimal parameter values for the proposed control system in Equation (68) are $\varepsilon = 4.8$, $\beta = 10$ and

$$P = \begin{bmatrix} a_{11} & a_{12} \\ a_{21} & a_{22} \end{bmatrix} = \begin{bmatrix} 734.525 & 0.167 \\ 0.167 & 0.105 \end{bmatrix}$$

which are shown in Figure 13 and Figure 14. The output response with the proposed tuning parameters is the fast, smooth, and no oscillation, which approaches to the desired steady states at 0.25 and 2 minutes, respectively.

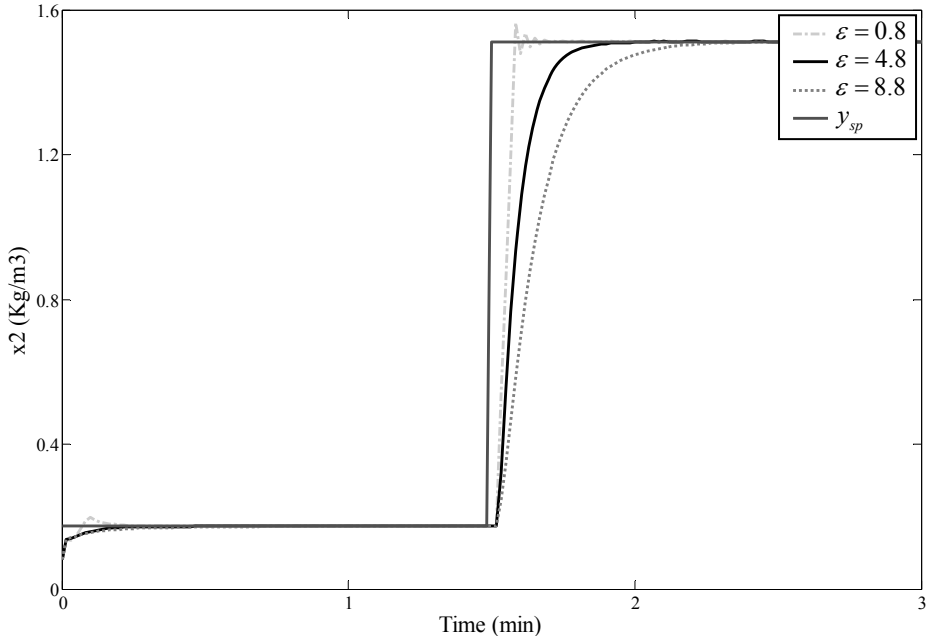

Figure 13 Closed-loop responses of controlled output by varying the tuning parameter, ε, under I/O linearization.

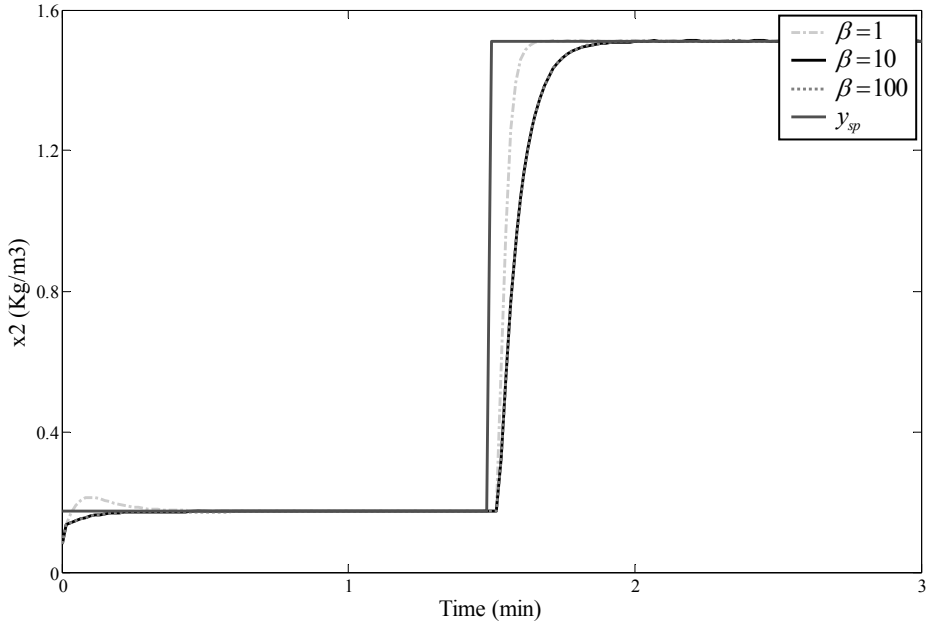

Figure 14 Closed-loop responses of controlled output by varying the tuning parameter, β, under Lyapunov stability constraint.

1.2.1.3 Simulation results of biochemical reactor without uncertainty

The control technique developed in the previous section that is applied through biochemical reactor without uncertainty. The substrate concentration is controlled at the desired setpoints. The performance of the controller is investigated in terms of performing a smooth and fast startup of the process, the stability of closed-loop system, and tracking step changes in the setpoints. Figure 15(a) shows the closed-loop response of biomass concentration. The controller successfully operates the biochemical reactor at the desired setpoints whether unstable, minimum phase and stable, minimum phase. The profiles of the substrate concentration is shown in Figure 15(b) from the loading instant at $t = 0$ until the reactor reaches steady state conditions. The substrate concentration response is a smooth and fast startup. Moreover, it is no oscillation when move from one set point to another without offset. The controller adjusts the maximum dilution rate in Figure 15(c) to bring the substrate concentration to a new setpoint value as soon as possible. The Lyapunov function profile in Figure 16(a) continuously decrease, which indicate that the closed-loop response is stable. Furthermore, it is also asymptotically stable when the time derivatives of Lyapunov function in Figure 16(b) converge to zero corresponding to stability analysis. Figure 16(c) shows the constraint flag of the closed-loop response. The value of constraint flag at one indicate that the Lyapunov stability constraint is active when the substrate concentration is controlled at unstable, minimum phase steady state. Only I/O linearization technique cannot control the substrate concentration at unstable, minimum phase steady state because its domain of solution is not cover the dynamic behavior with unstable, minimum-phase. Thus, Lyapunov stability constraint must continuously be active to maintain the substrate concentration at the desired steady state.

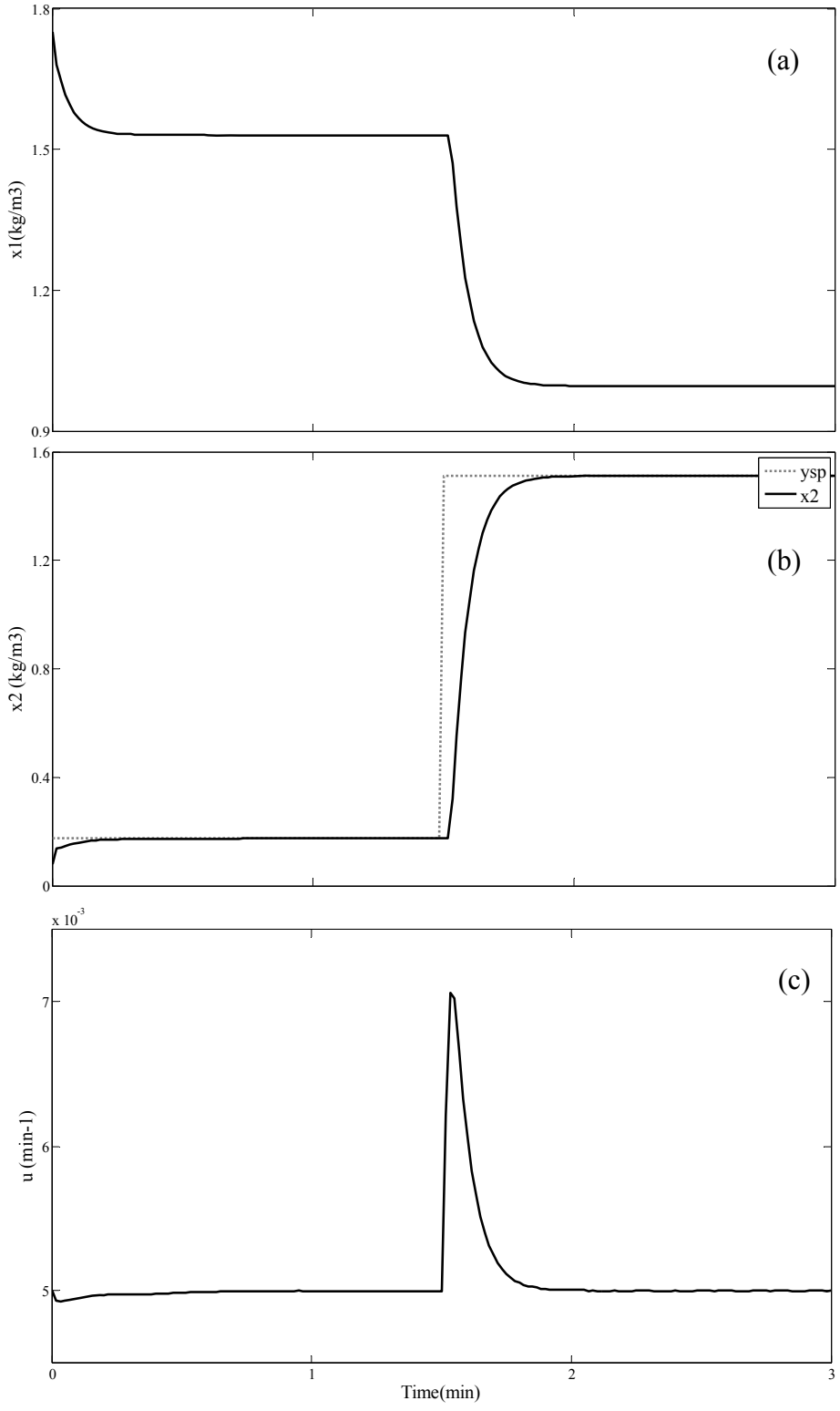

Figure 15 Closed-loop responses of (a) biomass concentration, (b) substrate concentration and (c) dilution rate for biochemical reactor without uncertainty.

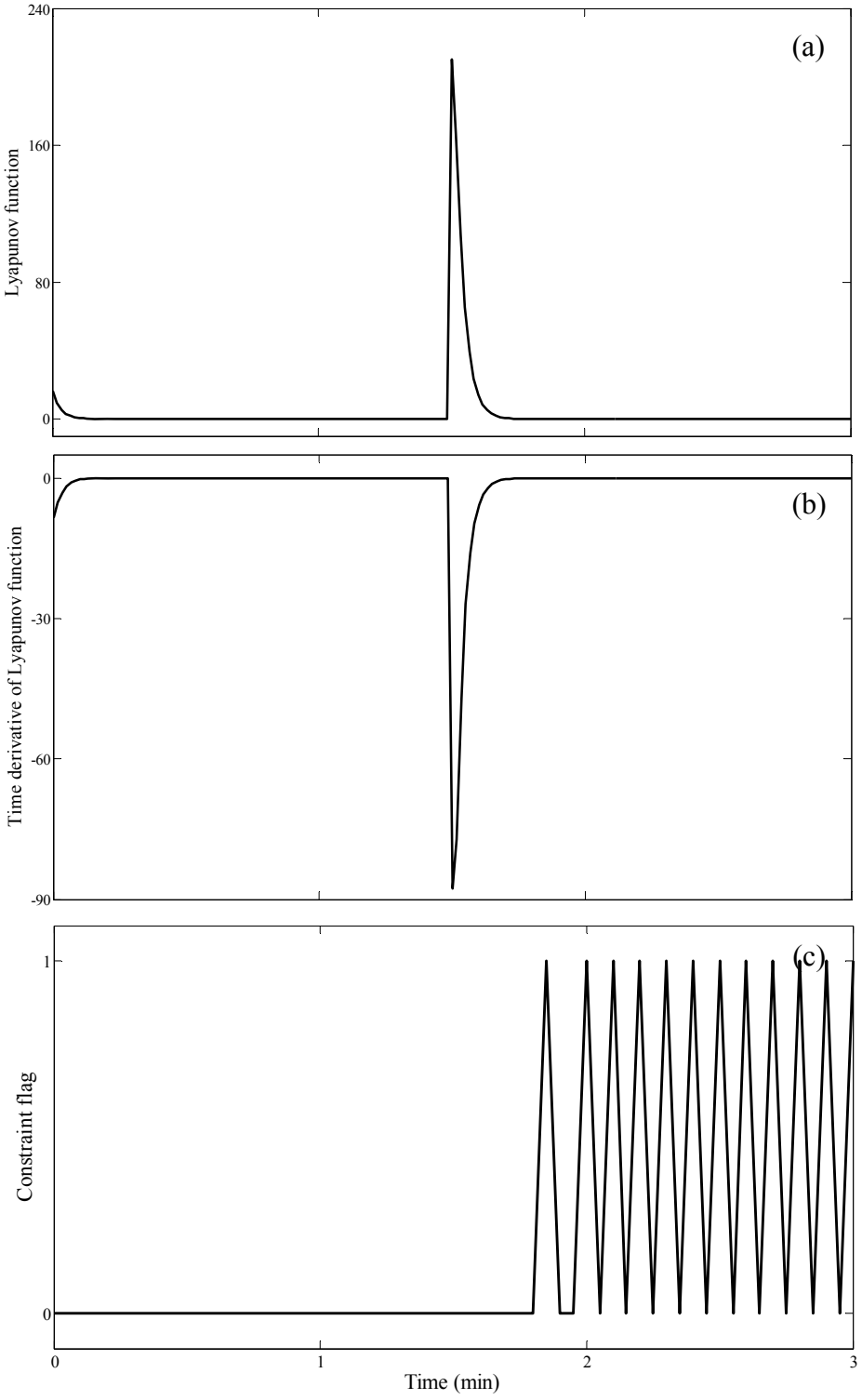

Figure 16 Closed-loop responses of (a) Lyapunov function profile, (b) time derivative of Lyapunov function and (c) constraint flag for biochemical reactor without uncertainty.

1.2.1.4 Simulation results of biochemical reactor with uncertainty

The proposed control technique is applied through biochemical reactor with uncertainty to control the substrate concentration at the desired setpoints. The performance of the controller is investigated in terms of tracking step changes in the setpoints, the stability of closed-loop system and the robustness property of controller. The parametric uncertainty and unmeasured disturbances are considered, which are simulated with random noise of the maximum growth rate (μ_{max}) and the dilution rate (D), respectively. The different experimental conditions of the various data sources and the extensive parameter variation among individual cells are increasing the complexity of the rate term $\mu(S)$ that causes the uncertainty in maximum growth rate. On the other hand, the sensitivity of online measurements such as flow sensor generates the uncertainty in the dilution rate, which significantly affect the substrate concentration.

Case 1: Uncertainty in the maximum growth rate (μ_{max})

To test the robustness property of the proposed controller, the controller can maintain the substrate concentration at the maximum of $\pm$ 40% uncertainty in the maximum growth rate. Figure 17(a) shows the closed-loop response of biomass concentration. The controller successfully operates the biochemical reactor at the desired setpoints whether unstable, minimum phase and stable, minimum phase. The profiles of the substrate concentration is shown in Figure 17(b) from the loading instant at t = 0 until the reactor reaches steady state conditions. The substrate concentration can effectively move from one set point to another. The controller adjusts the dilution rate as shown in Figure 18(a) to bring the substrate concentration at a new setpoint value as soon as possible. The approximation of uncertainty in each state is shown in Figure 18(b). The uncertainty has a significant effect on the substrate concentration to compensate the disturbance to obtain the desired output. The Lyapunov function profile in Figure 18(c) continuously decrease, which indicate that the closed-loop response is stable. Furthermore, it is also asymptotically stable when

the time derivatives of Lyapunov function in Figure 19(a) converge to zero. Figure 19(b) shows the constraint flag of the closed-loop response. The Lyapunov stability constraint is active in some ranges of stable, minimum phase steady state, which may cause the wide range of uncertainty in the maximum growth rate. Moreover, it is active at unstable, minimum phase steady state when the output tracking cannot stabilize the closed-loop system. Thus, Lyapunov stability constraint must continuously be active to maintain the substrate concentration at the desired steady state.

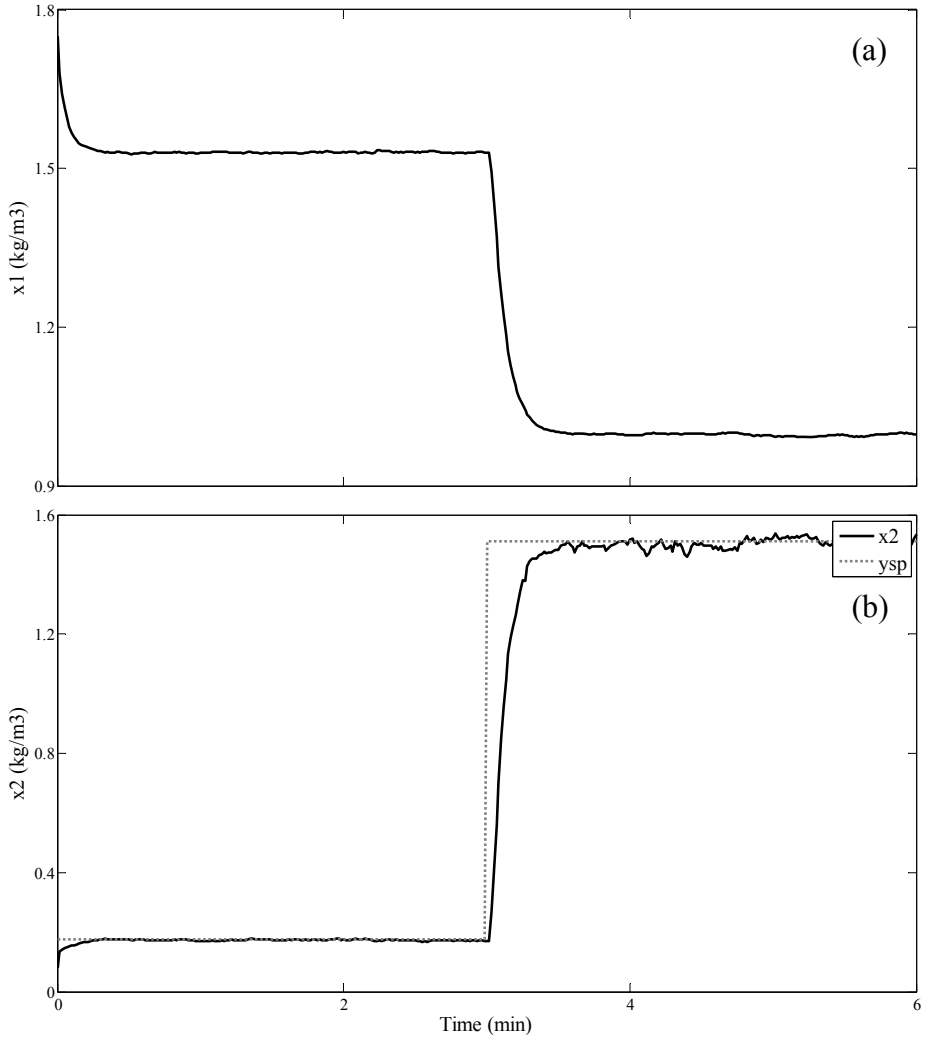

Figure 17 Closed-loop responses of (a) biomass concentration, and (b) substrate concentration with ± 40% uncertainty in maximum growth rate (μ_{max}).

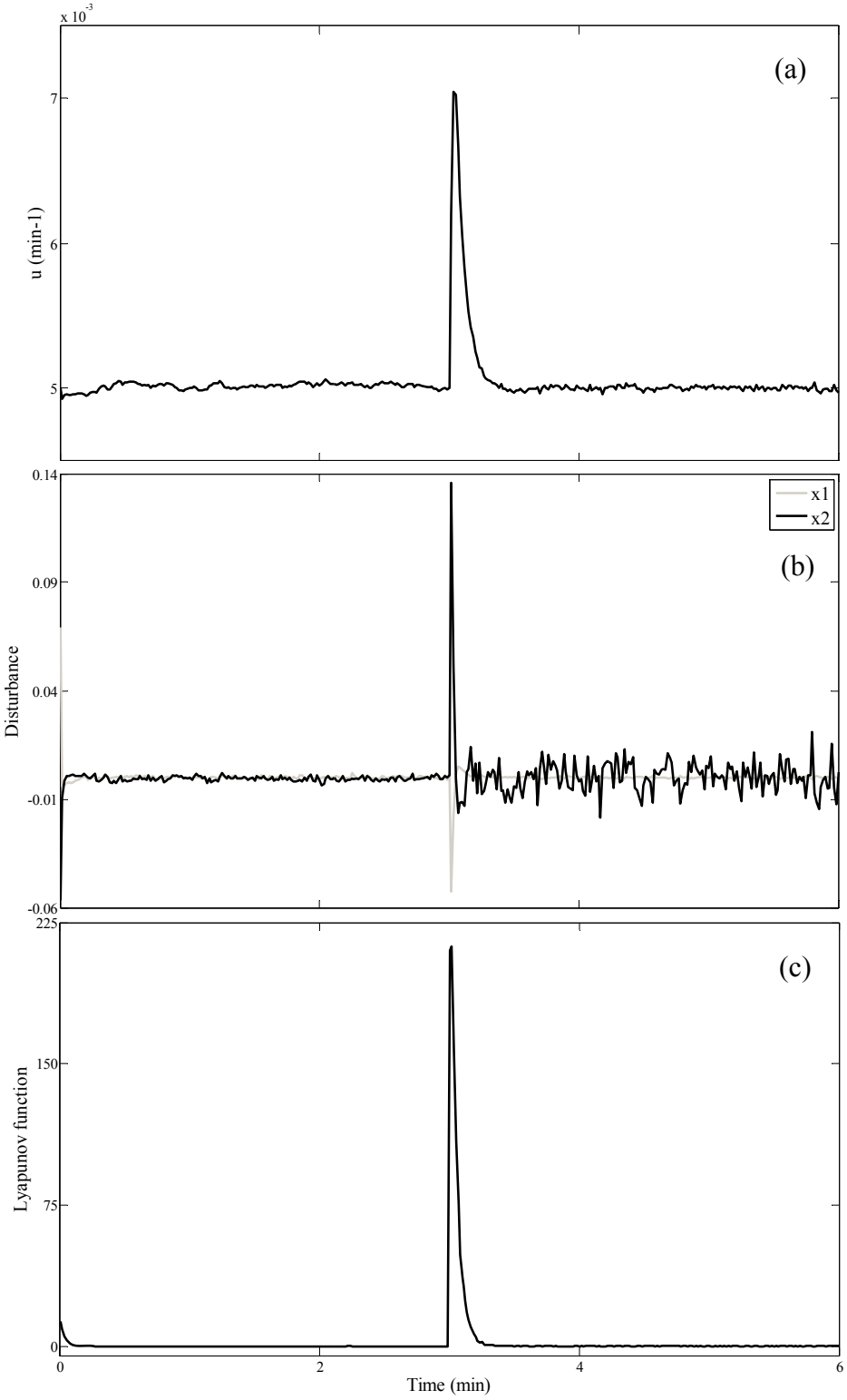

Figure 18 Closed-loop responses of (a) dilution rate, (b) unmeasured disturbance, and (c) Lyapunov function for biochemical reactor with $\pm 40\%$ uncertainty in maximum growth rate (μ_{max}).

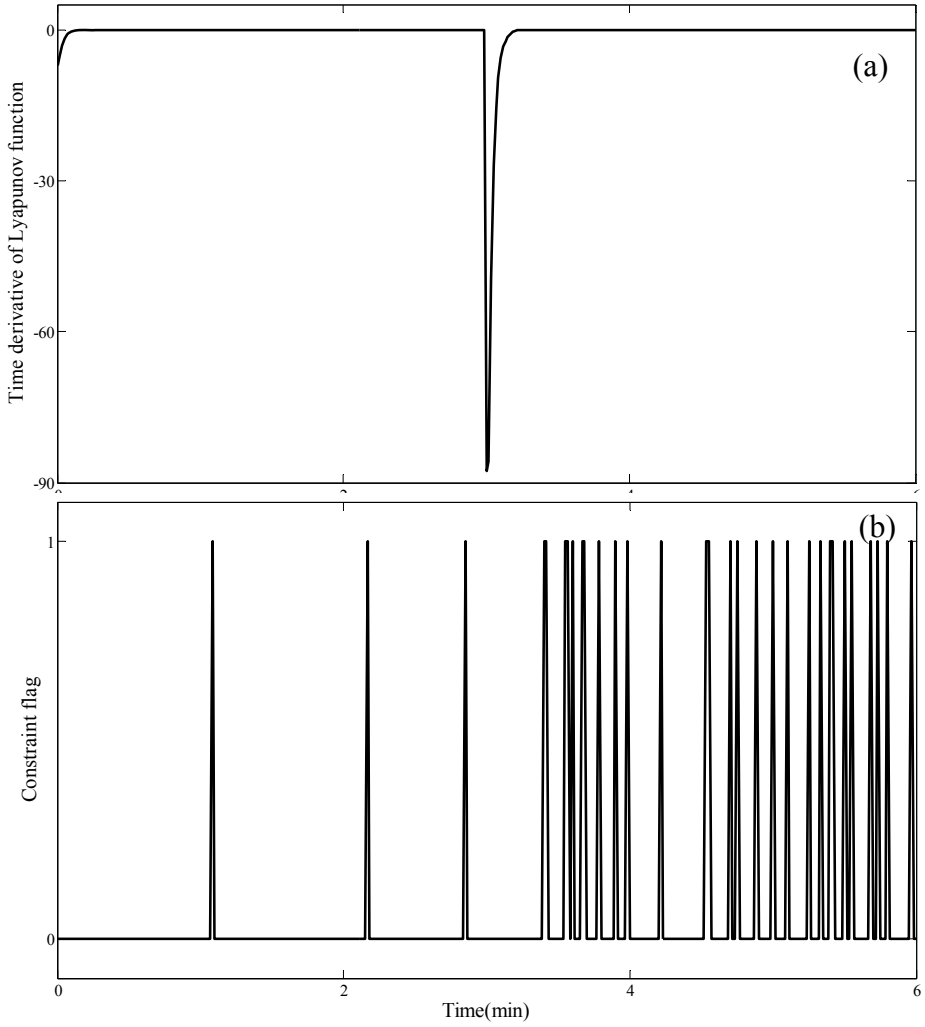

Figure 19 Closed-loop responses of (a) time derivative of Lyapunov function, and (b) constraint flag for biochemical reactor with $\pm 40\%$ uncertainty in maximum growth rate (μ_{max}).

Case 2: Uncertainty in the dilution rate (*D*)

To test the robustness property of the proposed controller, the controller can maintain the substrate concentration at the maximum of $\pm 20\%$ uncertainty in the dilution rate. Figure 20(a) shows the closed-loop response of biomass concentration. The controller successfully operates the biochemical reactor at the desired setpoints whether unstable, minimum phase and stable, minimum phase. The profiles of the substrate concentration is shown in Figure 20(b) from the loading instant at $t = 0$ until

the reactor reaches steady state conditions. The substrate concentration can effectively move from one set point to another. The controller adjusts the dilution rate as shown in Figure 20(c) to bring the substrate concentration at a new setpoint value as soon as possible. The approximation of uncertainty in each state is shown in Figure 21(a). The uncertainty has a significant effect on the substrate concentration to compensate the disturbance to obtain the desired output. The Lyapunov function profile in Figure 21(b) continuously decrease, which indicate that the closed-loop response is stable. Furthermore, it is also asymptotically stable when the time derivatives of Lyapunov function in Figure 21(c) converge to zero. Figure 22 shows the constraint flag of the closed-loop response. The Lyapunov stability constraint is active in some ranges of stable, minimum phase steady state, which may cause the wide range of uncertainty in the maximum growth rate. Moreover, it is active at unstable, minimum phase steady state when the output tracking cannot stabilize the closed-loop system. Thus, Lyapunov stability constraint must continuously be active to maintain the substrate concentration at the desired steady state.

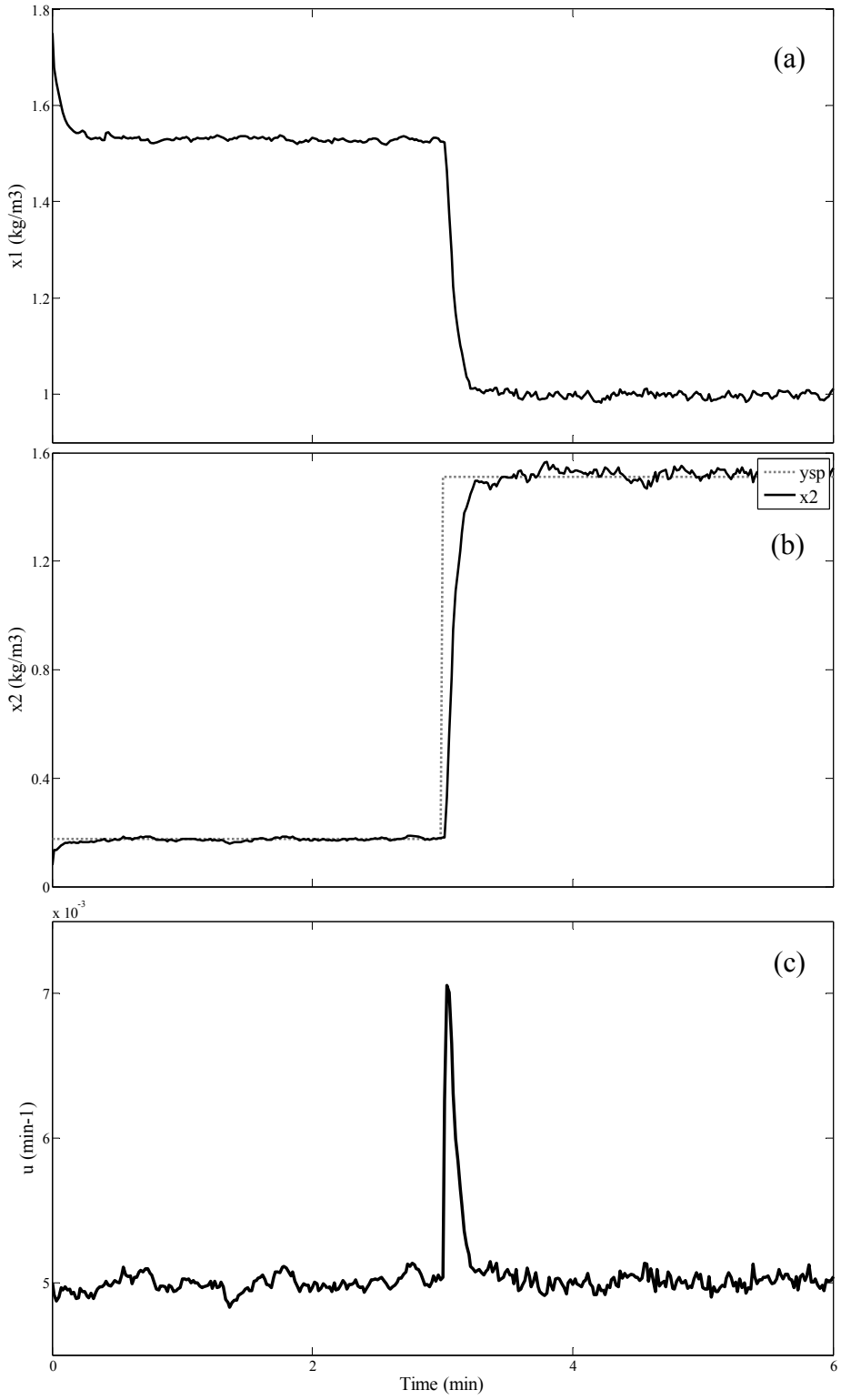

Figure 20 Closed-loop responses of (a) biomass concentration, (b) substrate concentration, and (c) dilution rate for biochemical reactor with ± 20% uncertainty in dilution rate (*D*).

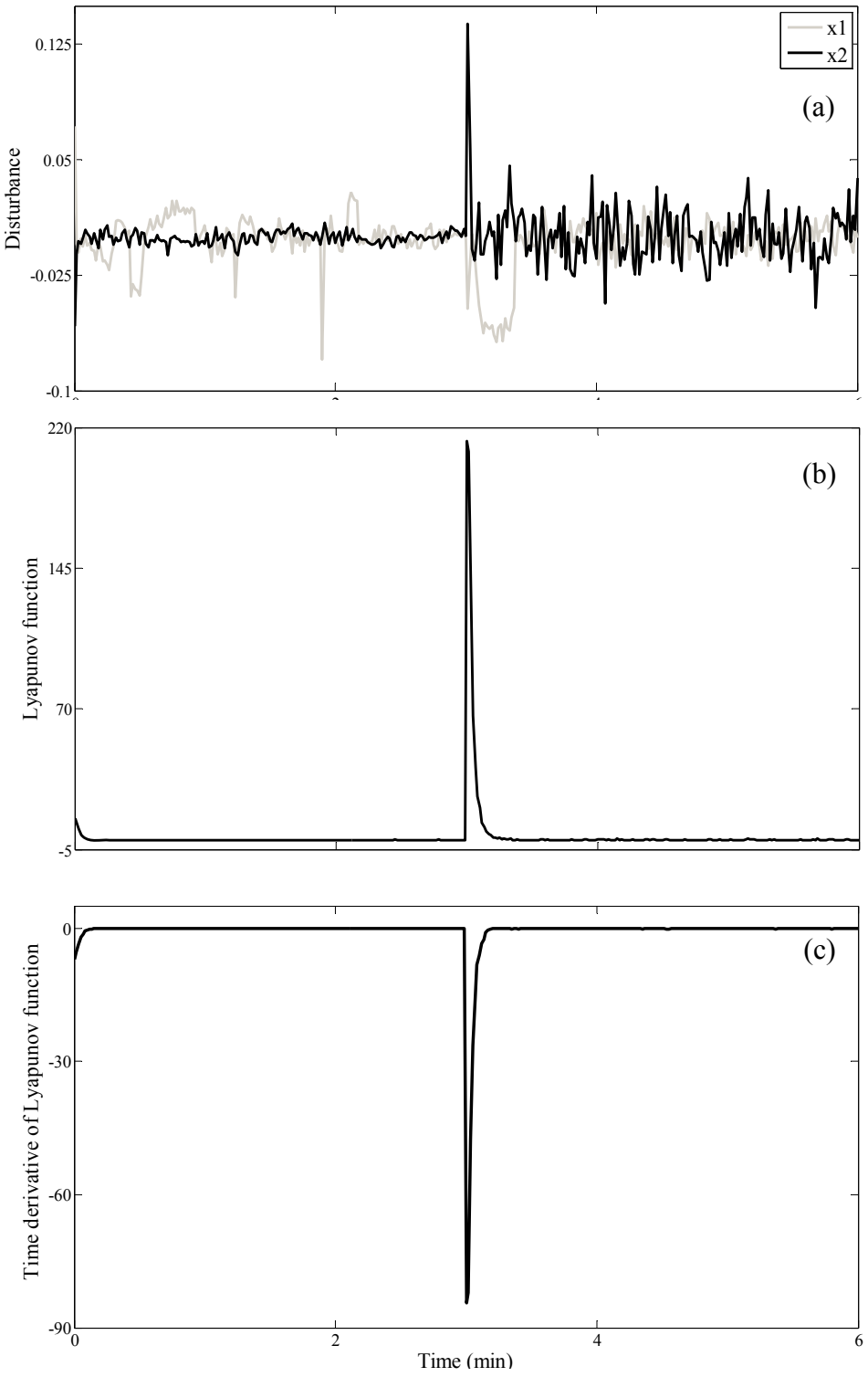

Figure 21 Closed-loop responses of (a) unmeasured disturbance, (b) Lyapunov function profile, and (c) time derivative of Lyapunov function for biochemical reactor with ± 20% uncertainty in dilution rate (*D*).

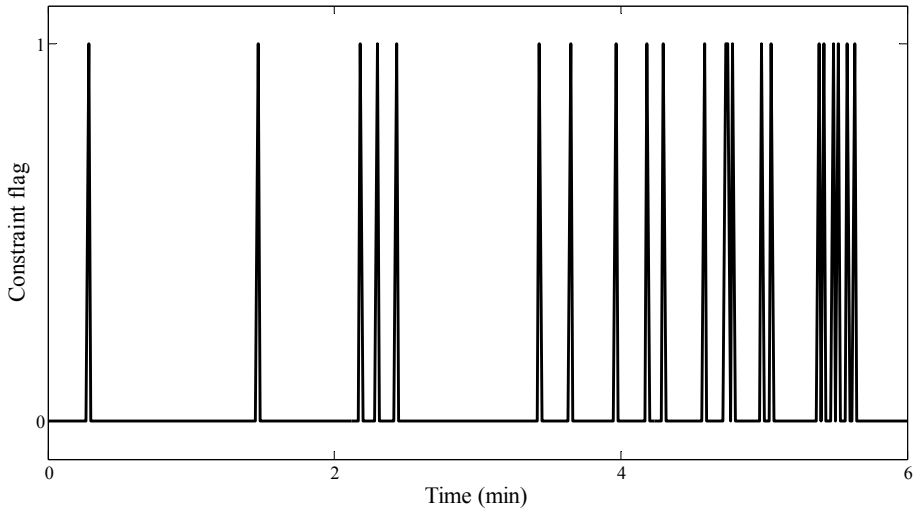

Figure 22 The constraint flag for biochemical reactor with ± 20% uncertainty in dilution rate (*D*).

1.2.2 Single-input single-output styrene polymerization reactor

To apply the proposed control technique through the process with complex reaction, a challenge control problem such the styrene polymerization reactor (Russo and Bequette, 1998) is presented, which exhibit non-minimum phase behavior in three steady states. The free radical polymerization kinetic mechanism is modeled as

$$I \xrightarrow{k_d} 2R \qquad \text{(initiator decomposition)}$$

$$M + R \xrightarrow{k_i} P_1 \qquad \text{(chain initiator)}$$

$$P_n + M \xrightarrow{k_p} P_{n+1} \qquad \text{(propagation)}$$

$$P_n + P_m \xrightarrow{k_{td}} T_n + T_m \qquad \text{(termination)}$$

$$P_n + P_m \xrightarrow{k_{tc}} T_{n+m} \qquad \text{(termination)}$$

where *I*, *R*, *M*, *P*, and *T* are the initiator, the radical produced by initiator decomposition, the monomer species, the growing polymer chain, and the terminated polymer chain, respectively. The reaction is initiated by azobisisobutyronitrile (AIBN), which dissolve in isopropyl benzene to keep both conversion and viscosity

low. The monomers of styrene are converted to polystyrene, which the reaction is complex and highly exothermic. To remove excess heat from the reactor, a cold liquid is pumped through the jacket. The process diagram for the jacketed styrene polymerization CSTR is shown in Figure 23.

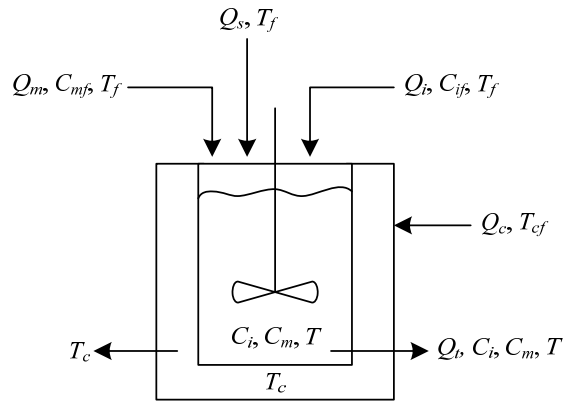

Figure 23 Process diagram for the jacketed styrene polymerization CSTR.

Material and energy balances result in five states that appear in four differential equations and one algebraic equation as described by Equation (69). The physical properties of the reaction mixture such as density, heat capacity, heat transfer coefficient are assumed constant.

$$\frac{dC_i}{dt} = \frac{\left(Q_i C_{if} - \left(Q_i + Q_m + Q_s\right) C_i\right)}{\mathrm{V}} - k_{d0} C_i$$

$$\frac{dC_m}{dt} = \frac{\left(Q_m C_{mf} - \left(Q_i + Q_m + Q_s\right) C_m\right)}{\mathrm{V}} - k_{p0} C_m C_{gp}$$

$$\frac{dT}{dt} = \frac{\left(Q_i + Q_m + Q_s\right)\left(T_f - T\right)}{\mathrm{V}} + \frac{\left(-\Delta H_r\right)}{\rho C_p} k_{p0} C_m C_{gp} - \frac{UA}{\rho C_p \mathrm{V}}\left(T - T_c\right) \qquad (69)$$

$$\frac{dT_c}{dt} = \frac{Q_c\left(T_{cf} - T_c\right)}{\mathrm{V}_c} + \frac{UA}{\rho_c C_{pc} \mathrm{V}_c}\left(T - T_c\right)$$

$$C_{gp} = \sqrt{\frac{2 f k_{d0} C_i}{k_{t0}}}$$

where C_i, C_m, T, T_c, C_{gp} and Q_c are the initiator concentration, monomer concentration, reactor temperature, cooling jacket temperature, growing polymer concentration, and cooling jacket flowrate, respectively. The method of moments is used to characterize the polymer property distribution, which two polymer chain moment equations are defined by

$$\frac{d\lambda_0}{dt} = 0.5k_{tc}C_{gp}^2 - \frac{Q_t}{\mathrm{V}}\lambda_0$$
$$\frac{d\lambda_1}{dt} = k_{p0}C_m C_{gp} - \frac{Q_t}{\mathrm{V}}\lambda_1 \tag{70}$$

where λ_0 is the total molar concentration of dead polymer and λ_1 is the total molar concentration of monomer units.

From Equation (69)-(70), the model for polystyrene polymerization reactor can be written in the following dimensionless form

$$\frac{dx_1}{dt} = q_i x_{1f} - \left(q_i + q_m + q_s\right)x_1 - \phi_d \kappa_d\left(x_3\right)x_1$$
$$\frac{dx_2}{dt} = q_m x_{2f} - \left(q_i + q_m + q_s\right)x_2 - \phi_p \kappa_p\left(x_3\right)x_2 x_5$$
$$\frac{dx_3}{dt} = \left(q_i + q_m + q_s\right)\left(x_{3f} - x_3\right) + \beta\phi_p \kappa_p\left(x_3\right)x_2 x_5 - \delta\left(x_3 - x_4\right)$$
$$\frac{dx_4}{dt} = \delta_1\left(q_c\left(x_{4f} - x_4\right) + \delta\delta_2\left(x_3 - x_4\right)\right)$$
$$x_5 = \sqrt{\frac{2f\phi_d \kappa_d\left(x_3\right)}{\phi_t \kappa_t\left(x_3\right)}}x_1$$
$$\frac{dx_6}{dt} = 0.5\phi_t \kappa_t\left(x_3\right)x_5^2 - x_6$$
$$\frac{dx_7}{dt} = \phi_p \kappa_p\left(x_3\right)x_2 x_5 - x_7$$
$$y = x_3 \tag{71}$$

where x_1, x_2, x_3, x_4, x_5, x_6, x_7 and q_c are the dimensionless initiator concentration, monomer concentration, reactor temperature, cooling jacket temperature, growing polymer concentration, concentration of dead polymer, concentration of monomer units and cooling jacket flowrate, respectively.

The objective of this control problem is a control of reactor temperature (x_3) by manipulating the dimensionless cooling jacket flowrate q_c with and without uncertainty. The cooling jacket flowrate is adjusted to obtain the desired temperature profile until t = 30 minutes. Let $u=q_c$, and $y=x_3$. A styrene polymerization reactor operated at the initial condition $\left[x_1(0), x_2(0), x_3(0), x_4(0), x_6(0), x_7(0)\right]=\left[3.7\times10^{-3}, 0.175, 1.2, 1, 2.4\times10^{-4}, 0.225\right]$ in stable non-minimum phase region for all steady states. The controller implemented every sampling time of 5 seconds. The optimal tuning parameter under I/O linearization is investigated in the following section that is described by the best response of the controlled output. The relation between the dimensionless parameters and variables and the physical variables for the four-state polymerization reactor model are shown in Table 3. The nominal parameter values are shown in Table 4.

Table 3 The dimensionless parameters and variables for the four-state polymerization reactor model

Dimensionless parameters and variables		
$x_1 = \frac{C_i}{C_{mf0}}$	$x_{1f} = \frac{C_{if}}{C_{mf0}}$	$\phi_d = \frac{\mathrm{V}}{Q_{d0}} k_{p0} \exp\left(-\gamma_d \gamma_p\right)$
$x_2 = \frac{C_m}{C_{mf0}}$	$x_{2f} = \frac{C_{mf}}{C_{mf0}}$	$\phi_t = \frac{VC_{mf0}}{Q_{t0}} k_{t0} \exp\left(-\gamma_t \gamma_p\right)$
$x_3 = \frac{T - T_{f0}}{T_{f0}} \gamma_p$	$x_{3f} = \frac{T_f - T_{f0}}{T_{f0}} \gamma_p$	$\phi_p = \frac{VC_{mf0}}{Q_{t0}} k_{p0} \exp\left(-\gamma_p\right)$
$x_4 = \frac{T_c - T_{f0}}{T_{f0}}$	$x_{4f} = \frac{T_{cf} - T_{f0}}{T_{f0}} \gamma_p$	$\tau = \frac{Q_{t0}}{V} t$

Table 3 (Continued)

Dimensionless parameters and variables		
$x_5 = \frac{C_{gp}}{C_{mf0}}$	$\gamma_d = \frac{E_d}{E_p}$	$\kappa_d(x_3) = \exp\left(\frac{\gamma_d x_3}{1+\frac{x_3}{\gamma_p}}\right)$
$x_6 = \frac{\lambda_0}{C_{mf0}}$	$\gamma_t = \frac{E_t}{E_p}$	
$x_7 = \frac{\lambda_1}{C_{mf0}}$	$\gamma_p = \frac{E_p}{RT_{f0}}$	$\kappa_t(x_3) = \exp\left(\frac{\gamma_t x_3}{1+\frac{x_3}{\gamma_p}}\right)$
$q_i = \frac{Q_i}{Q_{t0}}$	$\delta_1 = \frac{\mathrm{V}}{\mathrm{V}_c}$	
$q_m = \frac{Q_m}{Q_{t0}}$	$\delta_2 = \frac{\rho C_p}{\rho C_{pc}}$	$\kappa_p(x_3) = \exp\left(\frac{x_3}{1+\frac{x_3}{\gamma_p}}\right)$
$q_s = \frac{Q_s}{Q_{t0}}$	$\delta = \frac{UA}{\rho C_p Q_{t0}}$	$\beta = \frac{(-\Delta H_r) C_{mf0}}{\rho C_p T_{f0}} \gamma_p$
$q_c = \frac{Q_c}{Q_{t0}}$		

Table 4 The parameter values of the styrene polymerization reactor

Parameter	Value	Parameter	Value
f	0.6	Q_i	0.03 l s^{-1}
k_{d0}	5.95×10^{13} s^{-1}	Q_s	0.1275 l s^{-1}
E_d	123,853.658 J mol^{-1}	Q_m	0.105 l s^{-1}
k_{t0}	1.25×10^{9} J mol^{-1} s^{-1}	Q_c	0.131 l s^{-1}
E_t	7008.702 J mol^{-1}	V	3000 l
k_{p0}	1.06×10^{7} l mol^{-1} s^{-1}	V_c	3312.4 l
E_p	29572.898 J mol^{-1}	C_{if}	0.5888 mol l^{-1}
$-\Delta H_r$	69,919.56 J mol^{-1}	C_{mf}	8.6981 mol l^{-1}

Table 4 (Continued)

Parameter	Value	Parameter	Value
UA	293.076 J s^{-1} K^{-1}	T_f	330 K
ρC_p	1507.248 J l^{-1} K^{-1}	T_{cf}	295 K
$\rho_c C_{pc}$	4045.7048 J l^{-1} K^{-1}		

In the multiplicity analysis, the styrene polymerization reactor has three steady states under the parameter values (Table 5) that is described in Figure 24.

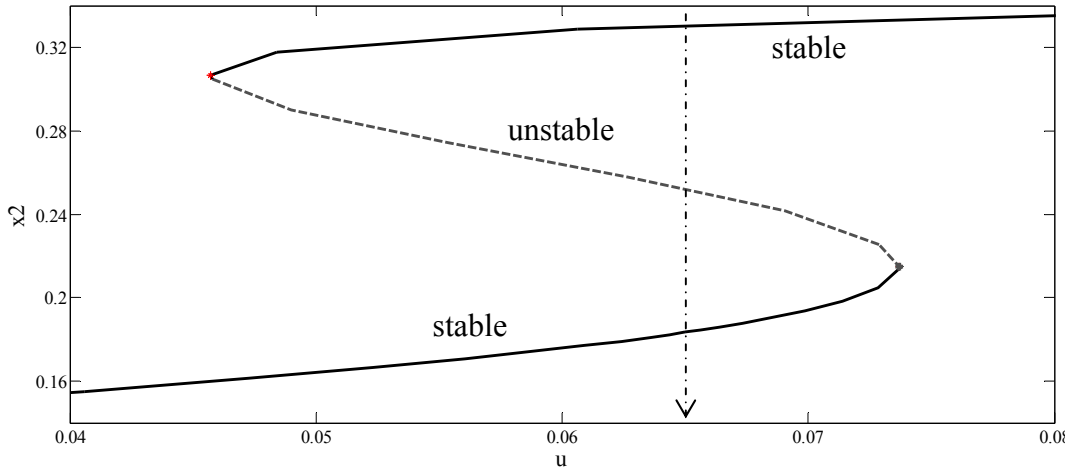

Figure 24 Bifurcation diagram of the styrene polymerization reactor.

The steady state of manipulated input is evaluated at u_{ss} = 0.065. The opened-loop dynamic behaviors are considered with eigenvalues of Jacobian matrix of both process and zero dynamics, which are shown in Table 5. The zero dynamics are analyzed to investigate the stability of internal dynamic that are given in Appendix B.

Table 5 Values of steady state pair and the opened-loop dynamic behavior analysis of styrene polymerization reactor.

Steady state pair $[x_{1ss}, x_{2ss}, x_{3ss}, x_{4ss}, x_{6ss}, x_{7ss}]$	Eigenvalues of Jacobian matrix		Opened-loop dynamic behavior
	Process	Zero dynamics	
$[7.347\times 10^{-3}$, 0.331, 0.367, 0.302, 2.336×10^{-4}, 0.069]	-1.036+0.432i, -1.036-0.432i, -1.044, -1, -1, -0.068	-1.113+0.143i, -1.113-0.143i, -1, -1, 0	Stable, non-minimum phase
[0.006, 0.251, 0.790, 0.650, 9.540×10^{-4}, 0.149]	-1.166, -0.746+0.744i, -0.746-0.744i, -1, -1, 0.063	-1.097+0.678i, -1.097-0.678i, -1, -1, 0	Unstable, non-minimum phase
[0.004, 0.183, 1.150, 0.948, 0.002, 0.217]	-0.829+1.500i, -0.829-1.500i, -1.475,-1,-1,-0.087	1.764, -1, -1, -0.243, 0	Stable, non-minimum phase

When the polymerization reactor is operated at lower steady state, we will obtain low monomer conversion. In addition, at upper steady state, we will obtain high monomer conversion but the gel effect may occur in the reactor. If the controller cannot effectively maintain the output at upper steady state, the effects are thermal runaway, low quality products, instabilities and even explosions in industrial applications. Moreover, all of steady states also exhibit non-minimum phase behavior, which may cause inverse response leading to difficult task.

1.2.2.1 Controller system

The continuous-time polymerization reactor model in (71) is approximated into the discrete-time model with Euler's method. The resulting discrete-time model is

$$
\begin{aligned}
x_1(k+1) &= x_1(k) + \Delta t\left(q_i x_{1f} - (q_i + q_m + q_s)x_1(k) - \phi_d \kappa_d\left[x_3(k)\right]x_1(k)\right)\\
x_2(k+1) &= x_2(k) + \Delta t\left[q_m x_{2f} - (q_i + q_m + q_s)x_2(k) - \phi_p \kappa_p\left[x_3(k)\right]x_2(k)x_5(k)\right]\\
x_3(k+1) &= x_3(k) + \Delta t\left[(q_i + q_m + q_s)\left(x_{3f} - x_3(k)\right) + \beta\phi_p\kappa_p\left[x_3(k)\right]x_2(k)x_5(k)\right.\\
&\quad \left. -\delta\left(x_3(k) - x_4(k)\right)\right]\\
x_4(k+1) &= x_4(k) + \Delta t\left[\delta_1\left(u(k)\left(x_{4f} - x_4(k)\right) + \delta\delta_2\left(x_3(k) - x_4(k)\right)\right)\right]\\
x_5(k) &= \sqrt{\frac{2f\phi_d\kappa_d\left[x_3(k)\right]}{\phi_t\kappa_t\left[x_3(k)\right]}}x_1(k)\\
x_6(k+1) &= x_6(k) + \Delta t\left[0.5\phi_t\kappa_t\left[x_3(k)\right]x_5^2(k) - x_6(k)\right]\\
x_7(k+1) &= x_7(k) + \Delta t\left[\phi_p\kappa_p\left[x_3(k)\right]x_2(k)x_5(k) - x_7(k)\right]\\
y(k) &= x_3(k)
\end{aligned}
\tag{72}
$$

The relative order of the process output with respect to the vector of manipulated input is $r = 2$. The application of the controller system of (63) takes the form:

$$
\begin{aligned}
\chi_1(k+1) &= \chi_1(k) + \Delta t\left(q_i x_{1f} - (q_i + q_m + q_s)\chi_1(k) - \phi_d\kappa_d\left[\chi_3(k)\right]\chi_1(k)\right)\\
&\quad + \check{D}_1\left(\chi(k), \nu(k)\right)\\
\chi_2(k+1) &= \chi_2(k) + \Delta t\left[q_m x_{2f} - (q_i + q_m + q_s)\chi_2(k) - \phi_p\kappa_p\left[\chi_3(k)\right]\chi_2(k)\chi_5(k)\right]\\
&\quad + \check{D}_2\left(\chi(k), \nu(k)\right)\\
\chi_3(k+1) &= \chi_3(k) + \Delta t\left[(q_i + q_m + q_s)\left(x_{3f} - \chi_3(k)\right) + \beta\phi_p\kappa_p\left[\chi_3(k)\right]\chi_2(k)\chi_5(k)\right.\\
&\quad \left. -\delta\left(\chi_3(k) - \chi_4(k)\right)\right] + \check{D}_3\left(\chi(k), \nu(k)\right)\\
\chi_4(k+1) &= \chi_4(k) + \Delta t\left[\delta_1\left(\psi\left(\hat{x}(k), \nu(k)\right)\left(x_{4f} - \chi_4(k)\right) + \delta\delta_2\left(\chi_3(k) - \chi_4(k)\right)\right)\right]\\
&\quad + \check{D}_4\left(\chi(k), \nu(k)\right)\\
\chi_5(k) &= \sqrt{\frac{2f\phi_d\kappa_d\left[\chi_3(k)\right]}{\phi_t\kappa_t\left[\chi_3(k)\right]}}\chi_1(k)\\
\chi_6(k+1) &= \chi_6(k) + \Delta t\left[0.5\phi_t\kappa_t\left[\chi_3(k)\right]\chi_5^2(k) - \chi_6(k)\right] + \check{D}_6\left(\chi(k), \nu(k)\right)\\
\chi_7(k+1) &= \chi_7(k) + \Delta t\left[\phi_p\kappa_p\left[\chi_3(k)\right]\chi_2(k)\chi_5(k) - \chi_7(k)\right] + \check{D}_7\left(\chi(k), \nu(k)\right)
\end{aligned}
$$

$$u(k)=\psi\left(\hat{x}(k),\nu(k)\right)=\min_{u(k)}\left(\frac{\varepsilon^2\left(x_2(k+2)\right)+2\varepsilon x_2(k+1)+\hat{x}_2(k)-\theta(k)}{\varepsilon}\right)^2$$

$$D(k)=\check{D}\left(\hat{x}(k),\nu(k)\right)=\min_{D(k)}\left(\frac{\varepsilon^2\left(x_2(k+2)\right)+2\varepsilon x_2(k+1)+\hat{x}_2(k)-\theta(k)}{\varepsilon}\right)^2 \quad (73)$$

subject to

$$0<u(k)<0.15$$

$$S(\hat{x}(k),\nu(k),u(k),D(k))\le 0$$

where

$$S(\hat{x}(k),\nu(k),u(k),D(k))=\beta\left(\frac{V[x(k+1)]+V[\hat{x}(k)]}{\Delta t}\right)-\begin{bmatrix}x_1(k+1)\\ \vdots \\ x_7(k+1)\end{bmatrix}\times\begin{bmatrix}x_1(k+1) & \cdots & x_7(k+1)\end{bmatrix}$$

$$V[\hat{x}(k)]=\begin{bmatrix}\hat{x}_1(k)-\nu_1(k)\\ \vdots \\ \hat{x}_7(k)-\nu_7(k)\end{bmatrix}\begin{bmatrix}a_{11} & a_{12} & a_{13} & a_{14}\\ a_{21} & a_{22} & a_{23} & a_{24}\\ a_{31} & a_{32} & a_{33} & a_{34}\\ a_{41} & a_{42} & a_{43} & a_{44}\end{bmatrix}\begin{bmatrix}\hat{x}_1(k)-\nu_1(k) & \cdots & \hat{x}_7(k)-\nu_7(k)\end{bmatrix}$$

$$\theta(k)=y_{sp}-x_3(k)+\chi_3(k)$$

1.2.2.2 Selection of tuning parameter of styrene polymerization reactor

To achieve the optimal response, the tuning parameters were determined by analyzing the stabilized domain of closed-loop system and bifurcation diagram. The details of controller tuning with bifurcation diagram will be referred to again in section 2. To test the effectiveness of the proposed controller, the reactor temperature in polymerization reactor is controlled with multiple steady states.

The process is initially at $y_{sp} = 0.367$ with stable, non-minimum phase behavior, and then it is adjusted to $y_{sp} = 0.79$ with unstable, non-minimum phase behavior and $y_{sp} = 1.15$ with stable, non-minimum phase behavior, respectively. The tuning parameter ε under I/O linearization technique is used to adjust the speed of the response of the closed-loop output. The tuning parameter β under Lyapunov stability constraint is used to set the rate of decay of Lyapunov function. The positive definite matrix P under Lyapunov stability constraint is chosen to satisfy the Riccati equation in Equation (52). The tuning results show that the optimal parameter values for the proposed control system in Equation (73) are $\varepsilon = 6,\ \beta = 50$ and

$$P = \begin{bmatrix} 2915.400 & 132.170 & 143.220 & 96.610 & 5.469\times10^{-3} & 5.480\times10^{-3} \\ 132.170 & 6.597 & 6.47040 & 4.417 & 7.243\times10^{-4} & 7.245\times10^{-4} \\ 143.220 & 6.470 & 10.934 & 5.512 & 5.478\times10^{-4} & 5.481\times10^{-4} \\ 96.619 & 4.417 & 5.512 & 14.745 & 5.762\times10^{-4} & 5.762\times10^{-4} \\ 5.469\times10^{-3} & 7.243\times10^{-4} & 5.478\times10^{-4} & 5.762\times10^{-4} & 4.876\times10^{-7} & 5.000\times10^{-4} \\ 5.480\times10^{-3} & 7.245\times10^{-4} & 5.481\times10^{-4} & 5.763\times10^{-4} & 5.000\times10^{-4} & 5.000\times10^{-4} \end{bmatrix}$$

At $\varepsilon = 2$ under I/O linearization, the output response is smooth and no oscillation in stable non-minimum phase region. However, the controller cannot maintain the output at middle steady state with unstable non-minimum phase. Then, the tuning parameter is adjusted to $\varepsilon = 10$, which the controller can maintain the output at three steady states. However, the output response has still oscillation. Thus, the optimal tuning parameter under I/O linearization is $\varepsilon = 6$ that is the fast response and no oscillation. For the tuning parameters under Lyapunov stability constraint, the output response under the proposed tuning parameters (β and P) is the fastest and no oscillation, which approaches to the three steady states.

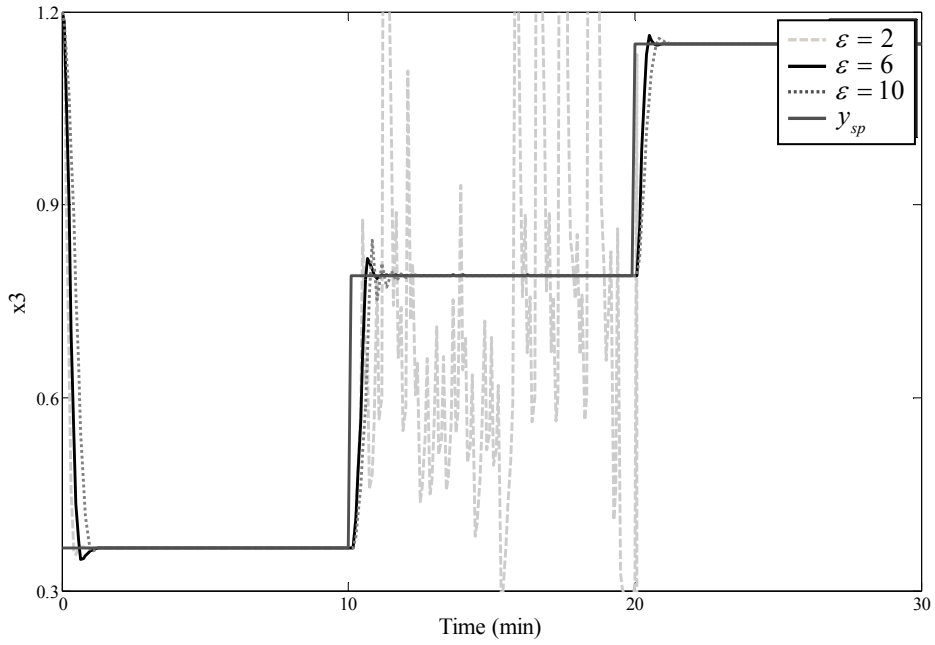

Figure 25 Closed-loop responses of controlled output by varying the tuning parameter, ε, under I/O linearization

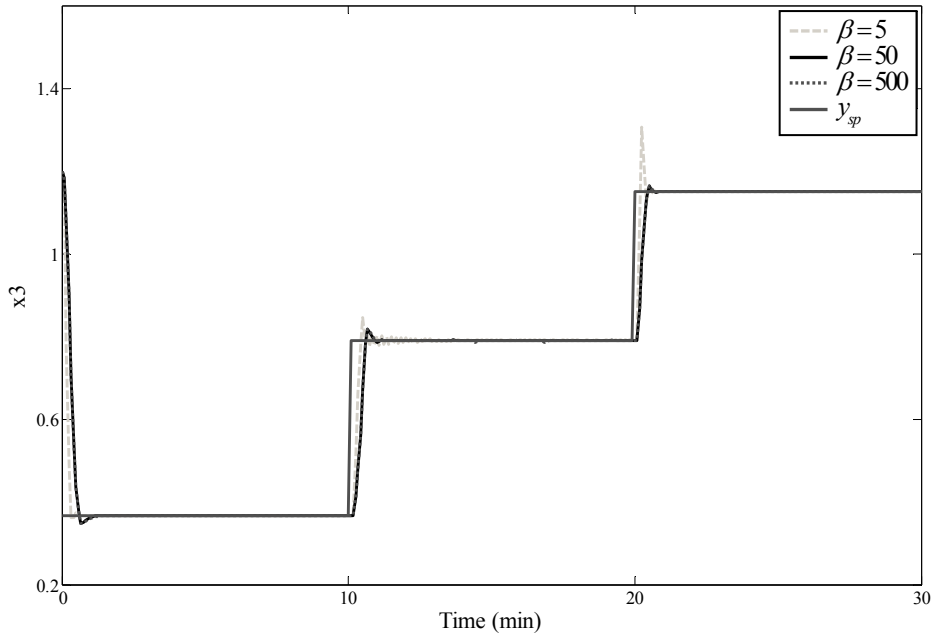

Figure 26 Closed-loop responses of controlled output by varying the tuning parameter, β, under Lyapunov stability constraint

1.2.2.3 Simulation results of styrene polymerization reactor without uncertainty

To apply the example with more complex reaction, the proposed control technique is applied through the styrene polymerization reactor without uncertainty in order to control the reactor temperature at the desired setpoints. The performance of the controller is investigated in terms of performing a smooth and fast startup of the process, ability in the process operation with initial condition in non-minimum phase region, the stability of closed-loop system, and tracking step changes in the setpoints. The controller successfully operates the styrene polymerization reactor, although the closed-loop response of the reactor temperature at unstable, non-minimum phase occur the oscillation. This problem causes the active constraint to achieve the desired output. Moreover, it can effectively control when the process is operated with initial conditions in non-minimum phase region. The closed-loop responses of the dimensionless of initiator concentration, monomer concentration, reactor temperature, cooling jacket temperature, dead polymer concentration and concentration of monomer units without uncertainty are shown in Figure 27-28. The reactor temperature response is a smooth and fast startup. It can effectively move from one set point to another. The controller adjusts the maximum cooling jacket flowrate in Figure 29(a) to bring the reactor temperature at the new setpoints value as soon as possible. The Lyapunov function profile in Figure 29(b) continuously decrease, which indicate that the closed-loop response is stable. Furthermore, it is also asymptotically stable when the time derivatives of Lyapunov function in Figure 29(c) converge to zero corresponding to stability analysis. The stability constraint is frequently active for all given desired setpoint whether unstable, non-minimum phase and stable non-minimum phase behavior as shown in Figure 30. Only I/O linearization technique cannot control the reactor temperature at non-minimum phase steady state because its domain of solution is not cover the dynamic behavior with non-minimum phase. Thus, Lyapunov stability constraint must continuously be active to maintain the controlled output at the desired steady state.

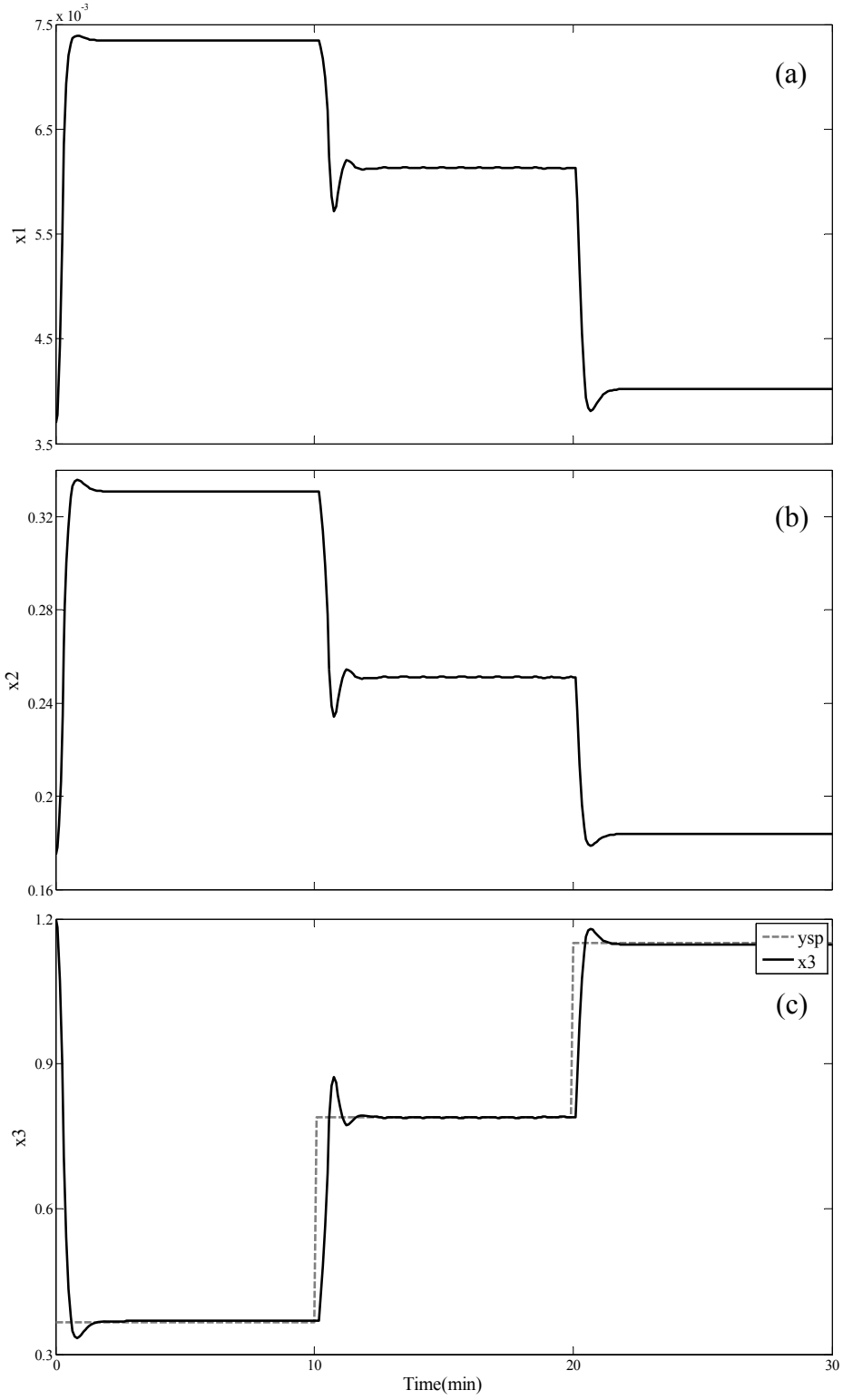

Figure 27 Closed-loop responses of the dimensionless of (a) initiator concentration, (b) monomer concentration and (c) reactor temperature of styrene polymerization reactor without uncertainty.

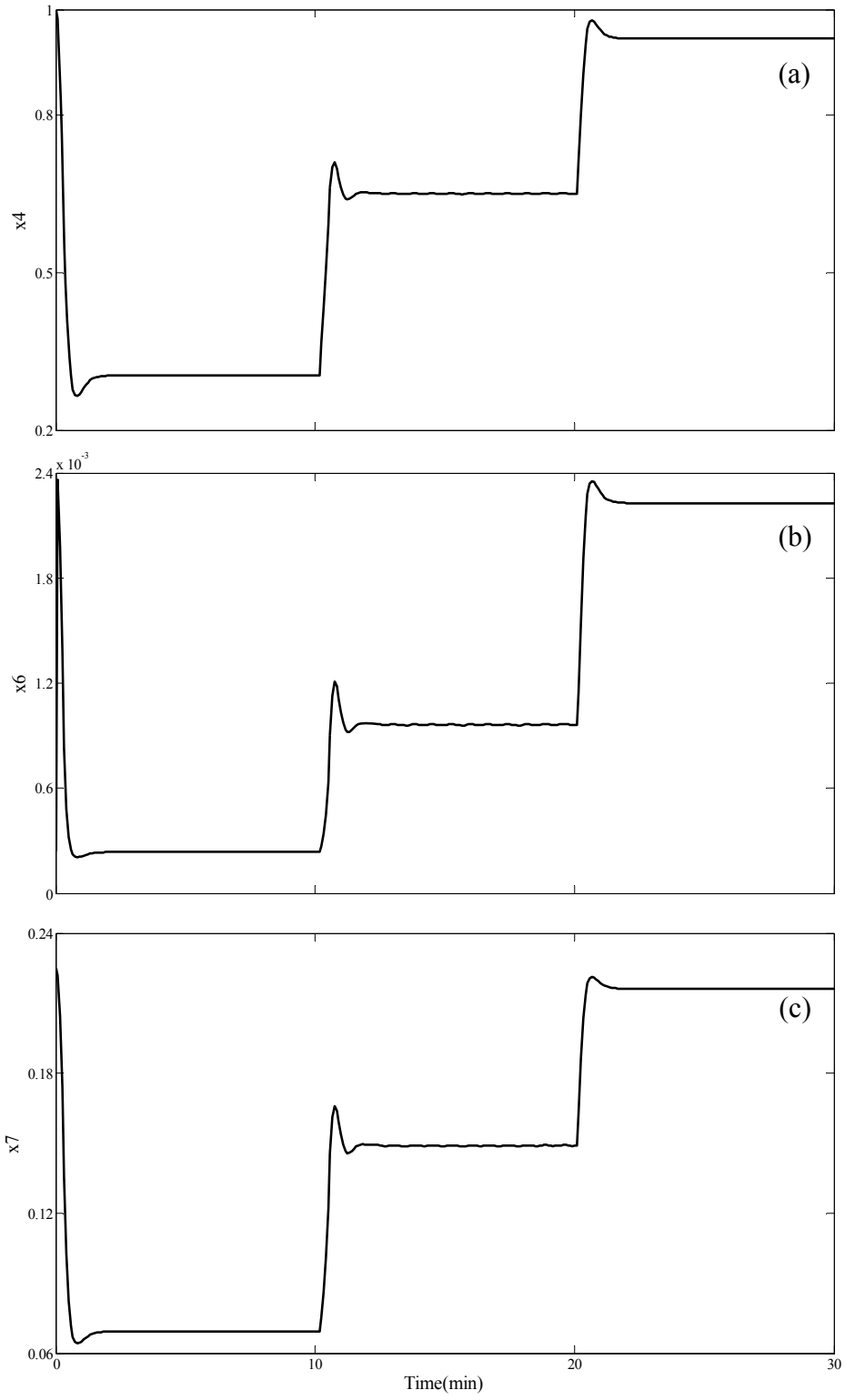

Figure 28 Closed-loop responses of the dimensionless of (a) cooling jacket temperature, (b) dead polymer concentration and (c) concentration of monomer units of styrene polymerization reactor without uncertainty.

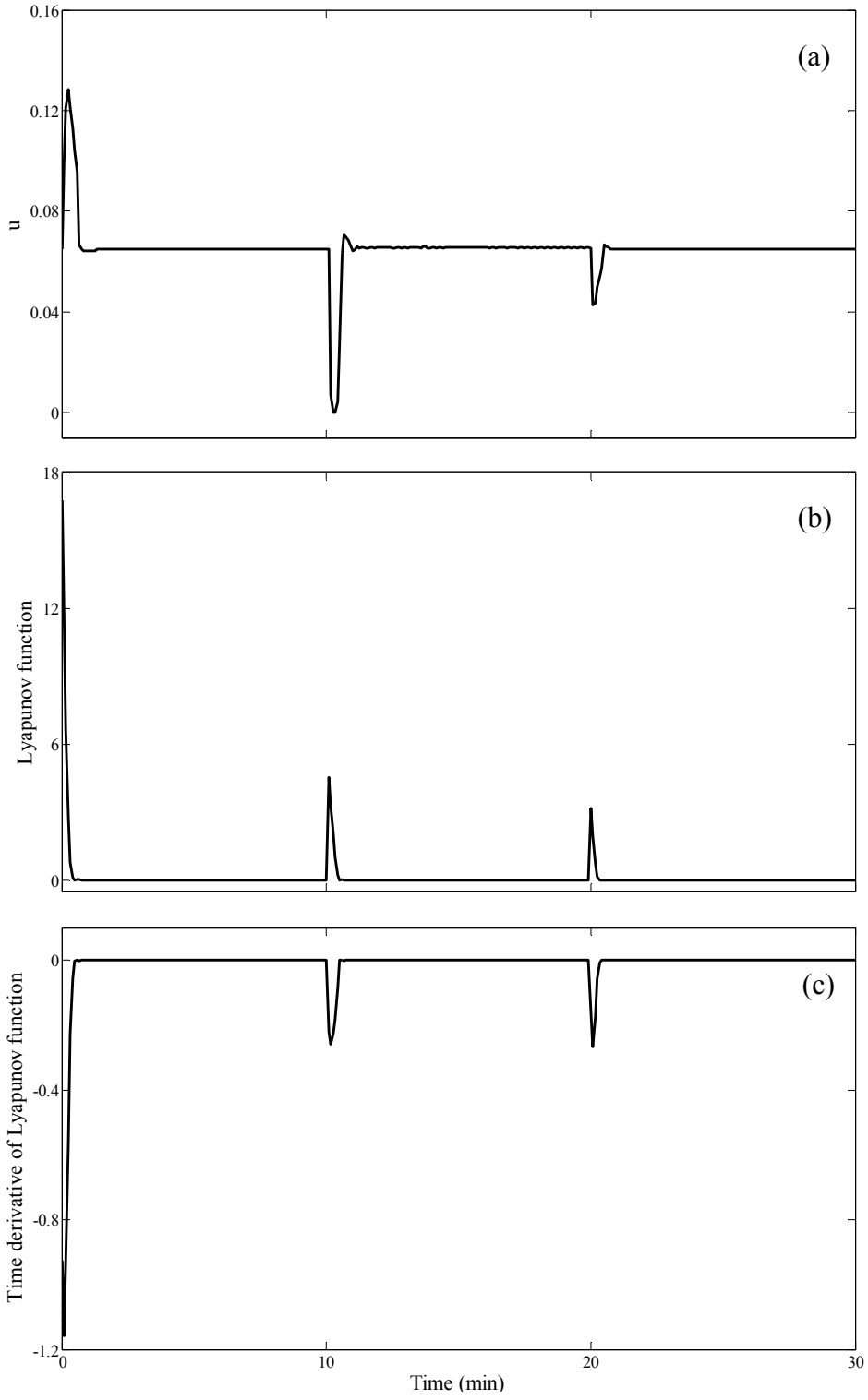

Figure 29 Closed-loop responses of (a) dilution rate, (b) Lyapunov function profile and (c) time derivative of Lyapunov function of styrene polymerization reactor without uncertainty.

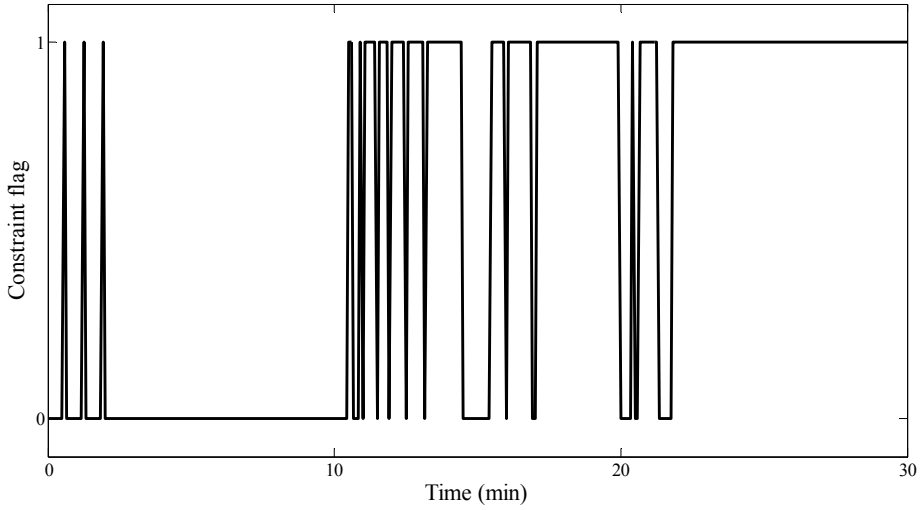

Figure 30 The constraint flag of styrene polymerization reactor without uncertainty.

1.2.2.4 Simulation results of styrene polymerization reactor with uncertainty

The proposed control technique is applied through styrene polymerization reactor with uncertainty to control the reactor temperature at the desired setpoints. The performance of the controller is investigated in terms of tracking step changes in the setpoints, the stability of closed-loop system and the robustness property of controller. The parametric uncertainty and unmeasured disturbances are considered, which are simulated with random noise of the heat transfer coefficient (U) and the dimensionless cooling jacket flowrate (q_c), respectively. The imperfect mixing may cause uncertainty in heat transfer coefficient. The concentrations of the various reacting species will be non-uniform, especially near the reactor wall. This uncertainty in the exact value of the heat transfer coefficient may lead to a loss in control performance. Moreover, the sensitivity of online measurements such as flow sensor generates the uncertainty in the cooling jacket flowrate, which significantly affect the substrate concentration.

Case 1: Uncertainty in the heat transfer coefficient (U)

To test the robustness of the proposed controller, the controller can maintain the reactor temperature at the maximum of $\pm$ 10% uncertainty in the heat transfer coefficient although it is operated with initial conditions in non-minimum phase region. The closed-loop responses of the dimensionless of initiator concentration, monomer concentration, reactor temperature, cooling jacket temperature, dead polymer concentration and concentration of monomer units in the presence of uncertainty in the heat transfer coefficient are shown in Figure 31-32. The controller can be forced the controlled output to the setpoint trajectory by manipulating the cooling jacket flowrate in Figure 33(a). Figure 33(b) shows the approximation of uncertainty in each state. The uncertainty has the significant effect on cooling jacket temperature because it depends on the manipulating of cooling jacket flowrate and the uncertainty in cooling jacket flowrate directly. The Lyapunov function profile in Figure 33(c) continuously decrease, which indicate that the closed-loop response is stable. However, it is not asymptotically stable because the time derivatives of Lyapunov function appear very small oscillation in Figure 34(a). Figure 34(b) shows the constraint flag of the closed-loop response. The Lyapunov stability constraint is continuously active especially, the last control range of stable, non-minimum phase steady state because it has two unstable zero dynamic.

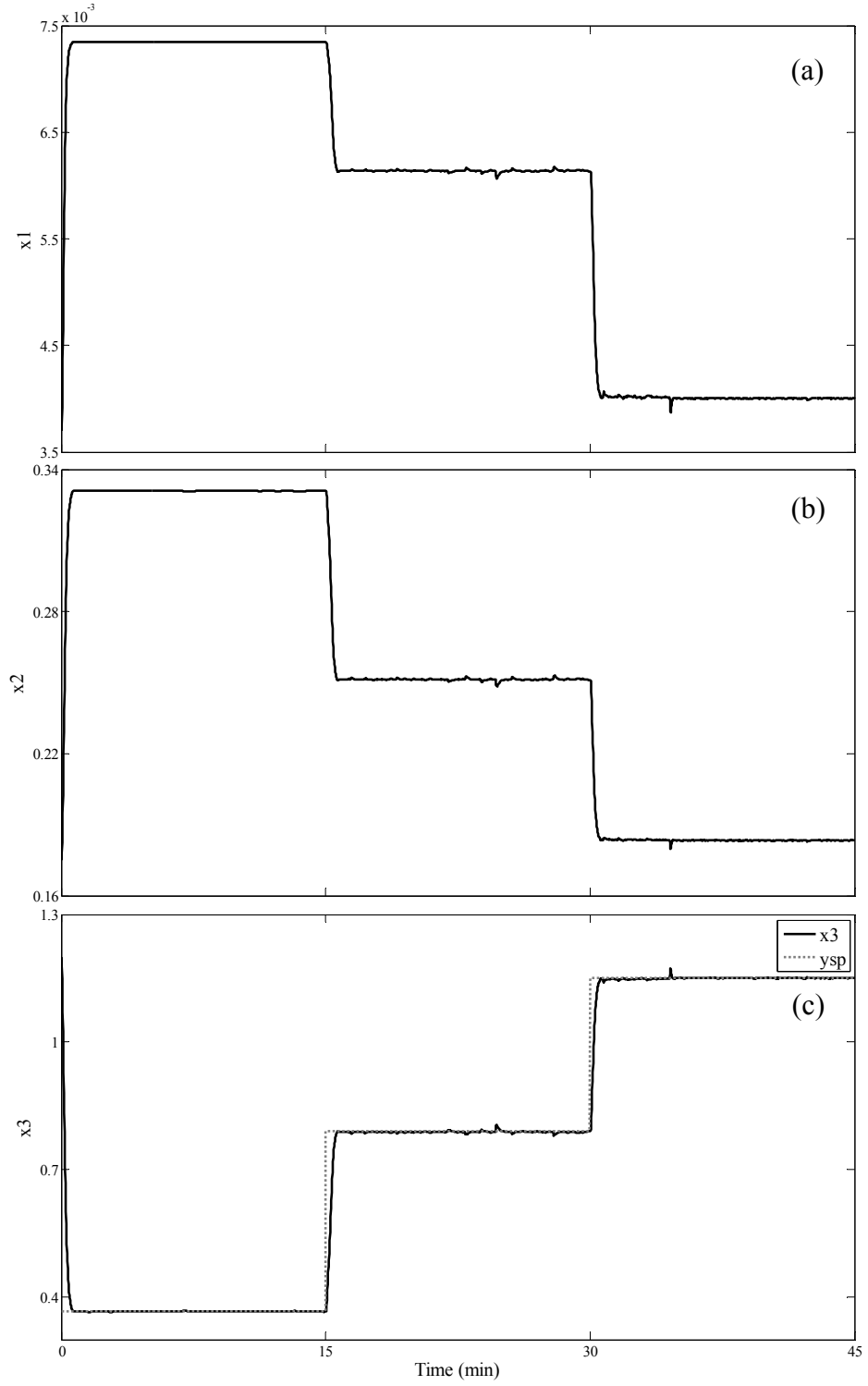

Figure 31 Closed-loop responses of the dimensionless of (a) initiator concentration, (b) monomer concentration and (c) reactor temperature for styrene polymerization reactor with ± 10% uncertainty of the heat transfer coefficient.

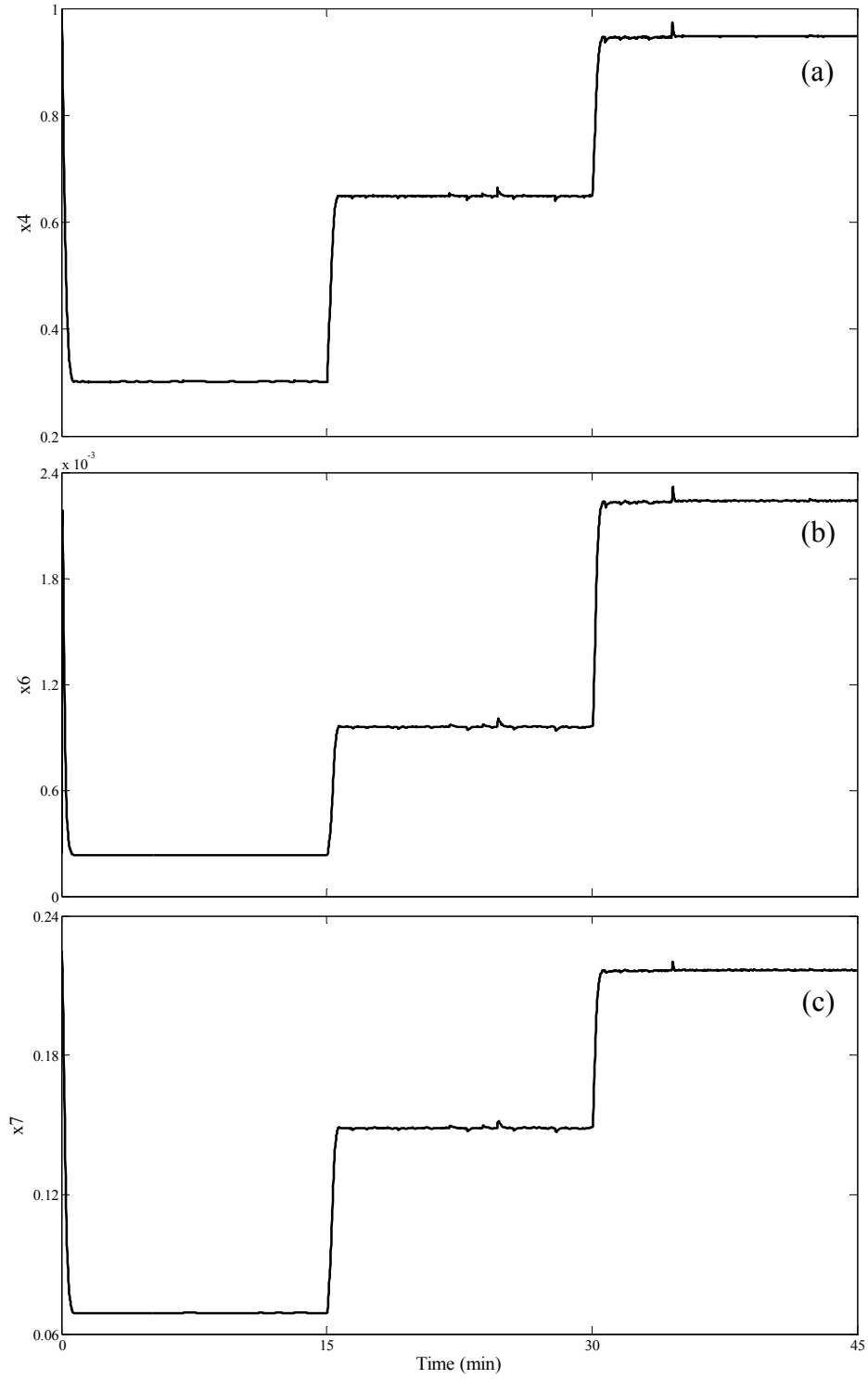

Figure 32 Closed-loop responses of the dimensionless of (a) cooling jacket temperature, (b) dead polymer concentration and (c) concentration of monomer units for styrene polymerization reactor with ± 10% uncertainty of the heat transfer coefficient.

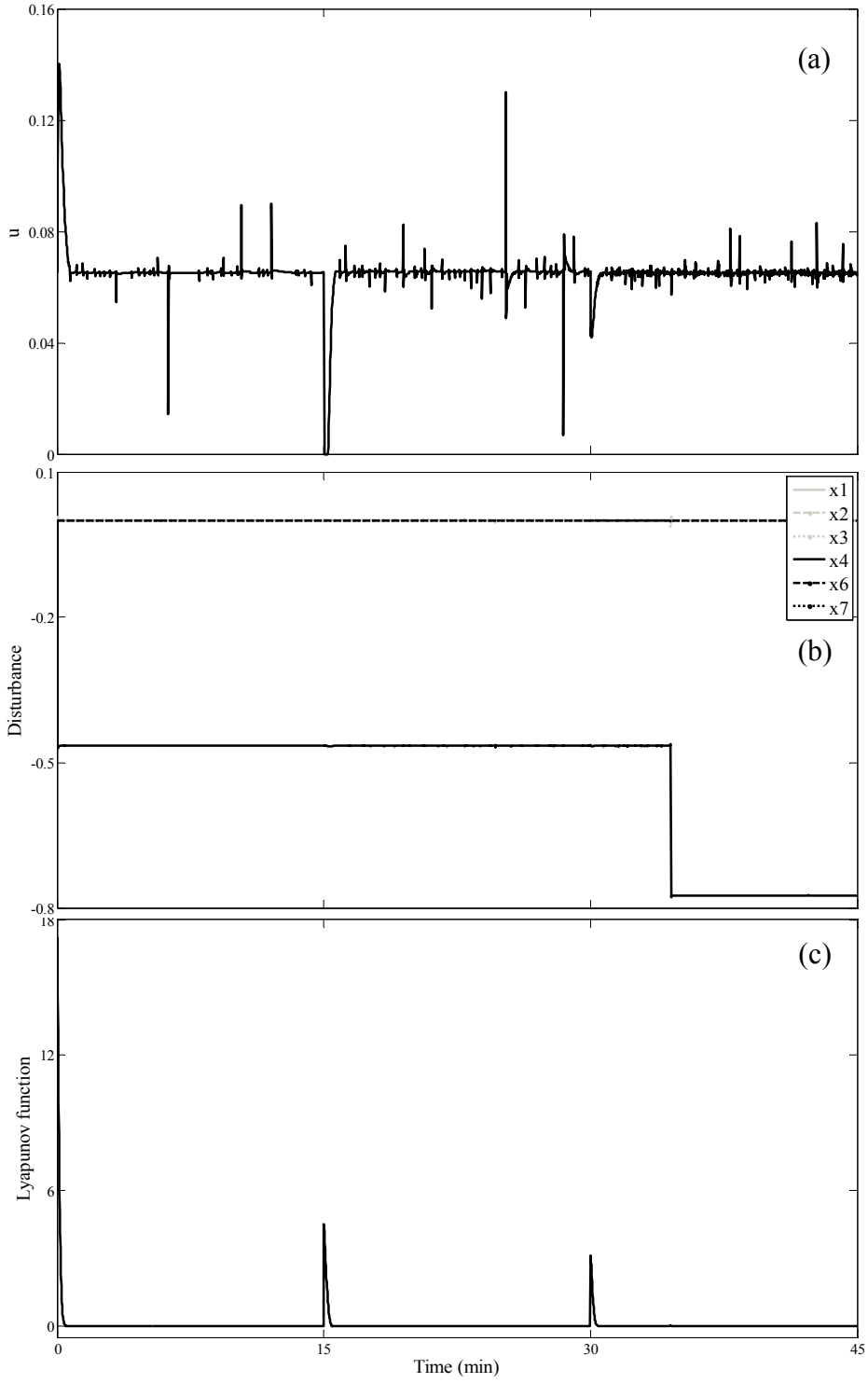

Figure 33 Closed-loop responses of the dimensionless (a) cooling jacket flowrate, (b) unmeasured disturbance and (c) Lyapunov function profile for styrene polymerization reactor with $\pm$ 10% uncertainty of the heat transfer coefficient.

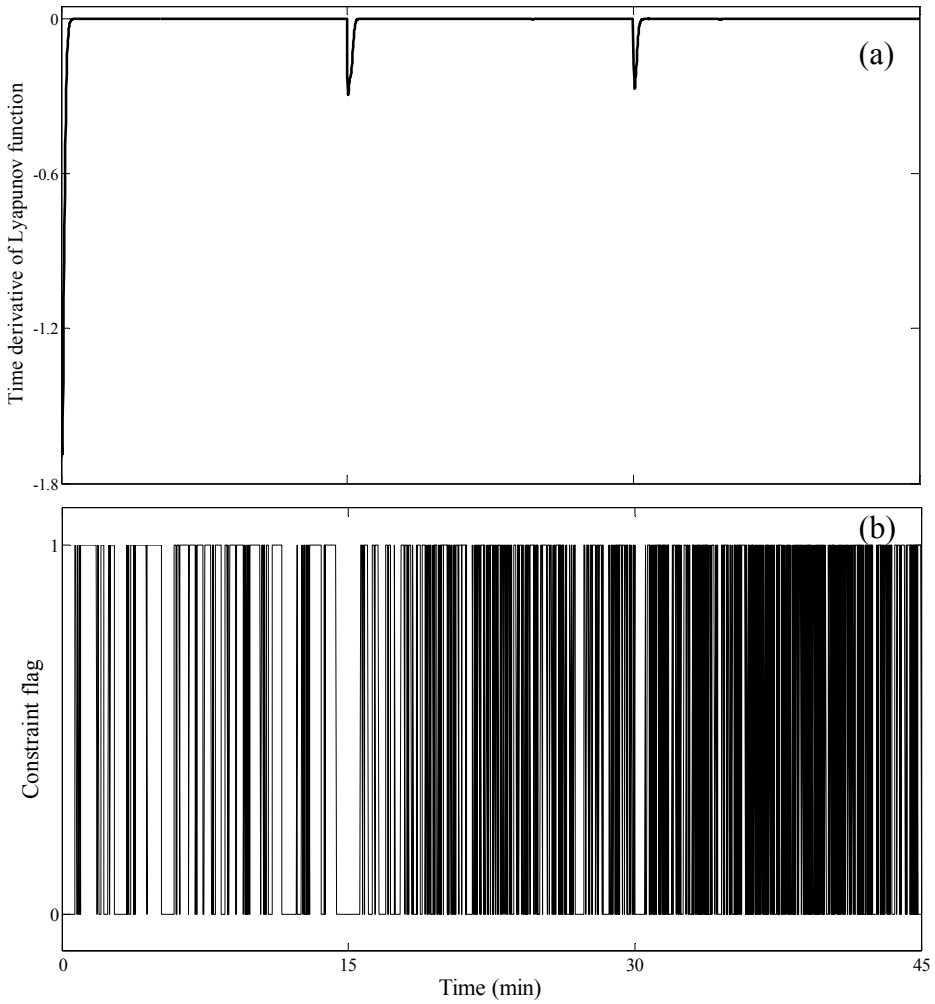

Figure 34 Closed-loop responses of (a) time derivative of Lyapunov function and (b) constraint flag for styrene polymerization reactor with ± 10% uncertainty of the heat transfer coefficient.

Case 2: Uncertainty in the dimensionless cooling jacket flowrate (q_c)

To test the robustness of the proposed controller, the controller can maintain the reactor temperature at the maximum of ± 10% uncertainty in the dimensionless cooling jacket flowrate although it is operated with initial conditions in non-minimum phase region. The closed-loop responses of the dimensionless of initiator concentration, monomer concentration, reactor temperature, cooling jacket temperature, dead polymer concentration and concentration of monomer units in the presence of uncertainty in the heat transfer coefficient are shown in Figure 35-36. The controller can be forced the controlled output to the setpoint trajectory by manipulating the cooling jacket flowrate in Figure 37(a). Figure 37(b) shows the approximation of uncertainty in each state. The uncertainty has the significant effect on cooling jacket temperature because it depends on the manipulating of cooling jacket flowrate and the uncertainty in cooling jacket flowrate directly. The Lyapunov function profile in Figure 37(c) continuously decrease, which indicate that the closed-loop response is stable. However, it is not asymptotically stable because the time derivatives of Lyapunov function appear very small of oscillation in Figure 38(a). Figure 38(b) shows the constraint flag of the closed-loop response. The Lyapunov stability constraint is continuously active especially, the last control range of stable, minimum phase steady state because it has two unstable zero dynamic.

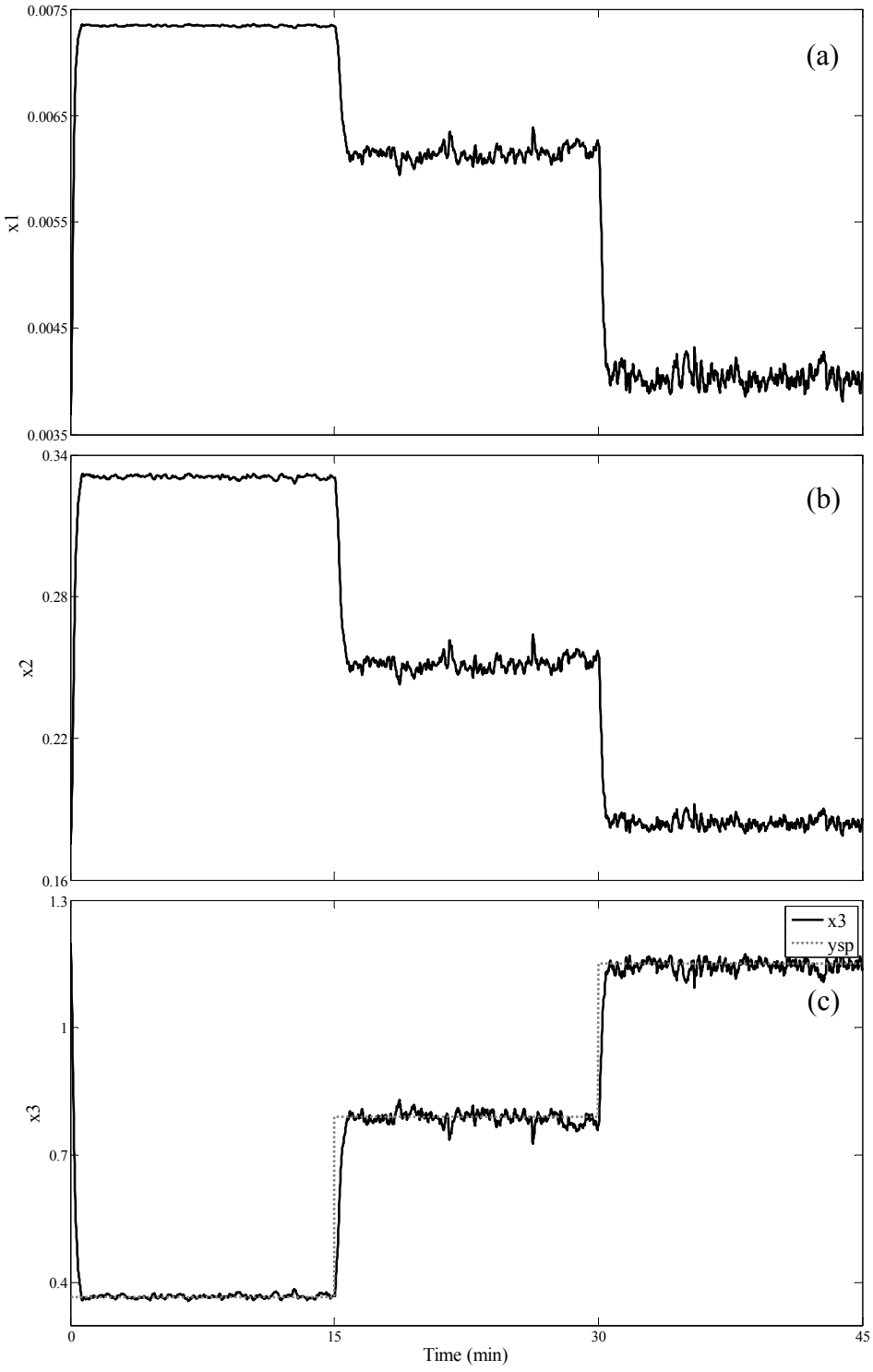

Figure 35 Closed-loop responses of the dimensionless of (a) initiator concentration, (b) monomer concentration and (c) reactor temperature for styrene polymerization reactor with $\pm$ 10% uncertainty of the dimensionless cooling jacket flowrate.

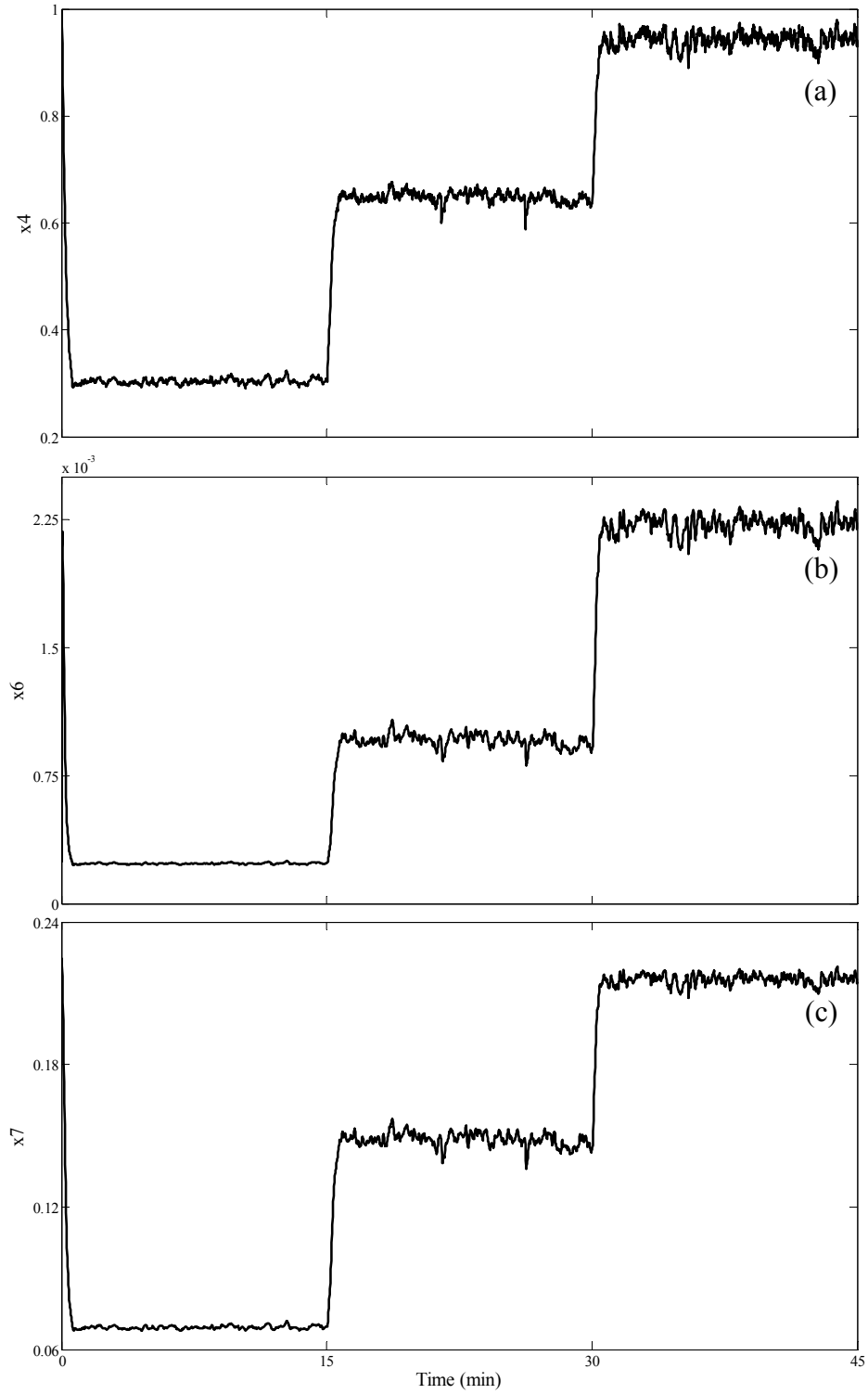

Figure 36 Closed-loop responses of the dimensionless of (a) cooling jacket temperature, (b) dead polymer concentration and (c) concentration of monomer units for styrene polymerization reactor with ± 10% uncertainty of the dimensionless cooling jacket flowrate.

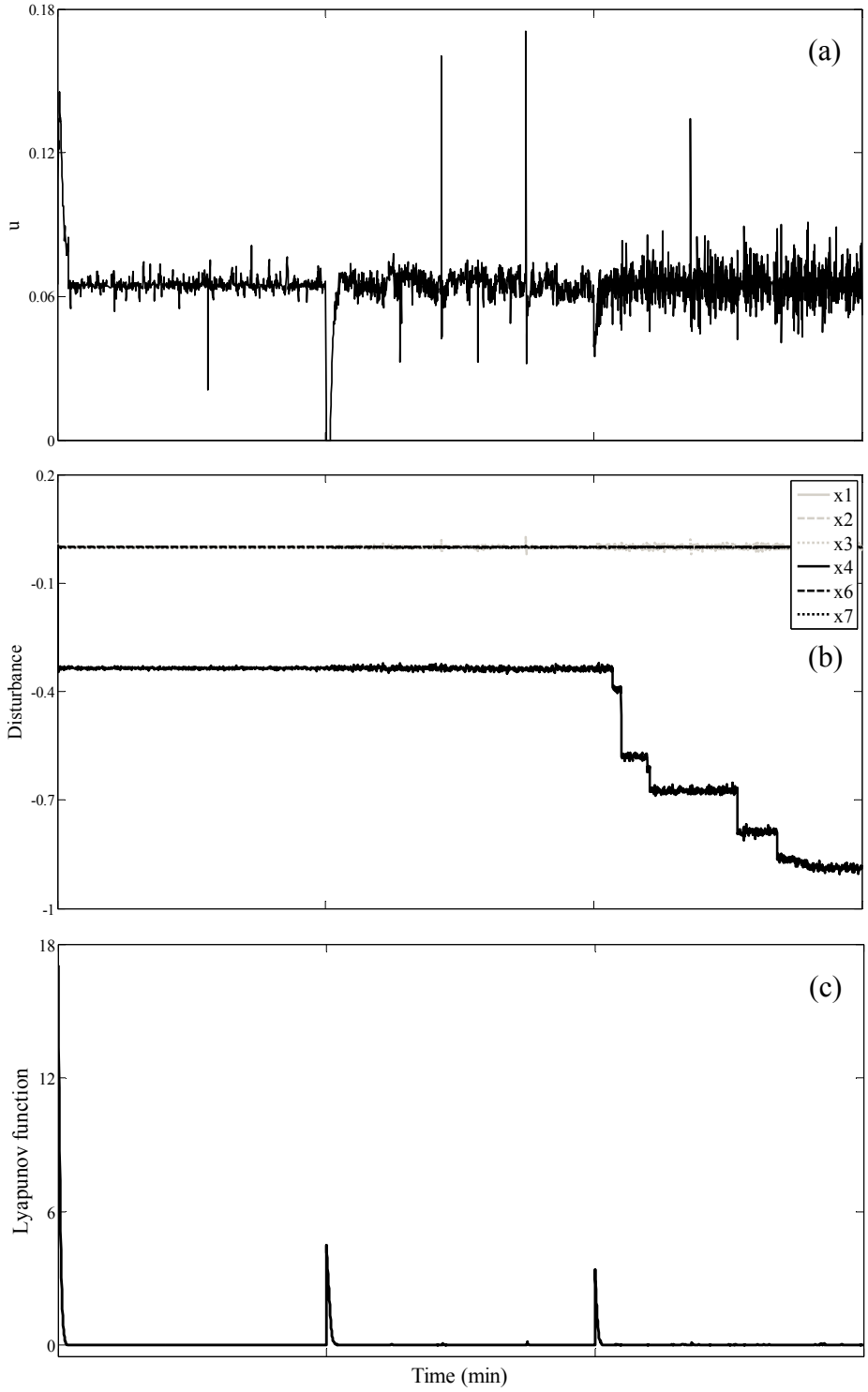

Figure 37 Closed-loop responses of the dimensionless of (a) cooling jacket flowrate, (b) unmeasured disturbance and (c) Lyapunov function profile for styrene polymerization reactor with $\pm$ 10% uncertainty of the dimensionless cooling jacket flowrate.

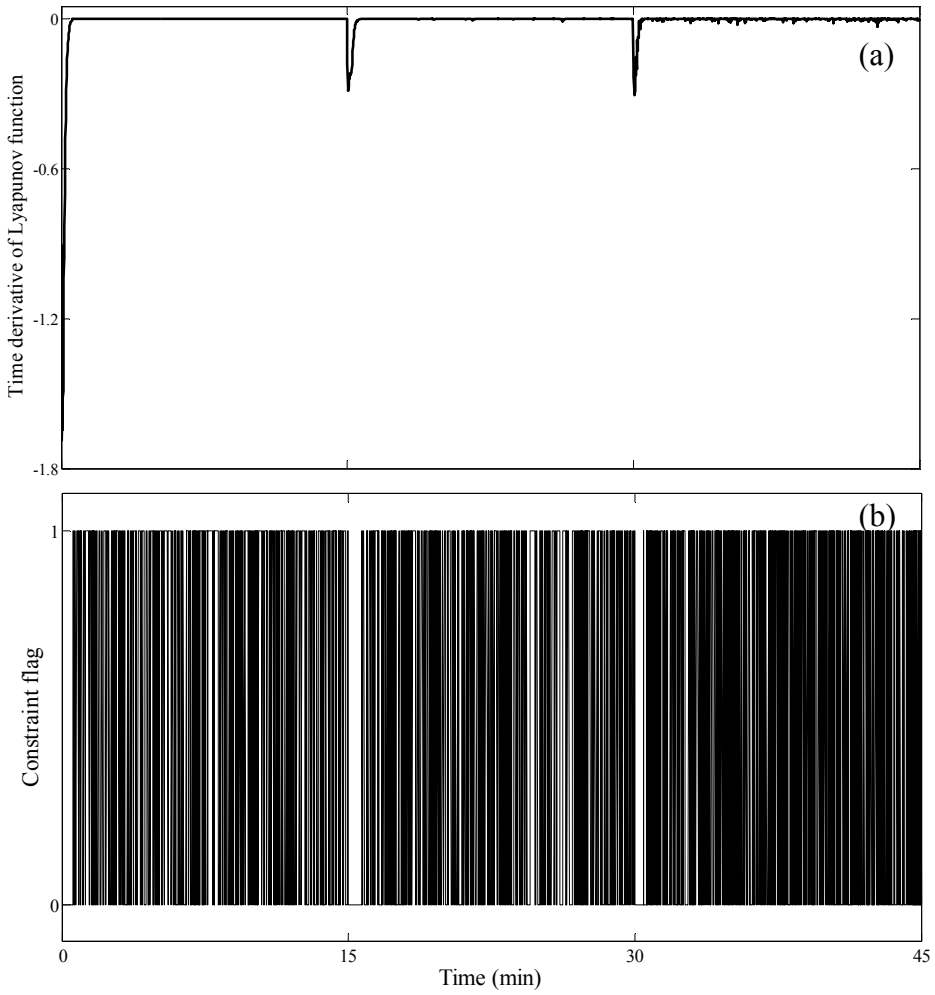

Figure 38 Closed-loop responses of (a) time derivative of Lyapunov function and (b) the constraint flag for styrene polymerization reactor with ± 10% uncertainty of the dimensionless cooling jacket flowrate.

1.2.3 Multi-input Multi-output styrene polymerization reactor

The same reactor of the previous example is considered, which the details of the process model are described in section 1.2.2. The model for polystyrene polymerization reactor can be written in the following dimensionless form

$$\frac{dx_1}{dt} = q_i x_{1f} - \left(q_i + q_m + q_s\right) x_1 - \phi_d \kappa_d \left(x_3\right) x_1$$

$$\frac{dx_2}{dt} = q_m x_{2f} - \left(q_i + q_m + q_s\right) x_2 - \phi_p \kappa_p \left(x_3\right) x_2 x_5$$

$$\frac{dx_3}{dt} = \left(q_i + q_m + q_s\right)\left(x_{3f} - x_3\right) + \beta \phi_p \kappa_p \left(x_3\right) x_2 x_5 - \delta\left(x_3 - x_4\right)$$

$$\frac{dx_4}{dt} = \delta_1 \left(q_c \left(x_{4f} - x_4\right) + \delta \delta_2 \left(x_3 - x_4\right)\right)$$

$$x_5 = \sqrt{\frac{2f\phi_d \kappa_d \left(x_3\right)}{\phi_t \kappa_t \left(x_3\right)}} x_1$$

$$\frac{dx_6}{dt} = 0.5 \phi_t \kappa_t \left(x_3\right) x_5^2 - x_6$$

$$\frac{dx_7}{dt} = \phi_p \kappa_p \left(x_3\right) x_2 x_5 - x_7$$

$$y_1 = x_2$$

$$y_2 = x_3 \qquad (74)$$

The dimensionless concentration monomer (x_2) and the dimensionless reactor temperature (x_3) are controlled by manipulating the dimensionless monomer flowrate q_m, and the dimensionless cooling jacket flowrate q_c with and without uncertainty. Let $u_1 = q_m$, $u_2 = q_c$, $y_1 = x_2$, and $y_2 = x_3$. A styrene polymerization reactor operated at the initial condition $\left[x_1(0), x_2(0), x_3(0), x_4(0), x_6(0), x_7(0) = \right[3.7\times10^{-3}, 0.175, 1.2, 1, 2.4\times10^{-4}, 0.225\left]\right.$ in stable non-minimum phase region for all steady states. The controller implemented every sampling time of 1 seconds. The relation between the dimensionless parameters and variables and the physical variables, the nominal parameter values, and the steady state pair and the opened-loop dynamic behavior analysis are shown Table 4, Table 5, and Table 6, recpectively. For this example, we consider the steady state pair at [x_{1ss}, x_{2ss}, x_{3ss}, x_{4ss}, x_{6ss}, x_{7ss}] =[7.347×10^{-3}, 0.331, 0.367, 0.302, 2.336×10^{-4}, 0.069] and [0.004, 0.183, 1.150, 0.948, 0.002, 0.217], respectively, which exhibit the stable non-minimum phase behavior. The tuning and simulation results are described by the following section.

1.2.3.1 Controller system

The continuous-time polymerization reactor model in (74) is approximated into the discrete-time model with Euler's method. The resulting discrete-time model is

$$
\begin{aligned}
x_1(k+1) &= x_1(k) + \Delta t\left(q_i x_{1f} - \left(q_i + u_1(k) + q_s\right)x_1(k) - \phi_d \kappa_d\left[x_3(k)\right]x_1(k)\right)\\
x_2(k+1) &= x_2(k) + \Delta t\left[u_1(k)x_{2f} - \left(q_i + u_1(k) + q_s\right)x_2(k) - \phi_p \kappa_p\left[x_3(k)\right]x_2(k)x_5(k)\right]\\
x_3(k+1) &= x_3(k) + \Delta t\left[\left(q_i + u_1(k) + q_s\right)\left(x_{3f} - x_3(k)\right) + \beta\phi_p\kappa_p\left[x_3(k)\right]x_2(k)x_5(k)\right.\\
&\qquad \left. -\delta\left(x_3(k) - x_4(k)\right)\right]\\
x_4(k+1) &= x_4(k) + \Delta t\left[\delta_1\left(u_2(k)\left(x_{4f} - x_4(k)\right) + \delta\delta_2\left(x_3(k) - x_4(k)\right)\right)\right]\\
x_5(k) &= \sqrt{\frac{2f\phi_d\kappa_d\left[x_3(k)\right]}{\phi_t\kappa_t\left[x_3(k)\right]}}\,x_1(k)\\
x_6(k+1) &= x_6(k) + \Delta t\left[0.5\phi_t\kappa_t\left[x_3(k)\right]x_5^2(k) - x_6(k)\right]\\
x_7(k+1) &= x_7(k) + \Delta t\left[\phi_p\kappa_p\left[x_3(k)\right]x_2(k)x_5(k) - x_7(k)\right]\\
y_1 &= x_2\\
y_2 &= x_3
\end{aligned}
\tag{75}
$$

The relative orders of the process outputs with respect to the vector of manipulated input are r_1=1, and r_2=2. The application of the controller system of (63) takes the form:

$$
\begin{aligned}
\chi_1(k+1) &= \chi_1(k) + \Delta t\left(q_i x_{1f} - \left(q_i + \psi_1\left(\hat{x}(k), \nu(k)\right) + q_s\right)\chi_1(k) - \phi_d\kappa_d\left[\chi_3(k)\right]\chi_1(k)\right)\\
&\quad + \check{D}_1\left(\chi(k), \nu(k)\right)\\
\chi_2(k+1) &= \chi_2(k) + \Delta t\left[\psi_1\left(\hat{x}(k), \nu(k)\right)x_{2f} - \left(q_i + \psi_1\left(\hat{x}(k), \nu(k)\right) + q_s\right)\chi_2(k)\right.\\
&\quad \left. -\phi_p\kappa_p\left[\chi_3(k)\right]\chi_2(k)\chi_5(k)\right] + \check{D}_2\left(\chi(k), \nu(k)\right)
\end{aligned}
$$

$$\chi_3(k+1)=\chi_3(k)+\Delta t\Big[\Big(q_i+\psi_1\big(\hat{x}(k),\nu(k)\big)+q_s\Big)\big(x_{3f}-\chi_3(k)\big)$$
$$+\beta\phi_p\kappa_p\big[\chi_3(k)\big]\chi_2(k)\chi_5(k)-\delta\big(\chi_3(k)-\chi_4(k)\big)\Big]+\check{D}_3\big(\chi(k),\nu(k)\big)$$
$$\chi_4(k+1)=\chi_4(k)+\Delta t\Big[\delta_1\Big(\psi_2\big(\hat{x}(k),\nu(k)\big)\big(x_{4f}-\chi_4(k)\big)+\delta\delta_2\big(\chi_3(k)-\chi_4(k)\big)\Big)\Big]$$
$$+\check{D}_4\big(\chi(k),\nu(k)\big)$$
$$\chi_5(k)=\sqrt{\frac{2f\phi_d\kappa_d\big[\chi_3(k)\big]}{\phi_t\kappa_t\big[\chi_3(k)\big]}\chi_1(k)}$$
$$\chi_6(k+1)=\chi_6(k)+\Delta t\Big[0.5\phi_t\kappa_t\big[\chi_3(k)\big]\chi_5^2(k)-\chi_6(k)\Big]+\check{D}_6\big(\chi(k),\nu(k)\big)$$
$$\chi_7(k+1)=\chi_7(k)+\Delta t\Big[\phi_p\kappa_p\big[\chi_3(k)\big]\chi_2(k)\chi_5(k)-\chi_7(k)\Big]+\check{D}_7\big(\chi(k),\nu(k)\big)$$

$$u(k)=\psi\big(\hat{x}(k),\nu(k)\big)=\min_{u(k)}\Bigg(\frac{\varepsilon_1 x_2(k+1)+\hat{x}_2(k)-\theta_1(k)}{\varepsilon_1}$$
$$+\frac{{\varepsilon_2}^2\big(x_3(k+2)\big)+2\varepsilon_2 x_3(k+1)+\hat{x}_3(k)-\theta_2(k)}{\varepsilon_2}\Bigg)^2$$

$$D(k)=\check{D}\big(\hat{x}(k),\nu(k)\big)=\min_{D(k)}\Bigg(\frac{\varepsilon_1 x_2(k+1)+\hat{x}_2(k)-\theta_1(k)}{\varepsilon_1}$$
$$+\frac{{\varepsilon_2}^2\big(x_3(k+2)\big)+2\varepsilon_2 x_3(k+1)+\hat{x}_3(k)-\theta_2(k)}{\varepsilon_2}\Bigg)^2 \tag{76}$$

subject to $\quad 0.25<u_1(k)<0.45,\quad 0.02<u_2(k)<0.1$

$$S(\hat{x}(k),\nu(k),u(k),D(k))\le 0$$

where $\quad S(\hat{x}(k),\nu(k),u(k),D(k))=\beta\big(V[x(k+I)]+V[\hat{x}(k)]\big)/\Delta t$
$$-\begin{bmatrix}x_1(k+1)\\ \vdots\\ x_7(k+1)\end{bmatrix}\times\begin{bmatrix}x_1(k+1) & \cdots & x_7(k+1)\end{bmatrix}$$

$$V[\hat{x}(k)]=\begin{bmatrix}\hat{x}_1(k)-\nu_1(k)\\ \vdots\\ \hat{x}_7(k)-\nu_7(k)\end{bmatrix}\cdot P\cdot\begin{bmatrix}\hat{x}_1(k)-\nu_1(k) & \cdots & \hat{x}_7(k)-\nu_7(k)\end{bmatrix}$$

$$\theta_1(k)=y_{1,sp}-x_2(k)+\chi_2(k),\quad \theta_2(k)=y_{2,sp}-x_3(k)+\chi_3(k)$$

1.2.3.2 Selection of tuning parameter of styrene polymerization reactor

To achieve the optimal response, the tuning parameters were determined by analyzing the stabilized domain of closed-loop system and bifurcation diagram. The details of controller tuning with bifurcation diagram will be referred to again in section 2. To test the effectiveness of the proposed controller, the monomer concentration and reactor temperature is controlled with multiple steady states. The process is initially at y_{sp1}=0.331 and y_{sp2}=0.367 with stable, non-minimum phase behavior, and then it is adjusted to y_{sp1}=0.183 and y_{sp2}=1.150 with stable, non-minimum phase behavior, respectively. The tuning parameter ε under I/O linearization technique is used to adjust the speed of the response of the closed-loop output. The tuning parameter β under Lyapunov stability constraint is used to set the rate of decay of Lyapunov function. The positive definite matrix P under Lyapunov stability constraint is chosen to satisfy the Riccati equation in Equation (52). The tuning results show that the optimal parameter values for the proposed control system in Equation (76) are $\varepsilon_1 = 0.85,\ \varepsilon_1 = 0.79, \beta = 50$ and

$$P = \begin{bmatrix} 173.380 & 5.794 & 11.025 & 4.168 & 1.654\times10^{-1} & 1.999 \\ 5.794 & 7.681\times10^{-1} & 4.263\times10^{-1} & 1.684\times10^{-1} & 9.207\times10^{-4} & 9.093\times10^{-2} \\ 11.025 & 4.263\times10^{-1} & 1.955 & 3.617\times10^{-1} & 3.908\times10^{-3} & 2.625\times10^{-2} \\ 4.168 & 1.684\times10^{-1} & 3.617\times10^{-1} & 1.716 & 7.709\times10^{-2} & 3.616\times10^{-2} \\ 1.654\times10^{-1} & 9.207\times10^{-4} & 3.908\times10^{-3} & 7.709\times10^{-2} & 9.998 & 4.883\times10^{-2} \\ 1.999 & 9.093\times10^{-2} & 2.625\times10^{-2} & 3.616\times10^{-2} & 4.883\times10^{-2} & 9.980\times10^{-1} \end{bmatrix}$$

The output response under the proposed tuning parameters is smooth and no oscillation, which can approach to the desired steady states at 0.2 and 3.2 minutes, respectively as shown in Figure 39.

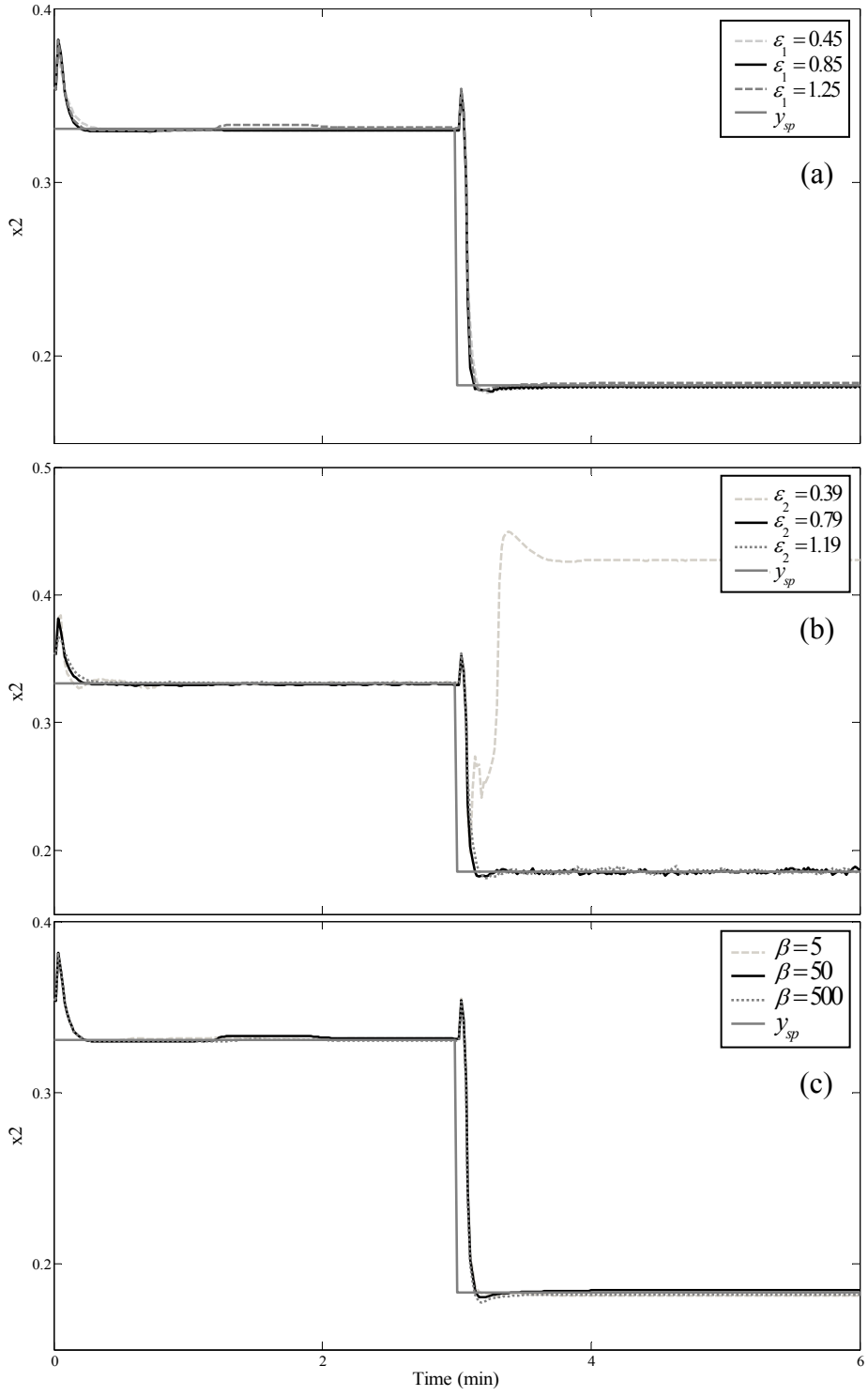

Figure 39 Closed-loop responses of controlled output by varying the tuning parameter, (a) ε_1 and (b) ε_2 under I/O linearization, and (c) β under Lyapunov stability constraint

1.2.3.3 Simulation results of styrene polymerization reactor without uncertainty

The proposed control technique is applied through the styrene polymerization reactor without uncertainty to control the monomer concentration and reactor temperature at the desired setpoints. The performance of the controller is investigated in terms of performing a smooth and fast startup of the process, ability in the process operation with initial condition in non-minimum phase region, the stability of closed-loop system, and tracking step changes in the setpoints. The controller successfully operates the styrene polymerization reactor at the three steady states. The closed-loop responses of the dimensionless of initiator concentration, monomer concentration, reactor temperature, cooling jacket temperature, dead polymer concentration and concentration of monomer units without uncertainty are shown in Figure 40-41. The monomer concentration and reactor temperature responses are a smooth and fast startup. It can effectively move from one set point to another. The controller adjusts the monomer flowrate and cooling jacket flowrate in Figure 42(a) to bring the outputs at the new setpoints value as soon as possible. The Lyapunov function profile in Figure 42(b) continuously decrease, which indicate that the closed-loop response is stable. Furthermore, it also is asymptotically stable when the time derivatives of Lyapunov function in Figure 42(c) approach to zero. The stability constraint is active as shown in Figure 43, which indicate that only I/O linearization technique cannot control the reactor temperature at non-minimum phase steady state. This cause from domain of solution that is not covers the dynamic behavior with non-minimum phase. Thus, Lyapunov stability constraint must continuously be active to maintain the controlled output at the desired steady state.

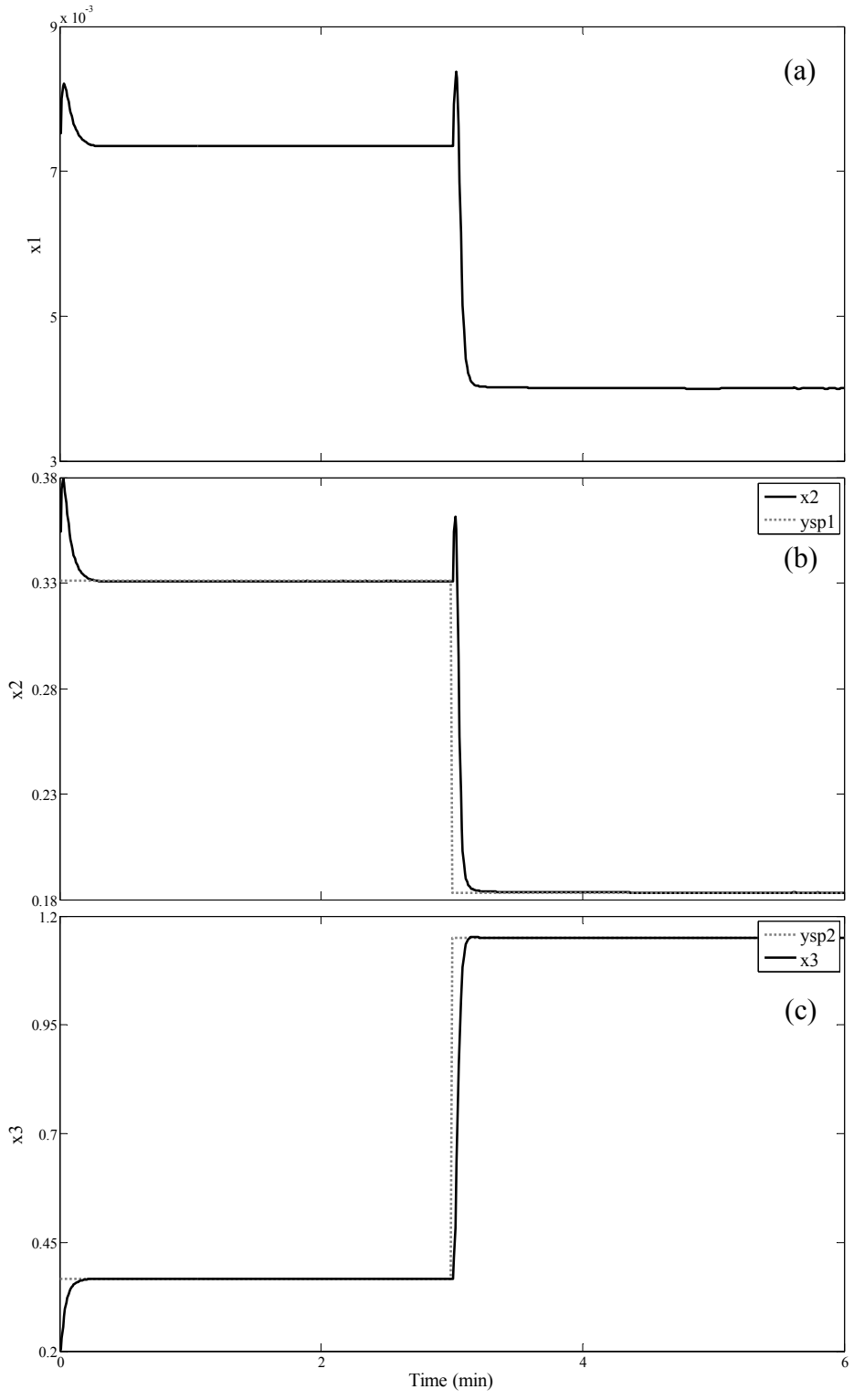

Figure 40 Closed-loop responses of the dimensionless of (a) initiator concentration, (b) monomer concentration and (c) reactor temperature of styrene polymerization reactor without uncertainty.

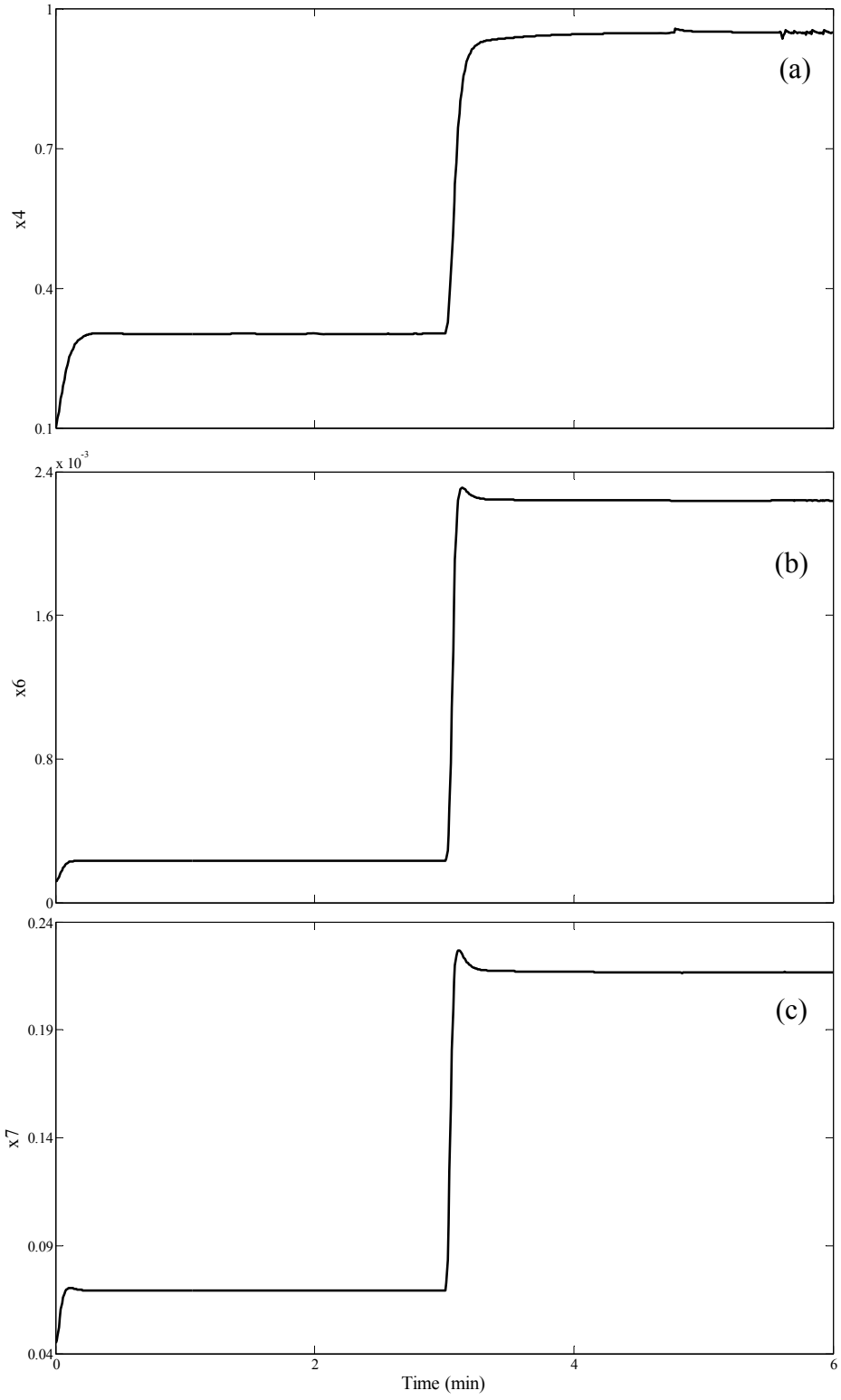

Figure 41 Closed-loop responses of the dimensionless of (a) cooling jacket temperature, (b) dead polymer concentration and (c) concentration of monomer units of styrene polymerization reactor without uncertainty.

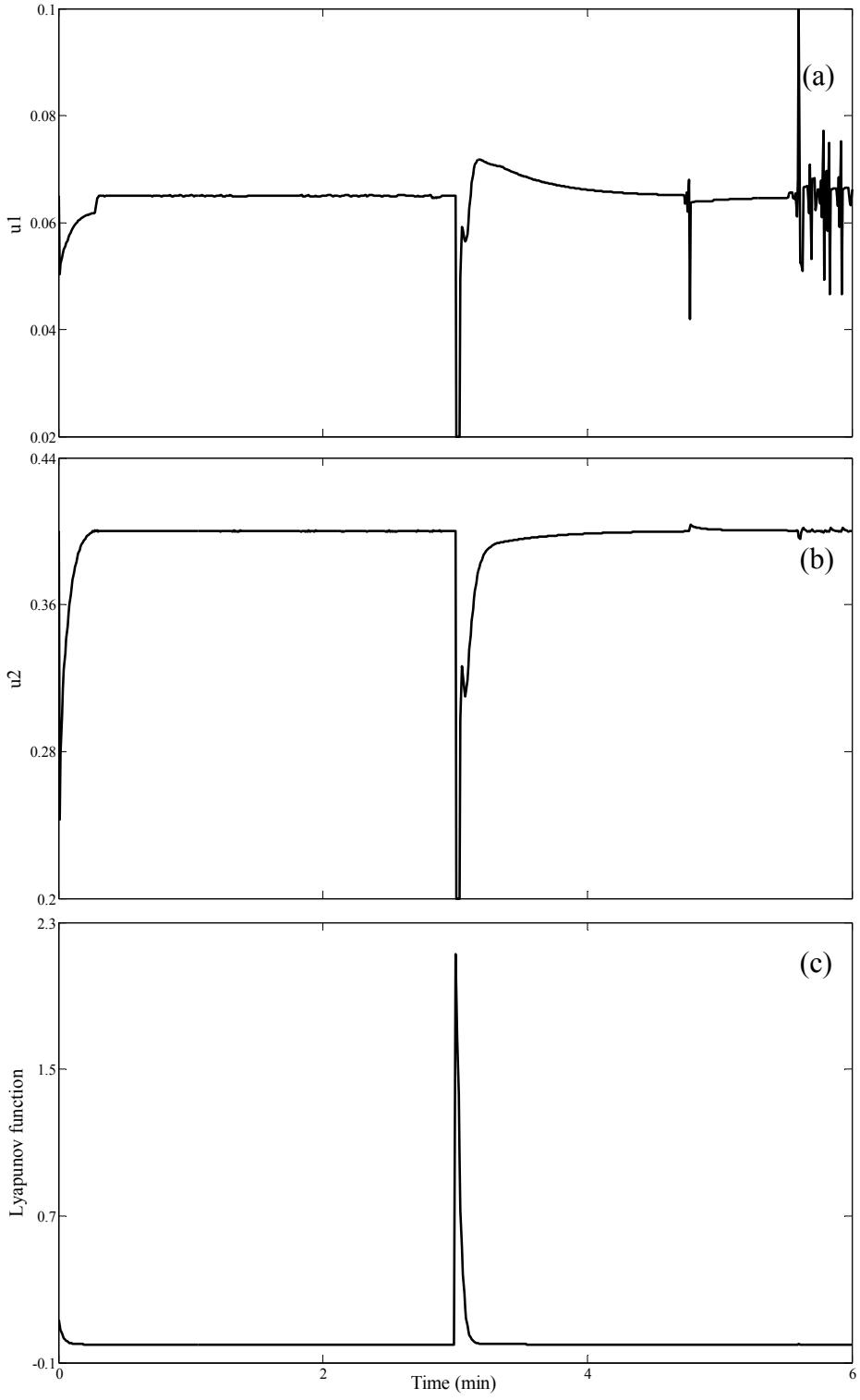

Figure 42 Closed-loop responses of the dimensionless of (a) monomer flowrate, (b) cooling jacket flowrate, and (c) Lyapunov function profile of styrene polymerization reactor without uncertainty.

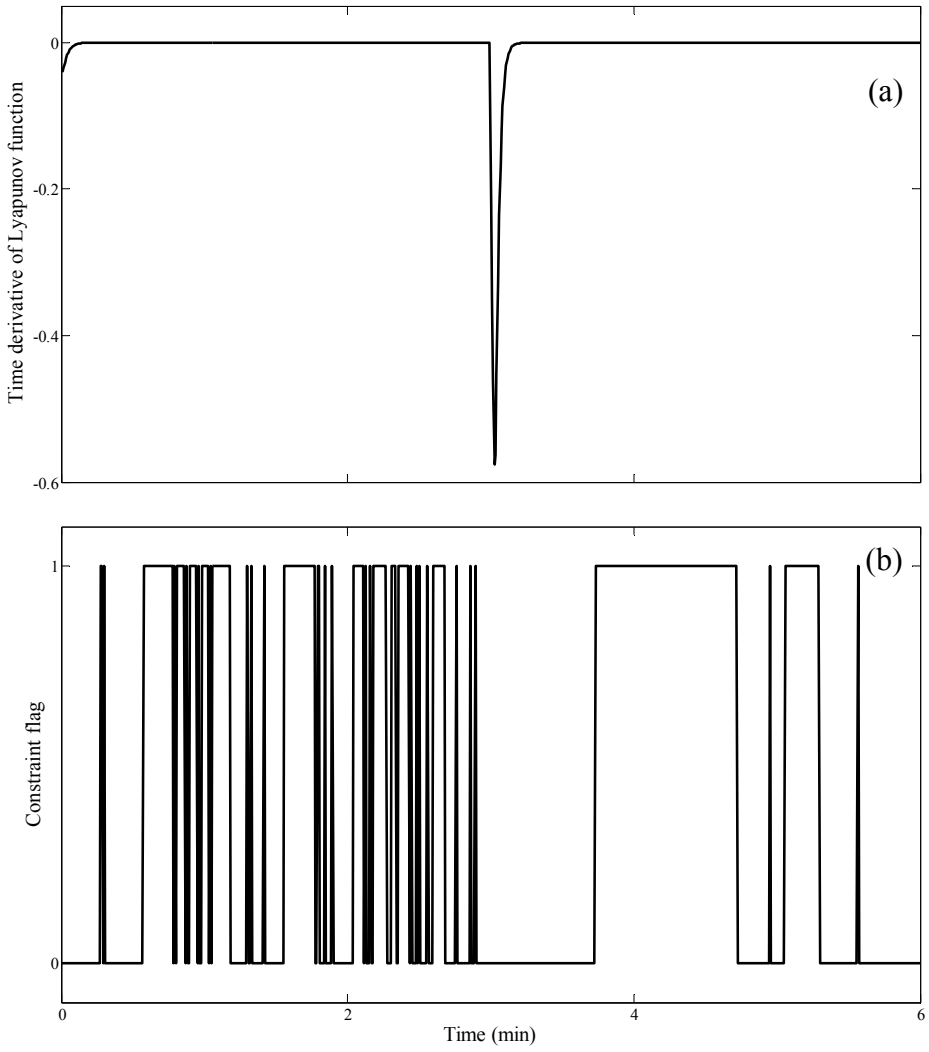

Figure 43 Closed-loop responses of (a) time derivative of Lyapunov function, and (b) the constraint flag and of styrene polymerization reactor without uncertainty.

1.2.3.4 Simulation results of styrene polymerization reactor with uncertainty

The performance of the controller is investigated in terms of tracking step changes in the setpoints, the stability of closed-loop system and the robustness property of controller. The parametric uncertainty and unmeasured disturbances are considered, which are simulated with random noise of the heat transfer coefficient (U) and the cooling jacket flowrate (q_c), respectively.

Case 1: Uncertainty in the heat transfer coefficient (U)

To test the robustness of the proposed controller, the controller can maintain the monomer concentration and the reactor temperature at the maximum of ± 10% uncertainty in the heat transfer coefficient although it is operated with initial conditions in non-minimum phase region. The closed-loop responses of the dimensionless of initiator concentration, monomer concentration, reactor temperature, cooling jacket temperature, dead polymer concentration and monomer concentration in the presence of uncertainty in the heat transfer coefficient are shown in Figure 44-45. The controller can be forced the controlled output to the setpoint trajectory by manipulating the monomer concentration and the cooling jacket flowrate in Figure 46(a) and Figure 46(b), respectively. Figure 46(c) shows the approximation of uncertainty in each state. The uncertainty is compensated in each state through the optimizer to obtain the desired output. The closed-loop response is stable, which show in Figure 47(a) and Figure 47(b). The Lyapunov stability constraint is continuously active especially, the last control range of stable, minimum phase steady state because it has two unstable zero dynamic as shown in Figure 47(c).

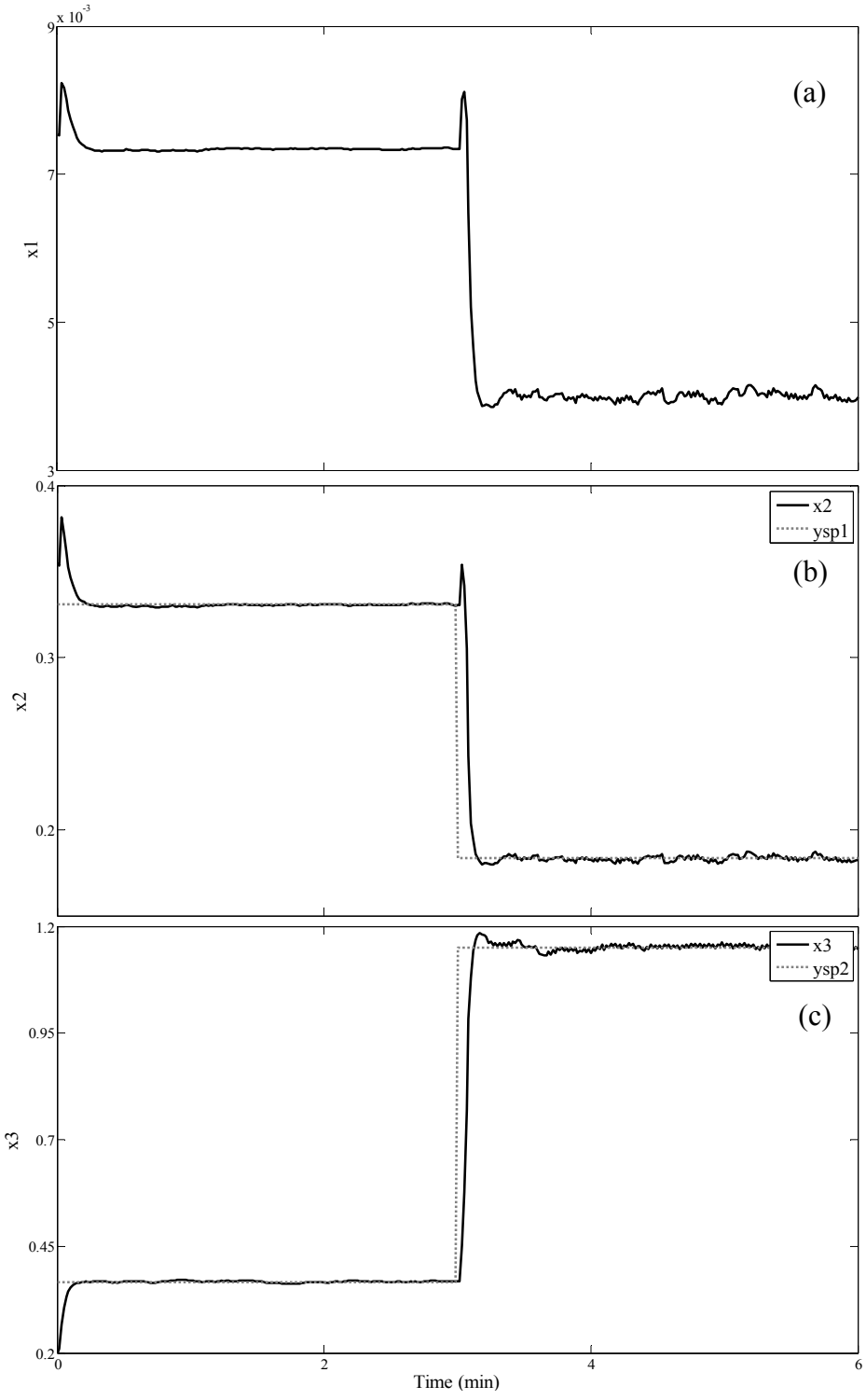

Figure 44 Closed-loop responses of the dimensionless of (a) initiator concentration, (b) monomer concentration, and (c) reactor temperature for styrene polymerization reactor with ± 10% uncertainty of the heat transfer coefficient.

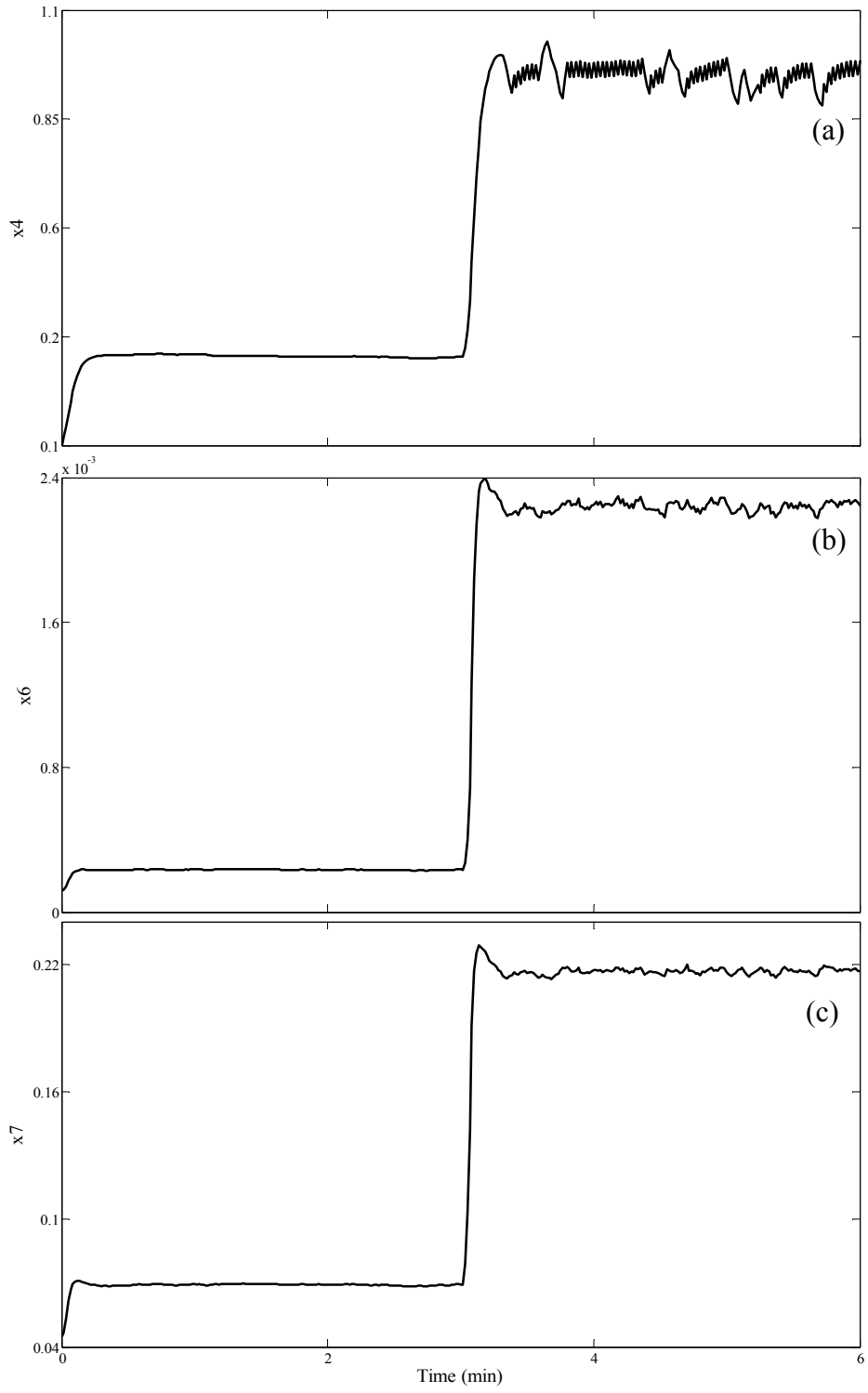

Figure 45 Closed-loop responses of the dimensionless of (a) cooling jacket temperature, (b) dead polymer concentration, and (c) concentration of monomer units for styrene polymerization reactor with ± 10% uncertainty of the heat transfer coefficient.

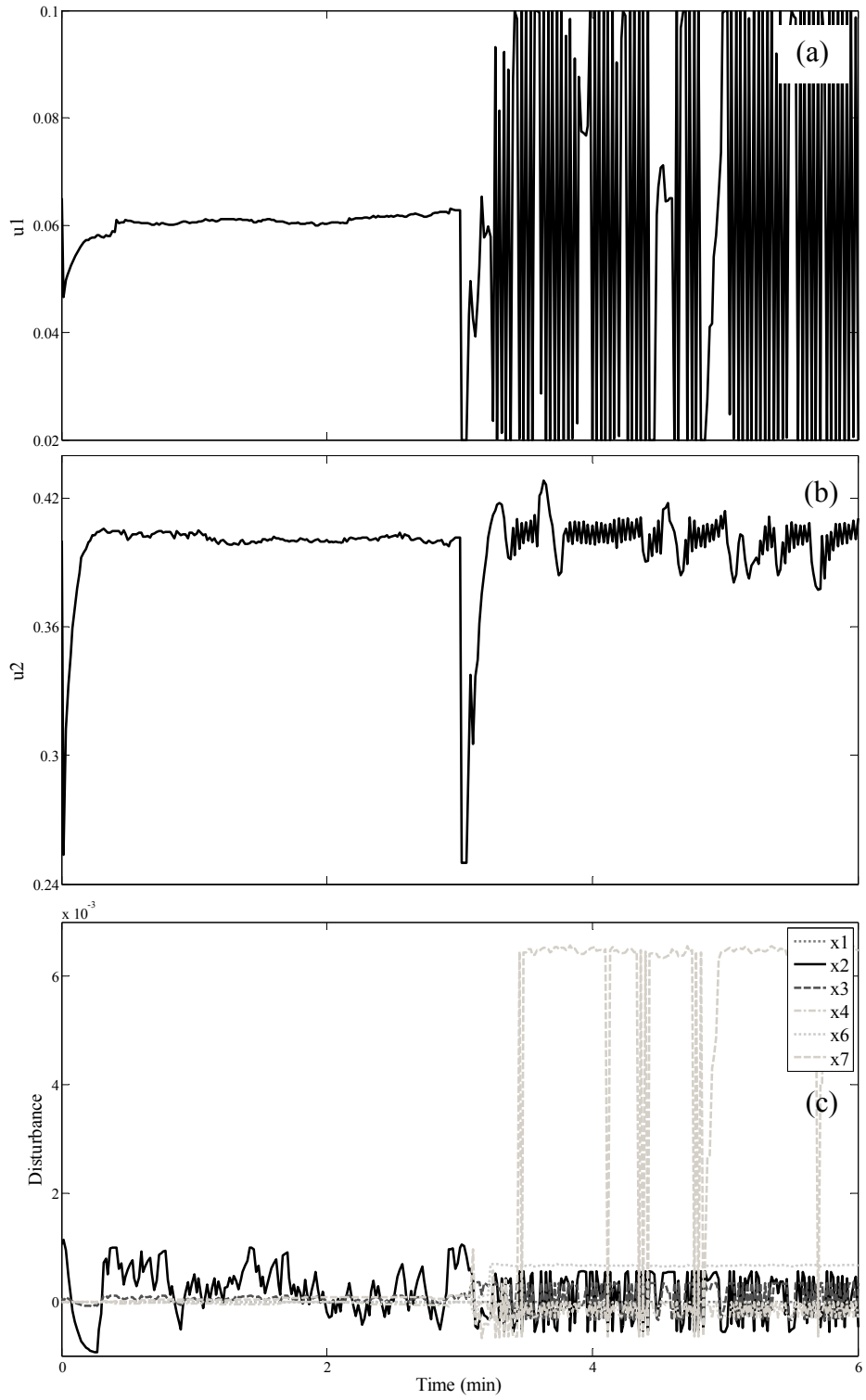

Figure 46 Closed-loop responses of the dimensionless of (a) monomer flowrate, (b) cooling jacket flowrate, and (c) unmeasured disturbance for styrene polymerization reactor with ± 10% uncertainty of the heat transfer coefficient.

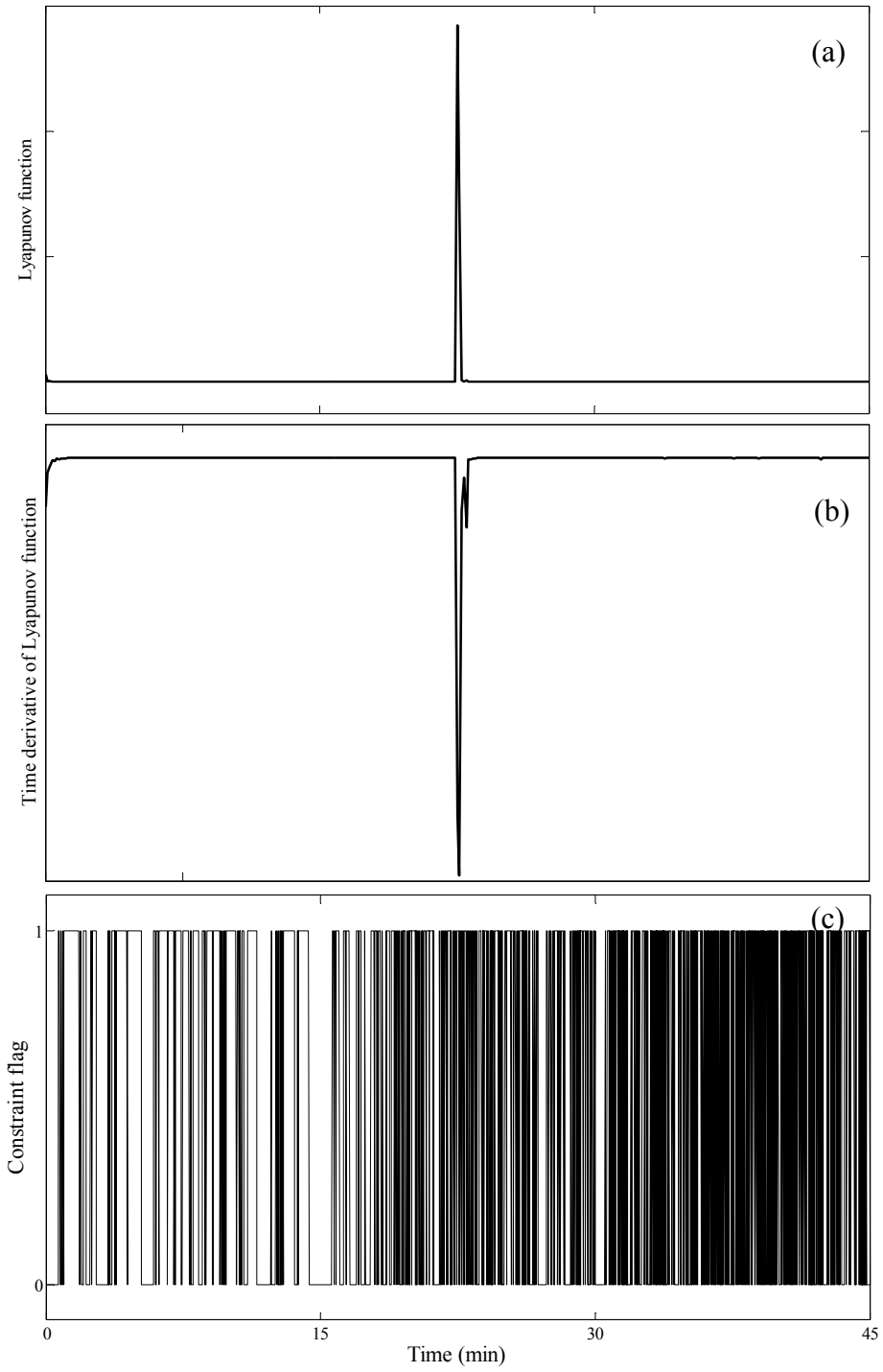

Figure 47 Closed-loop responses of the dimensionless (a) Lyapunov function profile, (b) time derivative of Lyapunov function, and (c) constraint flag for styrene polymerization reactor with ± 10% uncertainty of the heat transfer coefficient.

Case 2: Uncertainty in the cooling jacket flowrate (q_c)

The controller can maintain the monomer concentration and the reactor temperature at the maximum of $\pm$ 30% uncertainty in the monomer concentration although it is operated with initial conditions in non-minimum phase region. The closed-loop responses of the dimensionless of initiator concentration, monomer concentration, reactor temperature, cooling jacket temperature, dead polymer concentration and concentration of monomer units in the presence of uncertainty in the heat transfer coefficient are shown in Figure 48-49. The controller can be forced the controlled output to the setpoint trajectory by manipulating the monomer concentration and the cooling jacket flowrate in Figure 50(a) and Figure 50(b), respectively. Figure 50(c) shows the approximation of uncertainty in each state. The uncertainty is compensated in each state through the optimizer to obtain the desired output. The closed-loop is stable, which show in Figure 51(a), and Figure 51(b). Figure 51(c) shows the constraint flag of the closed-loop response. The Lyapunov stability constraint is continuously active especially, the last control range of stable, minimum phase steady state because it has two unstable zero dynamic.

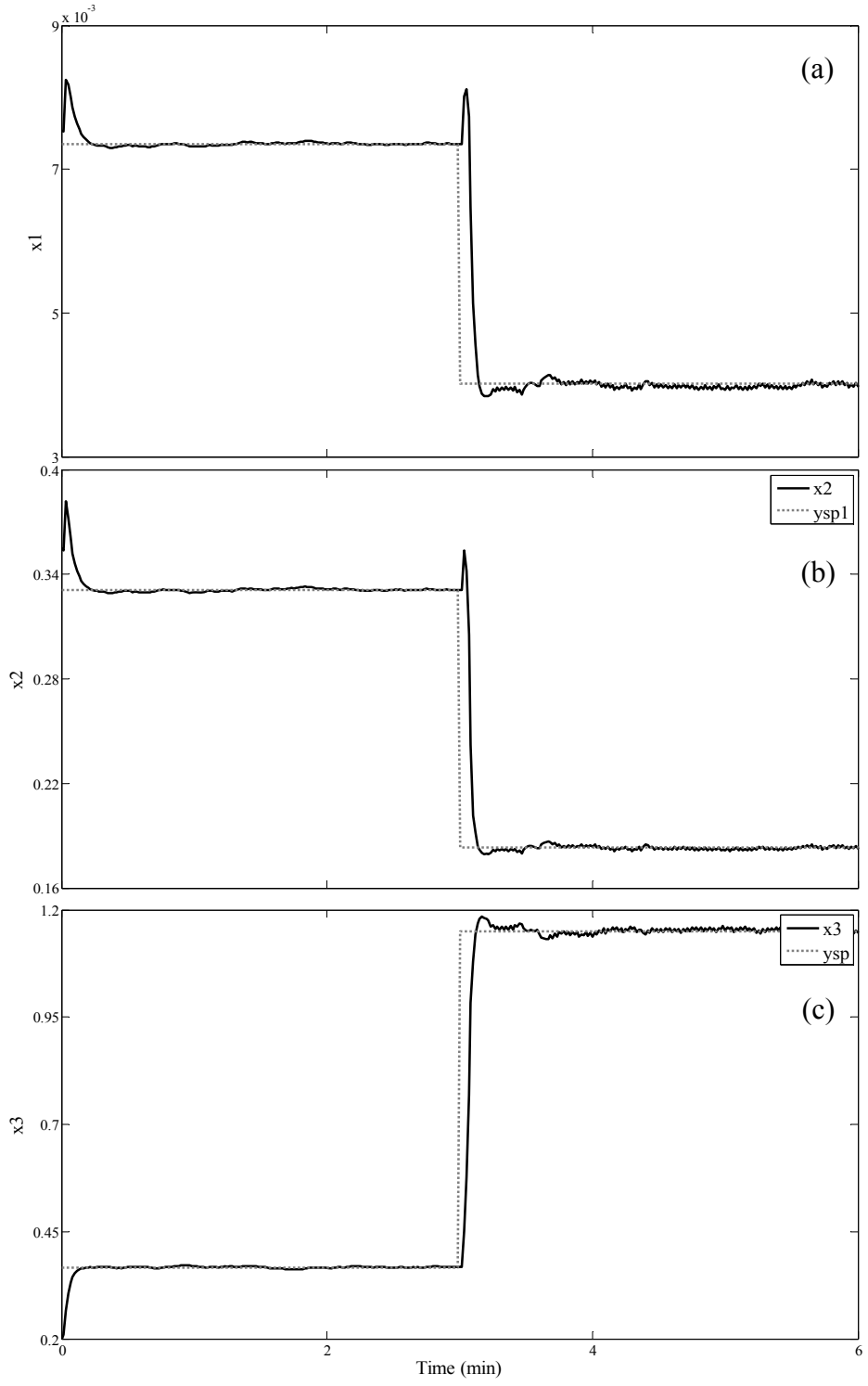

Figure 48 Closed-loop responses of the dimensionless of (a) initiator concentration, (b) monomer concentration and (c) reactor temperature for styrene polymerization reactor with $\pm$ 30% uncertainty of the dimensionless cooling jacket flowrate.

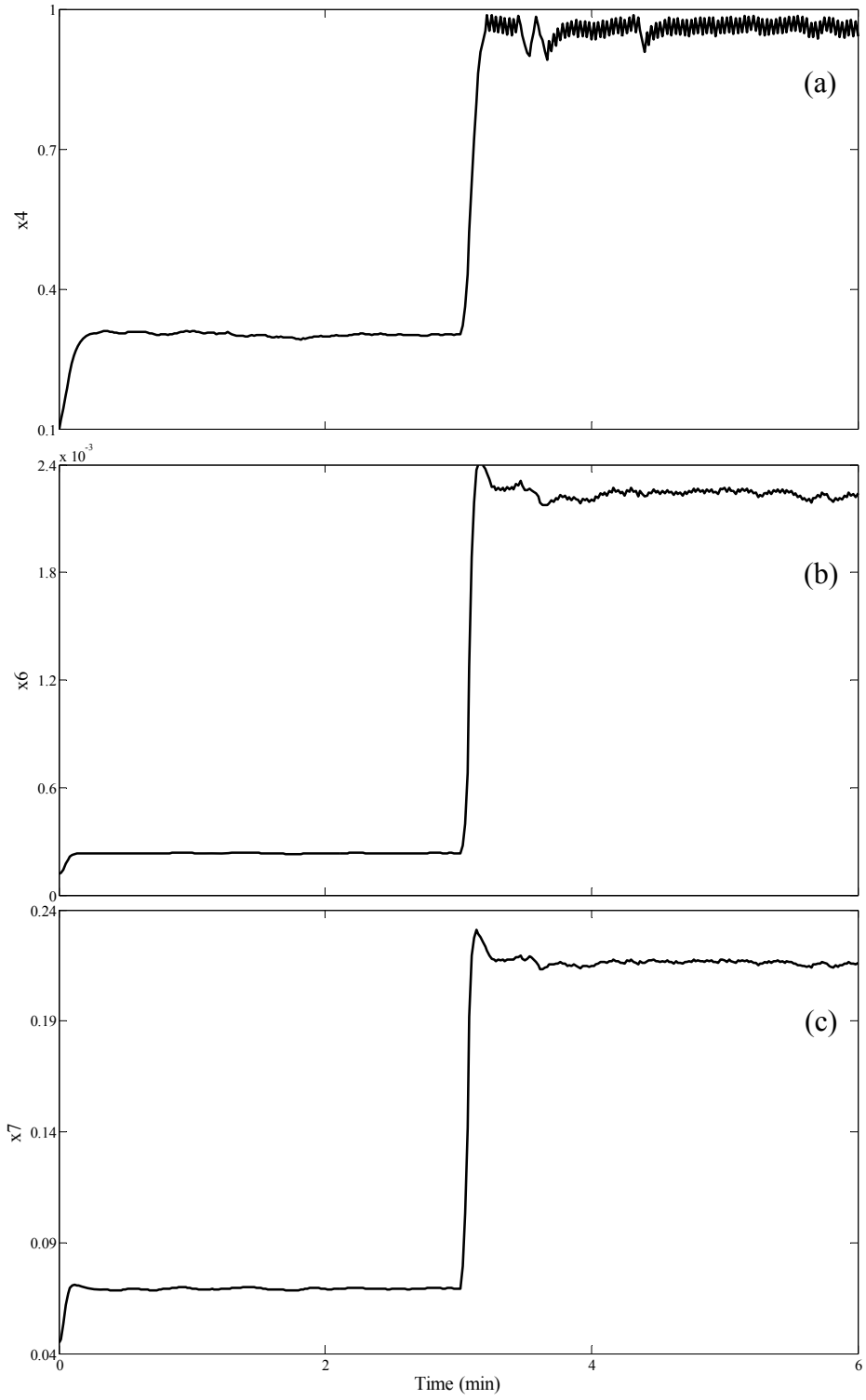

Figure 49 Closed-loop responses of the dimensionless of (a) cooling jacket temperature, (b) dead polymer concentration and (c) monomer concentration for styrene polymerization reactor with ± 30% uncertainty of the dimensionless cooling jacket flowrate.

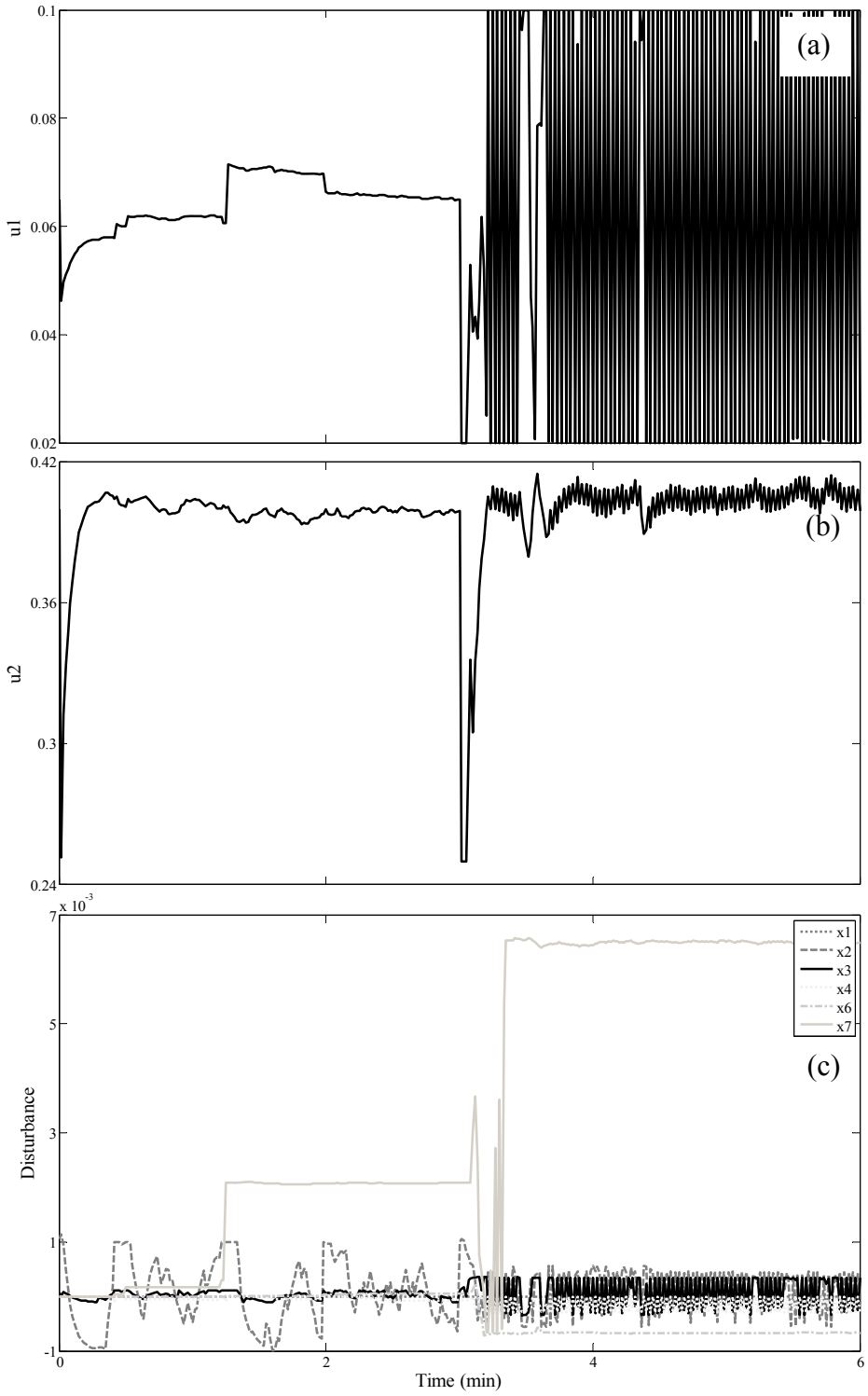

Figure 50 Closed-loop responses of the dimensionless of (a) cooling jacket temperature, (b) dead polymer concentration and (c) monomer concentration for styrene polymerization reactor with ± 30% uncertainty of the dimensionless cooling jacket flowrate.

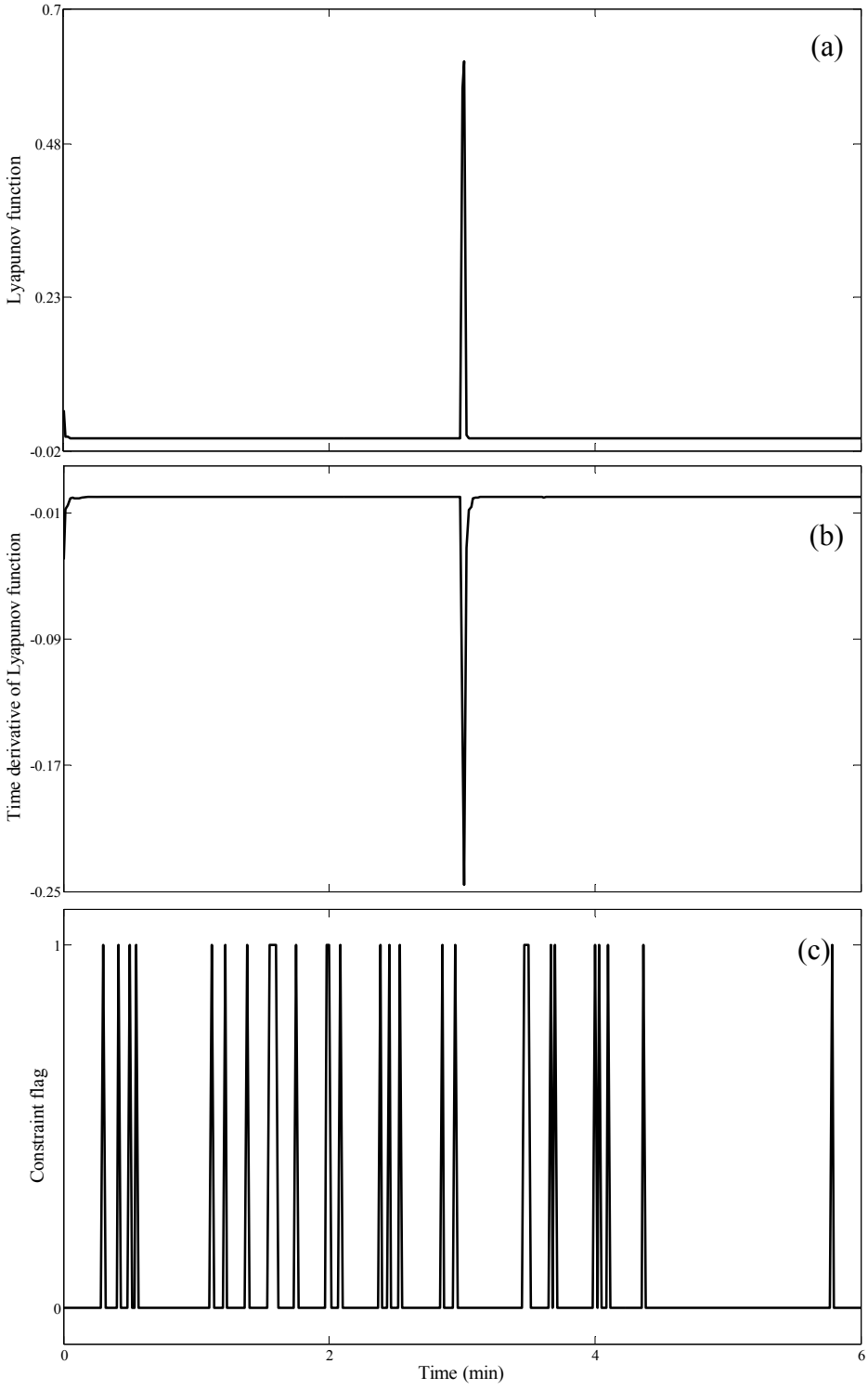

Figure 51 Closed-loop responses of the dimensionless of (a) cooling jacket flowrate, (b) unmeasured disturbance and (c) Lyapunov function profile for styrene polymerization reactor with $\pm$ 30% uncertainty of the dimensionless cooling jacket flowrate.

1.3 Comparison of control performance with a robust I/O linearizing controller using multi-model H_2 / H_∞ synthesis

To compare the control performance of the proposed controller, a popular alternative as robust I/O linearizing control using multi-model H_2 / H_∞ synthesis (Kolavennu *et al.*, 2000) is considered to reduce the effect of uncertainty. The multi-model H_2 / H_∞ synthesis placed the pole of the system to obtain good performance for all value of parametric uncertainty. The H_∞ objective canceled the effect of parametric uncertainty while the H_2 objective obtained the optimal linear quadratic Gaussian (LQG) control. LMI was used to solve the multi-objective optimization with pole placement constraints. The advantage of a robust I/O linearizing control using multi-model H_2 / H_∞ synthesis is reduce the effect of uncertainty with optimization problem, which can apply to multivariable systems with decoupling. Moreover, this approach does not require restrictive matching conditions to be satisfied. However, it is difficult to implement due to many tuning parameters. To illustrate the control performance, a chemical reactor is proposed in the following section.

1.3.1 Single-input single-output chemical reactor

A chemical reactor is considered with an isothermal, liquid phase, multi-component chemical reaction. The chemical reaction system is $x_1 \rightleftharpoons x_3 \rightarrow x_2$ with the rates of reaction described by

$$r_1 = k_1 x_1 - k_2 x_3^2$$
$$r_2 = k_2 x_3^2$$

There is an unmodeled first-order side reaction from x_3, which cause from the flowrate/valve-position relationship. This creates an error in measuring the molar feed rate of x_3. It is desired to control x_2 as close as possible to the steady state value by adjusting the molar feed rate of x_3. The process diagram is shown in Figure 52.

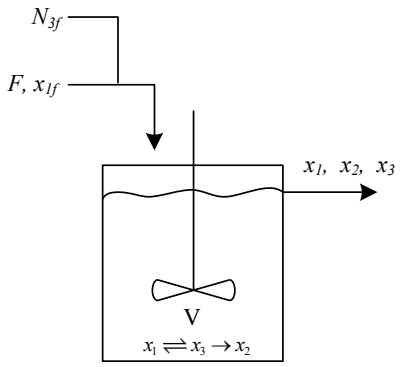

Figure 52 Process diagram for a chemical reactor.

The process models in terms of dimensionless variables are

$$\begin{aligned}
\frac{dx_1}{dt} &= -k_1 x_1 + \frac{F}{V}\left(x_{1f} - x_1\right) + k_2 x_3^2 \\
\frac{dx_2}{dt} &= -\frac{F}{V} x_2 + k_2 x_3^2 \\
\frac{dx_3}{dt} &= k_1 x_1 - \frac{F}{V} x_3 - \left(k_2 + k_3\right) x_3^2 + u \\
y &= x_2
\end{aligned} \tag{77}$$

where $u = N_{3f} / F x_{1f}$.

The objective of this control problem is a control of x_2 at a desired steady state by manipulating the molar feed rate *u*. The uncertainty occur from the parameter k_2 which is represented by

$$k_2 = \hat{k}_2 + c_2 D$$

where $\hat{k}_2$ is the nominal value of k_2, $c_2 = 2.9$ is a scaling constant representing the magnitude of the uncertainty, and *D* is set of parametric uncertainty. The relative order of the process output with respect to the vector of manipulated input is $r = 2$. The steady state is (x_{1ss}=2.180, x_{2ss}=3.933, x_{3ss}=0.887, u_{ss}=5). The eigenvalues of

Jacobian matrix of this process evaluated at steady state are (-15.5815, -1.6082, -1). The Jacobian of zero dynamics evaluated at desired steady state are (4, 1), which has eigenvalues in right half of real plane. Thus, the steady state is stable and non-minimum phase. The values of dimensionless parameters for process (77) are listed in Table 6.

Table 6 The dimensionless parameter values of chemical reactor

Parameter	value
k_1	1
k_2	3
k_3	5
F	3
V	3
x_{1f}	2

1.3.1.1 Controller system

The continuous-time chemical reactor model in (77) is approximated into the discrete-time model described by

$$\begin{aligned}
x_1(k+1) &= x_1(k) + \Delta t\left[-k_1 x_1(k) + \frac{F}{V}\left(x_{1f} - x_1(k)\right) + k_2 x_3^2(k)\right] \\
x_2(k+1) &= x_2(k) + \Delta t\left[-\frac{F}{V}x_2(k) + k_2 x_3^2(k)\right] \\
x_3(k+1) &= x_3(k) + \Delta t\left[k_1 x_1(k) - \frac{F}{V}x_3(k) - (k_2 + k_3)x_3^2(k) + u\right] \\
y(k) &= x_2(k)
\end{aligned} \tag{78}$$

The application of the controller system of (77) takes the form:

$$\chi_1(k+1)=\chi_1(k)+\Delta t\left[-k_1\chi_1(k)+\frac{F}{V}\left(x_{1f}-\chi_1(k)\right)+k_2\chi_3^2(k)\right]+\check{D}_1\left(\chi(k),\nu(k)\right)$$

$$\chi_2(k+1)=\chi_2(k)+\Delta t\left[-\frac{F}{V}\chi_2(k)+k_2\chi_3^2(k)\right]+\check{D}_2\left(\chi(k),\nu(k)\right)$$

$$\chi_3(k+1)=\chi_3(k)+\Delta t\left[k_1\chi_1(k)-\frac{F}{V}\chi_3(k)-(k_2+k_3)\chi_3^2(k)+\psi\left(\chi(k),\nu(k)\right)\right]$$
$$+\check{D}_3\left(\chi(k),\nu(k)\right)$$

$$u(k)=\psi\left(\hat{x}(k),\nu(k)\right)=\min_{u(k)}\left(\frac{\varepsilon^2\left(x_2(k+2)\right)+2\varepsilon x_2(k+1)+\hat{x}_2(k)-\theta(k)}{\varepsilon}\right)^2$$

$$D(k)=\check{D}\left(\hat{x}(k),\nu(k)\right)=\min_{D(k)}\left(\frac{\varepsilon^2\left(x_2(k+2)\right)+2\varepsilon x_2(k+1)+\hat{x}_2(k)-\theta(k)}{\varepsilon}\right)^2 \qquad (79)$$

subject to

$$2<u(k)<8$$

$$S(\hat{x}(k),\nu(k),u(k),D(k))\le 0$$

where

$$S(\hat{x}(k),\nu(k),u(k),D(k))=\beta V[x(k+1)]+V[\hat{x}(k)]$$
$$-\begin{bmatrix}x_1(k+1)\\x_2(k+1)\\x_3(k+1)\end{bmatrix}\times\begin{bmatrix}x_1(k+1) & x_2(k+1) & x_3(k+1)\end{bmatrix}$$

$$V[x(k)]=\begin{bmatrix}\hat{x}_1(k)-\nu_1(k)\\\hat{x}_2(k)-\nu_2(k)\\\hat{x}_3(k)-\nu_3(k)\end{bmatrix}\begin{bmatrix}a_{11} & a_{12} & a_{13}\\a_{21} & a_{22} & a_{23}\\a_{31} & a_{32} & a_{33}\end{bmatrix}\begin{bmatrix}\hat{x}_1(k)-\nu_1(k) & \hat{x}_2(k)-\nu_2(k) & \hat{x}_3(k)-\nu_3(k)\end{bmatrix}$$

$$\theta(k)=y_{sp}-x_2(k)+\chi_2(k)$$

A chemical reactor is operated with the various initial conditions $\left[x_1(0), x_2(0), x_3(0)\right]$ = [1, 8.33, 1], [4, 1.33, 6] and [4, 6.33, 1], respectively, which are in stable non-minimum phase region. The controller implemented every sampling time of 5 seconds. The controller parameter values are used to the control system of Equation (79) with $\varepsilon = 60, \beta = 6700$ and

$$P = \begin{bmatrix} 0.2619 & 1.5299 & 0.9518 \\ 1.5299 & 482.69 & 95.051 \\ 0.9517 & 95.051 & 28.933 \end{bmatrix}$$

The effectiveness of the proposed controller to regulate the controlled output x_2 of a chemical reactor is tested. The process is initially at $y_{sp} = 3.933$ with stable, non-minimum phase behavior. The results are shown in following section.

1.3.1.2 Simulation results of chemical reactor with uncertainty

The simulation results of the comparison of robust I/O linearization using multi-model H_2 / H_∞ synthesis (Kolavennu et al., 2000) with the proposed control technique under I/O linearization integrating with Lyapunov stability constraint are shown in Figure 53-58, respectively. It is observed that the controller of Kolevennu is unable to keep the system at the desired setpoint when the uncertainty in rate constant parameter is varied with $\pm 33\%$ and $\pm 67\%$. The closed-loop responses of the output show the offset setpoint at ± 0.1 and ± 0.2, respectively. For the proposed controller, it can efficiently maintain the output without offset when the uncertainty in rate constant parameter is varied with $\pm 33\%$. However, the proposed controller cannot control the output at $\pm 67\%$ uncertainty in rate constant parameter that appear the offset setpoint at ± 0.2. For the test the control performance with wide range of initial conditions, both the controller of Kolevennu and the proposed controller can effectively operate the reactor. However, the proposed controller can force the output to the desired steady states at t = 0.9, 1.2 and 0.9 minutes, respectively that is faster than the response of Kolevennu's controller.

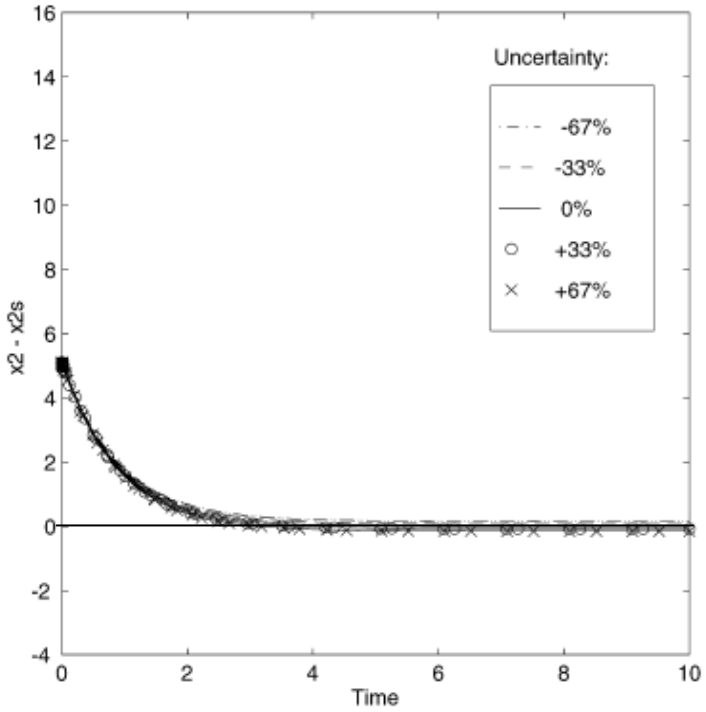

Figure 53 Closed-loop response of the deviation of controlled output under the control technique of Kolavennu at $x_0 = [1, 8.33, 1]$

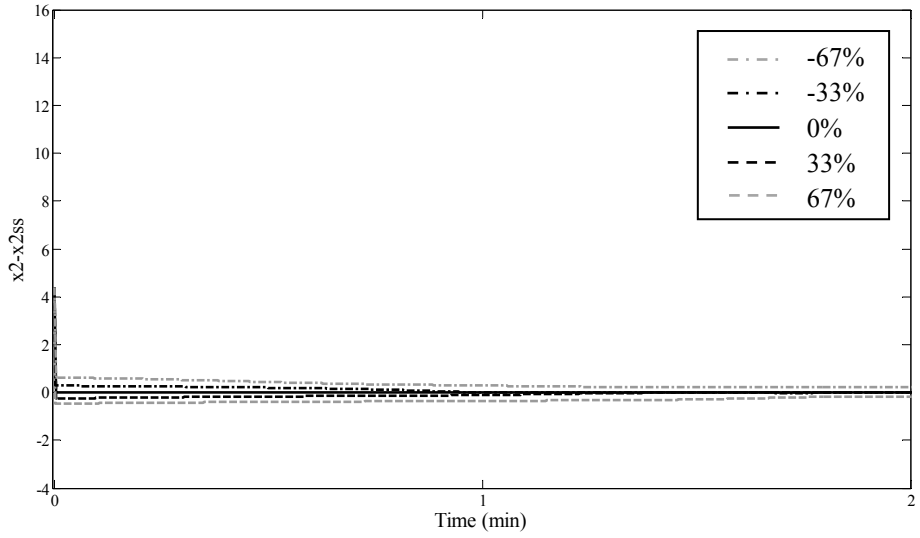

Figure 54 Closed-loop response of the deviation of controlled output under the proposed control technique at $x_0 = [1, 8.33, 1]$

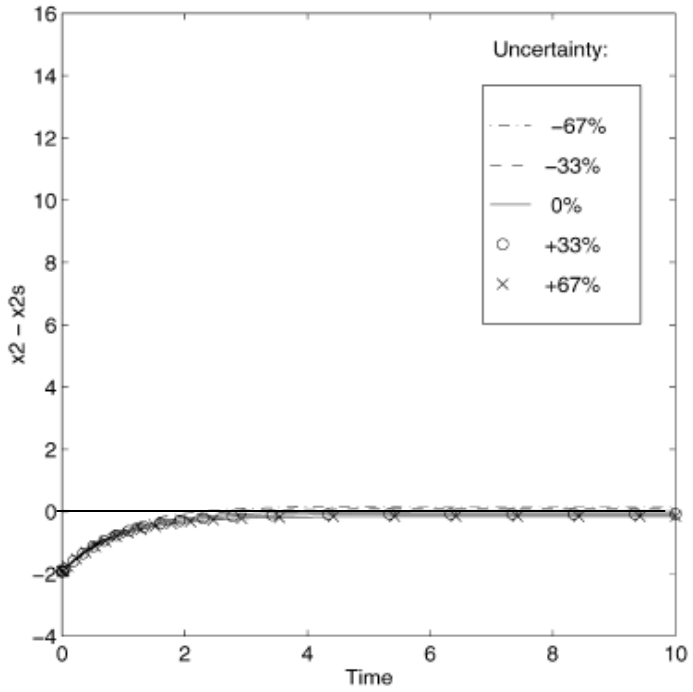

Figure 55 Closed-loop response of the deviation of controlled output under the control technique of Kolavennu at x_0 = [4, 1.33, 6]

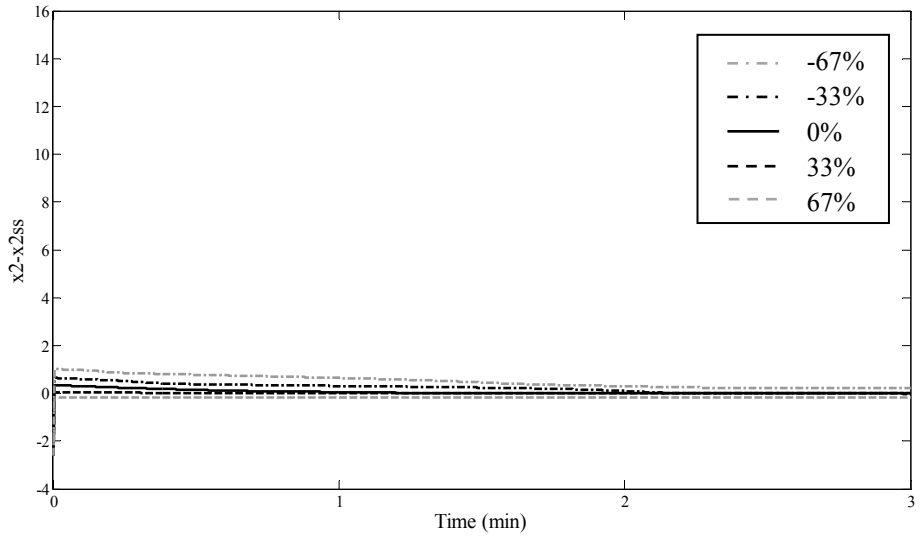

Figure 56 Closed-loop response of the deviation of controlled output under the proposed control technique at x_0 = [4, 1.33, 6]

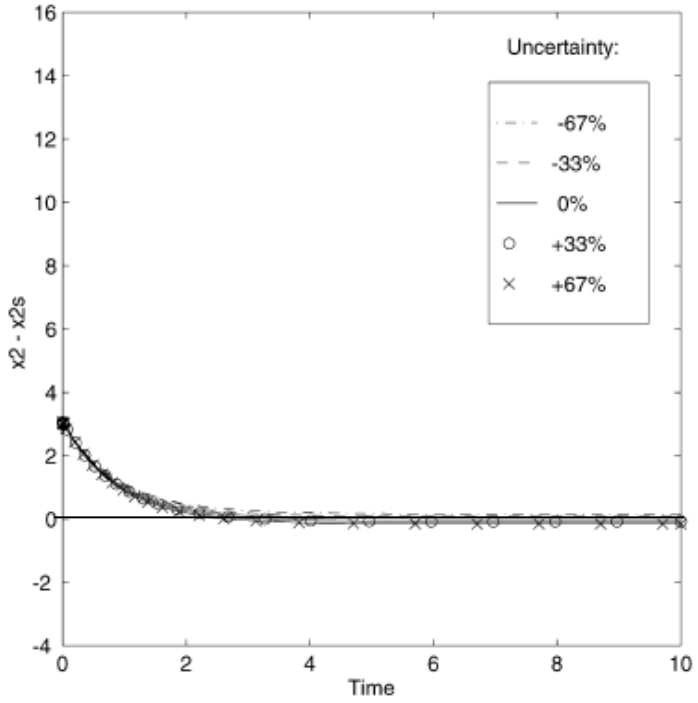

Figure 57 Closed-loop response of the deviation of controlled output under the control technique of Kolavennu at $x_0 = [4, 6.33, 1]$

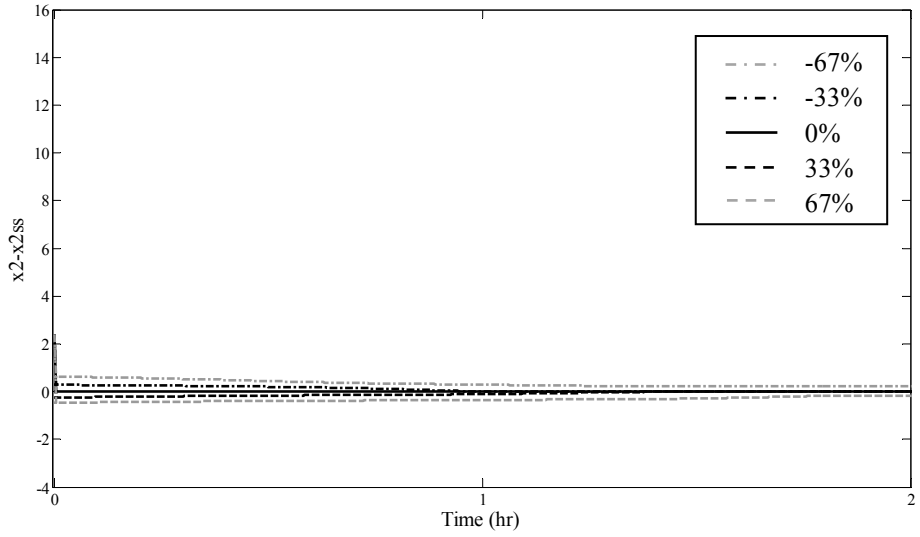

Figure 58 Closed-loop response of the deviation of controlled output under the proposed control technique at $x_0 = [4, 6.33, 1]$

From the comparison of control technique and simulation results of controller of Kolevennu (2000) with the proposed control technique, we can summarize the control performance as the following.

- The proposed controller can better control a process in presence of uncertainty and maintain a setpoint than the controller of Kolevennu.
- The proposed controller has the five tuning parameters while the controller of Kolevennu has the seven tuning parameters. It indicates that the proposed controller is easy to implement due to less tuning parameters.
- The responses of the proposed controller are faster than the controller of Kolevennu for every initial condition.
- The controller of Kolevennu is lack of guarantee for robustness.

2. Controller tuning with bifurcation analysis for uncertain chemical processes with multiplicity behavior

The determining of the optimal tuning parameters under stability region is important factor to achieve maximum productivity in the process operations. However, it must have an experience, knowledge of dynamical process behavior and control theory of the used control system. If the value of tuning parameters cannot be satisfied, the size of stability region is not suitable leading to the closed-loop instability. The stability region which is limited boundary of stability, seriously affect the control of highly nonlinear behavior and complex reaction, especially, the control of uncertain chemical process with multiplicity behavior. A controller must be tuned very carefully to obtain the desired steady state. If the controlled output cannot be maintained within the stability region, the result is uncontrollable leading to off-spec production.

Over the last decade, the bifurcation analysis was widely used to study dynamical behavior of the process whether in stable or unstable region. The majority of the literature in the control area has focused on the selecting of the suitable control range to maintain the closed-loop stability (Zhang et al., 2000, 2002, Monnigmann

and Marquardt, 2002, Gerhard and Monnigmann, 2004, Galluzzo et al., 2008), which not applied to controller tuning. Although Hahn et al. (2004, 2008) applied bifurcation analysis to be tuned controller for unstable reactor they used only simple feedback linearization technique, which cannot guarantee closed-loop stability. Moreover, the control performance of them may significantly degrade when it is used to chemical processes with multiplicity behavior.

Motivated by this limitation, the controller tuning with bifurcation analysis is applied to the proposed control technique for uncertain chemical processes with multiplicity behavior. The bifurcation analysis is used to

a) analyzing the opened-loop dynamic behavior of chemical process whether stable and/or unstable and the boundaries of the region of multiplicity behavior, and

b) tuning of the parameters under I/O linearizing feedback integrating with Lyapunov-based control.

Furthermore, the domain of solution under I/O linearizing feedback integrating with Lyapunov stability constraint is enlarged by the optimal tuning parameter to guarantee closed-loop stability. The advantage of the proposed tuning technique is easy to determine the optimal tuning parameters, which can identify the domain of stability under the proposed control technique.

2.1 Bifurcation analysis

Bifurcation analysis is an effective tool for studying the static and dynamic behavior of processes without having to solve completely the dynamics equations describing the processes. In this work, MATCONT continuation toolbox for MATLAB is used to bifurcation analysis for chemical multiplicity processes. The brief instruction to use such software is given in Appendix A. Consider an open-loop nonlinear dynamic process in the form of Equation (80):

$$\begin{aligned} \dot{x} &= f\left(x,u\right) \\ y &= h\left(x\right) \end{aligned} \tag{80}$$

where $x \in \mathbb{R}^n$, $u \in \mathbb{R}^m$ and $y \in \mathbb{R}^m$ denote the state variables, manipulated inputs, and controlled outputs, respectively. The equilibrium points of this process are the set of solutions obtained from the dynamic equations at steady state. The defining function is therefore:

$$f\left(x_{ss}, u_{ss}\right) = 0 \tag{81}$$

The approximated linearization of process model defined by Equation (80) is

$$\dot{x} = \tilde{A}x + \tilde{B}u \tag{82}$$

where x is an $n \times 1$ vector of state deviations from an operating point defined by the state vector, x, and the input vector, u,

u is an $m \times 1$ vector of input deviations from the input vector, u,

$\tilde{A}$ is the $n \times n$ Jacobian matrix, defined as:

$$\tilde{A} = \frac{\partial \mathrm{f}}{\partial \mathrm{x}} = \begin{bmatrix} \frac{\partial f_1}{\partial x_1} & \frac{\partial f_1}{\partial x_2} & \cdots & \frac{\partial f_1}{\partial x_n} \\ \frac{\partial f_2}{\partial x_1} & \frac{\partial f_2}{\partial x_2} & \cdots & \frac{\partial f_2}{\partial x_n} \\ \vdots & \vdots & \cdots & \vdots \\ \frac{\partial f_n}{\partial x_1} & \frac{\partial f_n}{\partial x_2} & \cdots & \frac{\partial f_n}{\partial x_n} \end{bmatrix}$$

$\tilde{B}$ is the $n \times m$ input-Jacobian matrix, defined as:

$$\tilde{B} = \frac{\partial \mathrm{f}}{\partial \mathrm{u}} = \begin{bmatrix} \frac{\partial f_1}{\partial u_1} & \frac{\partial f_1}{\partial u_2} & \cdots & \frac{\partial f_1}{\partial u_n} \\ \frac{\partial f_2}{\partial u_1} & \frac{\partial f_2}{\partial u_2} & \cdots & \frac{\partial f_2}{\partial u_n} \\ \vdots & \vdots & \cdots & \vdots \\ \frac{\partial f_n}{\partial u_1} & \frac{\partial f_n}{\partial u_2} & \cdots & \frac{\partial f_n}{\partial u_n} \end{bmatrix}$$

The stability of the steady states is determined by evaluating the eigenvalues of the Jacobian matrix of (82) at a steady state (x_{ss}, u_{ss}). The eigenvalues are found by setting the determinant to zero:

$$\left| J - \lambda I \right| = 0 \tag{83}$$

The character of a steady state can be summarized as follows:

vi) Stable node, if both eigenvalues are real and negative.

vii) Unstable node, if both eigenvalues are real and positive.

viii) Saddle node, if the eigenvalues are real with opposite signs.

ix) Stable focus, if the eigenvalues are complex conjugate with negative real parts.

x) Unstable focus, if the eigenvalues are complex conjugate with positive real parts.

To illustrative bifurcation analysis, isothermal continuous biochemical reactor is considered with Monod kinetics, constant volume V and constant physical-chemical properties (Bequette, 1998). The process model is described by Equation (84).

$$\begin{aligned}
\frac{dX_B}{dt} &= \mu(S)X_B - \frac{X_B F}{\mathrm{V}} \\
\frac{dS}{dt} &= -\frac{\mu(S)X_B}{Y} + \frac{(S_F - S)F}{\mathrm{V}} \\
\mu(S) &= \mu_{\max}\frac{S}{K_1 S^2 + S + K_m} \\
y &= S
\end{aligned} \tag{84}$$

where $D = F / V$.

Table 7 The parameter values of SISO biochemical reactor

Parameter	Value
D	0.1 m^3
S_F	4 kg m^{-3}
Y	0.4
$\mu_{\max}$	8.82×10^{-3} min^{-1}
K_1	0.12 m^3 kg^{-1}
K_m	4.55×10^{-1} kg m^{-3}

The dilution rate, which is manipulated input (u) is used as a continuation parameter to trace the steady state branches and construct the bifurcation diagram shown in Figure 59.

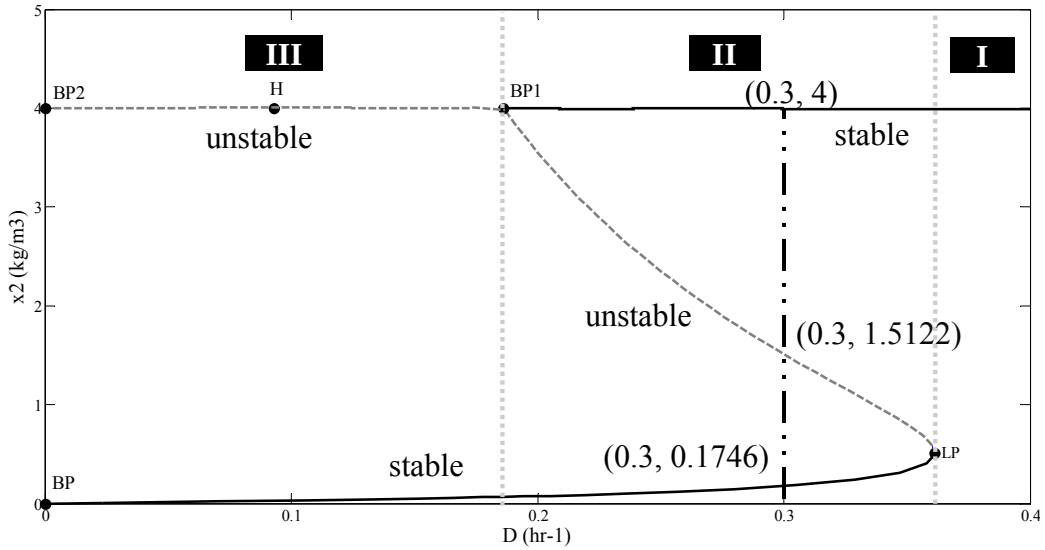

Figure 59 Bifurcation diagram of substrate concentration.

The stability of the steady states has been determined by evaluating the eigenvalues of the Jacobian matrix of the approximated model (84). Three steady-states (equilibrium) for this set of parameters (u_{ss}=0.3) are

Equilibrium 1 $x_{1ss} = 0$ $x_{2ss} = 4$

The eigenvalues of Jacobian matrix are (-0.3, -0.1139), which lie in the open left half of real plane. Then the steady state is stable node. This steady-state is known as the wash-out steady-state, because no biomass is produced and the substrate concentration in the reactor is equal to the feed substrate concentration.

Equilibrium 2 $x_{1ss} = 0.9951$ $x_{2ss} = 1.5122$

The eigenvalues of Jacobian matrix are (-0.3, 0.1698), which has at least one eigenvalue in the open right half of real plane. Then the steady state is unstable (it is a saddle point).

Equilibrium 3 $x_{1ss} = 1.5302 \quad x_{2ss} = 0.1746$

The eigenvalues of Jacobian matrix are (-2.262, -0.3), which lie in the open left half of real plane. Then the steady state is stable node.

A transcritical bifurcation occurs at the branch point 1 (BP1), which is a changing of stability between the washout steady state and a normal steady state. The continuation algorithm after computing the branch of washout steady states switches branches and computes the branch of normal steady states. At the limit point (LP), bifurcation occurs that connect two normal steady states together: one stable and one saddle. However, in the bifurcation diagram of Figure are shown only the important steady states. Three ranges of the dilution rate where qualitatively different behaviors are exhibited by the system. In the range of I, only the washout steady state exists and is stable. In the range of II, the washout steady state is still stable, but there are also two normal steady states, one stable and one saddle. In the range of III, the washout steady state is saddle and there is only one normal steady state which is stable.

From bifurcation analysis, it is possible to determine regions of stability not just for the parameter space but for the state space corresponding to the operating region of a process.

2.2 Tuning of parameter under input/output linearizing feedback controller with bifurcation analysis

The I/O linearizing feedback control technique has to adjust the optimal parameter to control the output under the desired domain of solution. The proposed tuning technique can use in order to tune the controller while ensuring that all steady states within this operating region will be stable. For I/O linearization method, the tuning parameter ε is used to adjust the speed response. The optimal tuning parameter should be small value because the eigenvalue of Jacobain matrix tend to left half plane. However, in practical, the small value of tuning parameter ε may not always good answer. The optimal tuning parameter should be adjusted corresponding with dynamical process behavior. Thus, this research work proposed controller tuning

technique under I/O linearizing feedback control. The following steps should be included in the controller tuning as shown in Figure 60.

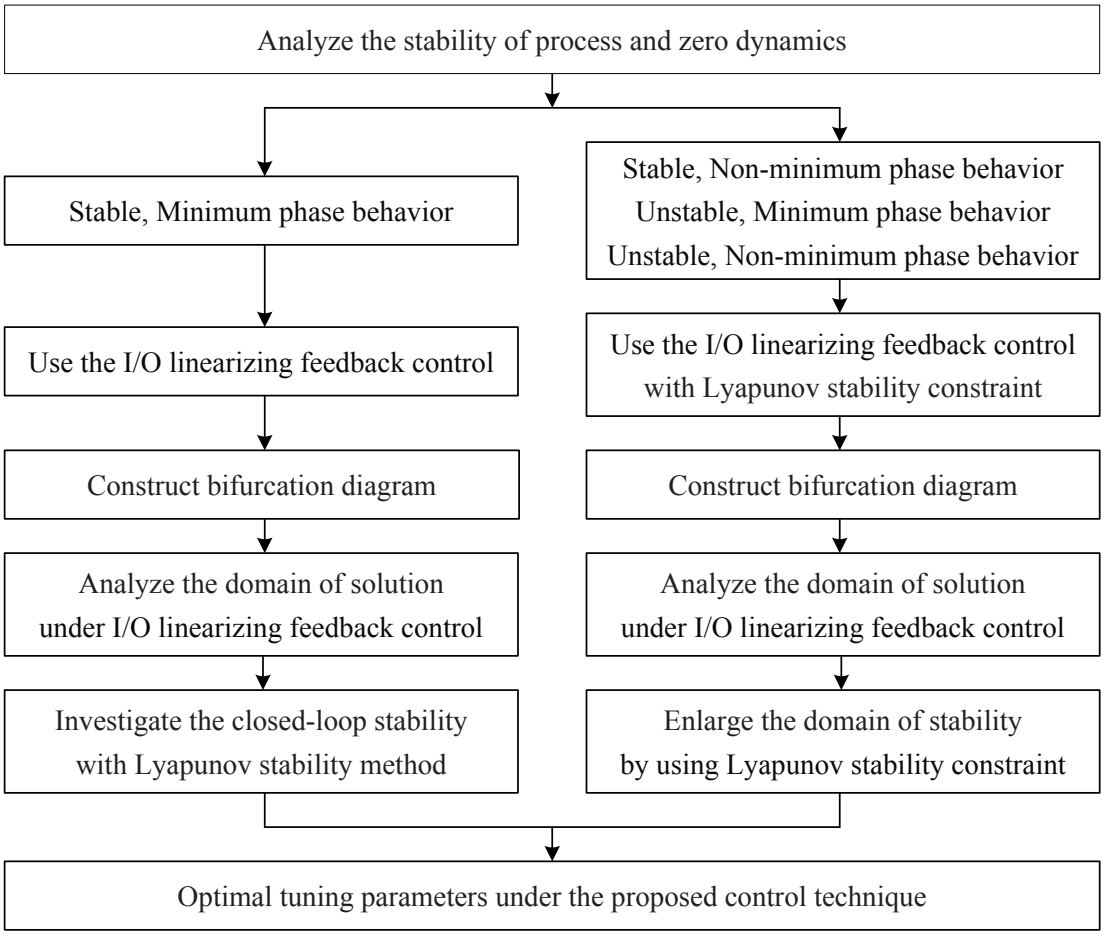

Figure 60 Controller tuning technique under I/O linearization integrating with Lyapunov stability constraint

First, the stability of process and zero dynamics is analyzed to investigate stable, unstable, minimum phase, and non-minimum phase behavior because the behavior such unstable and non-minimum phase cannot be controlled with only I/O linearizing feedback control technique. The stability region is enlarged by using Lyapunov stability constraint to account unstable and non-minimum phase behavior. Then, the bifurcation diagram is constructed to analyze the domain of solution and the domain of stability by varying the tuning parameters under I/O linearizing feedback control and Lyapunov stability constraint. The output response with the optimal tuning

parameter must cover the bifurcation diagram. The system trajectories will be ensured the stability under the designed domain. This requirement is an important point in order to guarantee stability of the controller. These steps will result in the controller tuning to achieve stability of operating points over the entire region of operation.

2.3 Illustrative examples for controller tuning with bifurcation analysis under input/output linearizing feedback control integrating with Lyapunov stability constraint

To illustrate the proposed tuning technique, a chemical reactor and bioreactor are tested. A chemical reactor will be operated with stable minimum phase behavior while a bioreactor will be operated both stable minimum phase and unstable minimum-phase behavior.

2.3.1 Single-input single-output chemical reactor

A well-mixed continuous stirred-tank reactor is applied in which the reaction A $\rightarrow$ B takes place in the liquid phase**.** The reactor dynamics are represented by

$$\begin{aligned} \frac{dC_A}{dt} &= \left(-k_0 \exp\left(\frac{-E_a}{RT} \right) \right) C_A + \left(C_{Ai} - C_A \right) \frac{F}{\mathrm{V}} \\ \frac{dT}{dt} &= \gamma \left(k_0 \exp\left(\frac{-E_a}{RT} \right) \right) C_A + \left(T_i - T \right) \frac{F}{\mathrm{V}} + q \\ y &= T \end{aligned} \tag{85}$$

The objective is the control of the temperature T by manipulating the feed flowrate $\frac{F}{\mathrm{V}}$ at the stable, minimum phase steady state (x_{1ss}=6.319, x_{2ss}=302, u_{ss}=0.45). All state variables are assumed to be measured, $u = \frac{F}{\mathrm{V}}$, $x_1 = C_A$ and $y = x_2 = T$. The values of model parameters for process are listed in Table 8.

Table 8 The parameter values of SISO chemical reactor

Parameter	Value
V	0.1 m^3
γ	3.9 m^3 K $kmol^{-1}$
k_0	5 x 10^{-8} s^{-1}
$\frac{E_a}{R}$	8100 K
q	-2.519 x 10^{-2} K s^{-1}
C_{Ai}	12 kmol m^{-3}

The manipulated input (u) is used as a continuation parameter to trace the steady state branches in constructing the bifurcation diagram as shown in Figure 60.

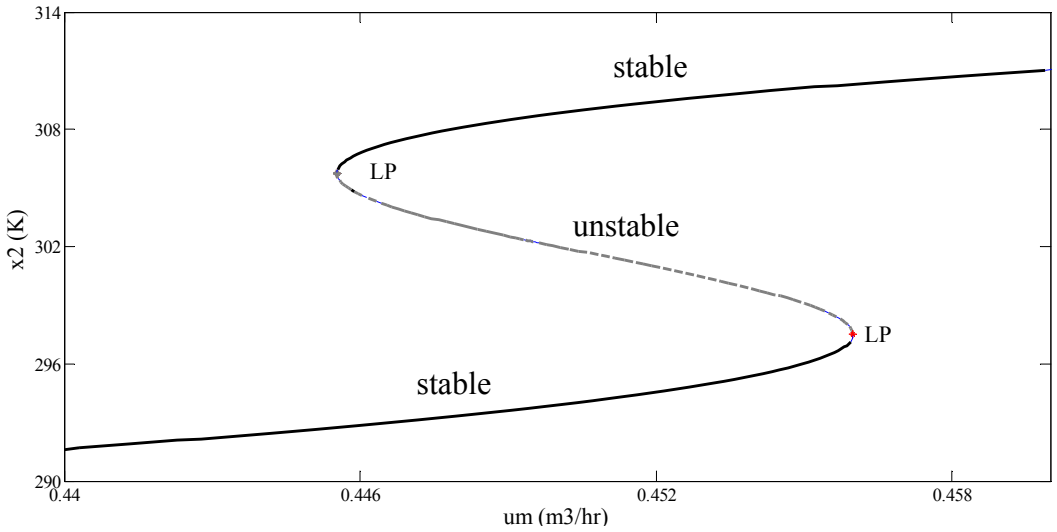

Figure 61 Bifurcation diagram of SISO chemical reactor

Controller tuning results under the proposed I/O linearizing method integrating with Lyapunov stability constraint

For the tuning procedure, the bifurcation diagram is considered to analyze the domain of solution under the I/O linearization technique. The optimal domain of solution should cover the bifurcation diagram, which describe the opened-loop dynamic behavior of chemical reactor. The tuning parameter under I/O linearizing technique is ε, which is used to adjust the speed response of system. If any value of tuning parameter can generate the largest domain of solution, the closed-loop response of controlled output with that value is the best response. In this example, we select the initial value of tuning parameter at ε=0.001 to ε=0.01, 0.1, 1, 10 and 20, respectively. The optimal range of tuning parameter is ε=0.001-0.1 because it cover the bifurcation diagram at stable, minimum phase behavior (low steady state). Then, we adjust the tuning parameter at ε=0.001, 0.005, 0.01, 0.05, and 0.1, respectively. The optimal range of tuning parameter is ε=0.001-0.005 due to the largest domain of solution. To investigate the closed-loop response of the controlled output, the chemical reactor under the tuning parameter at ε=0.001, 0.002, 0.003, 0.004, 0.005 is simulated that is show in Figure 63. The simulation results show that the best value of tuning parameter under I/O linearization technique is ε=0.002 because the closed-loop response of the output is the fastest, no oscillation and overshoot. To clearly illustrate the domain of solution and the closed-loop response under the various tuning parameter, Figure 62 and Figure 64 show the domain of solution and the closed-loop response of the controlled output at ε=0.002, 0.02, 0.2, 2, and 20. To guarantee the stability, the closed-loop response of the controlled output is plotted under domain of solution of I/O linearization method and the domain of stability of Lyapunov stability constraint. The tuning parameter under Lyapunov method is β=20 and

$$P = \begin{bmatrix} 8.200 & 0.756 \\ 0.756 & 778.953 \end{bmatrix}$$

When the response time is infinity, the closed-loop response of the controlled output is stable. Although the output response at $[x_1, x_2, u] = [9.994, 290.009, 0.139]$ appears outside the domain of solution of I/O linearization with the eigenvalues of Jacobian matrix of process at (3.674, -1.25×10^{-3}), the setpoint trajectory can track the output to the desired steady state without Lyapunov stability constraint. We observe from Lyapunov stability constraint that is not active in Figure 65.

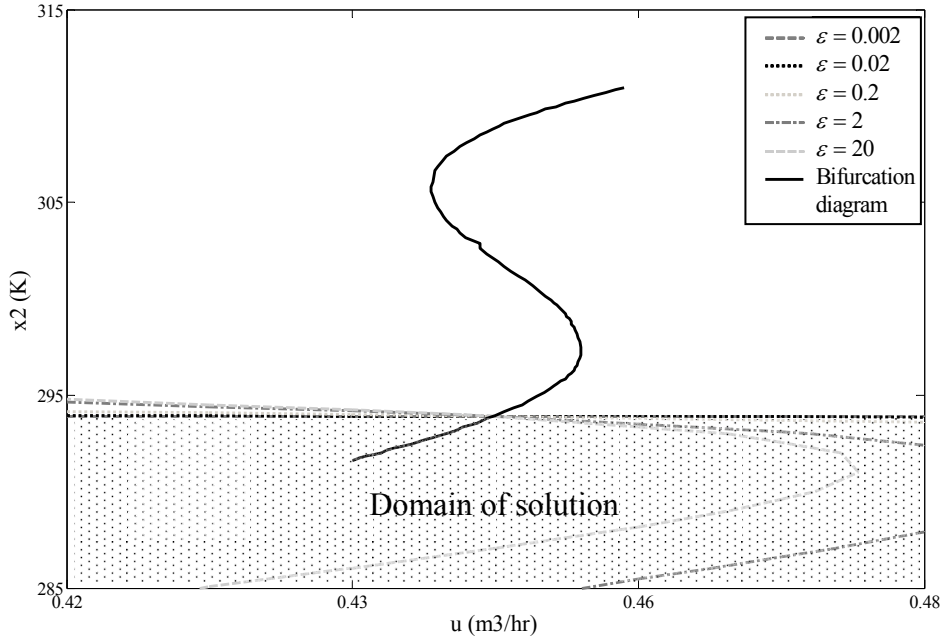

Figure 62 Domain of solution of controlled output for chemical reactor with stable minimum phase steady state by varying parameter (ε) under proposed I/O linearizing feedback control.

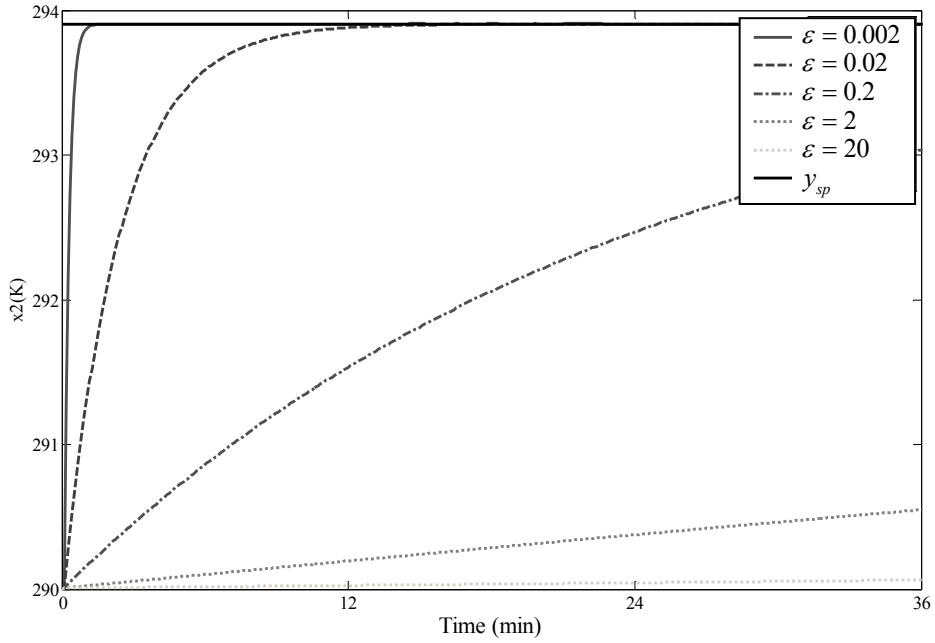

Figure 63 Closed-loop responses of controlled output for chemical reactor with stable minimum phase steady state by varying parameter (ε) under proposed I/O linearizing feedback control.

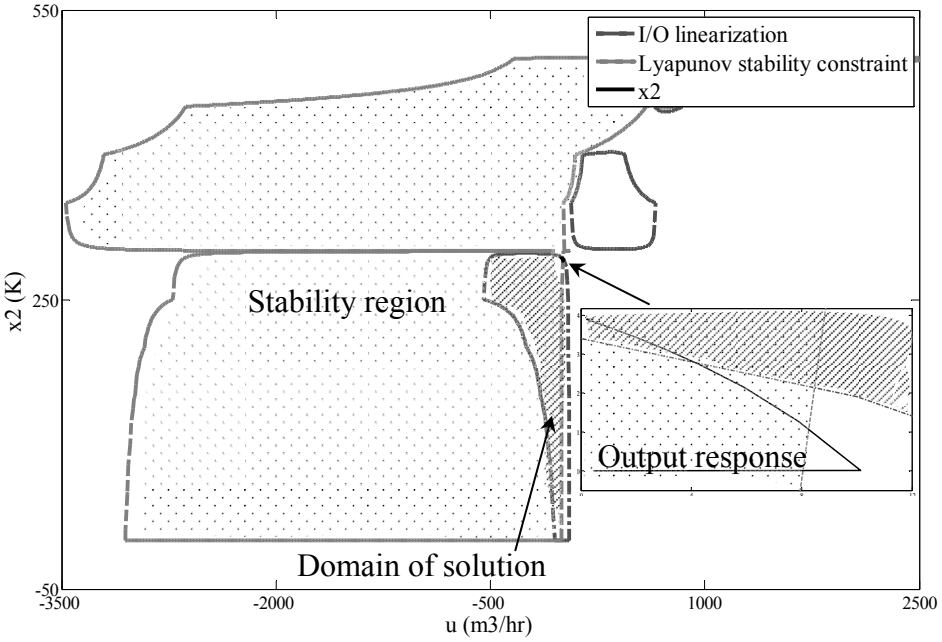

Figure 64 Domain of stability for chemical reactor with stable minimum phase, under proposed method.

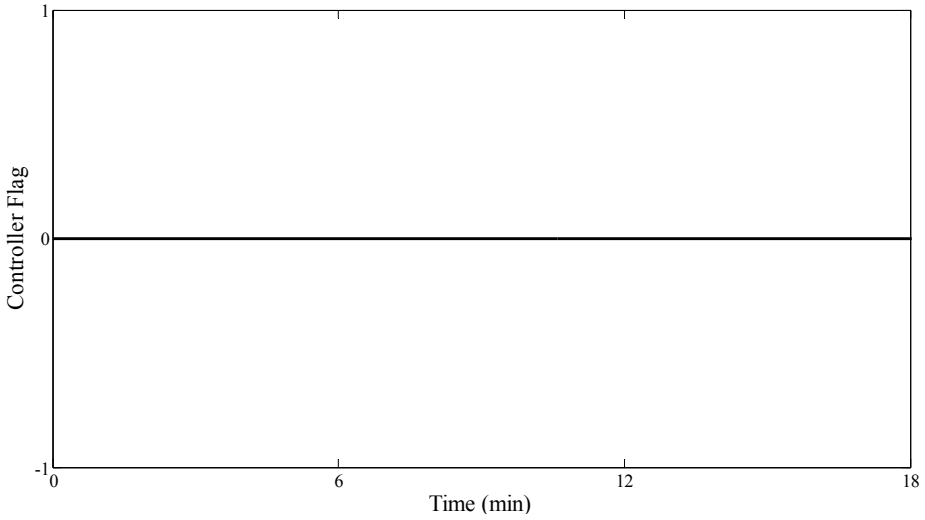

Figure 65 The corresponding controller flag for chemical reactor with stable minimum phase steady state.

2.3.2 Single-input single-output biochemical reactor

The considered biochemical reactor is a perfectly stirred continuous reactor with constant volume V and constant physical-chemical properties. Its state-space model is given by (Bequette, 1998):

$$\begin{aligned} \frac{dX_B}{dt} &= \mu(S)X_B - \frac{X_B F}{\mathrm{V}} \\ \frac{dS}{dt} &= -\frac{\mu(S)X_B}{Y} + \frac{(S_F - S)F}{\mathrm{V}} \\ \mu(S) &= \mu_{\max}\frac{S}{K_1 S^2 + S + K_m} \\ y &= S \end{aligned} \tag{86}$$

The objective is the control of the substrate concentration S by manipulating the dilution rate $D = \frac{F}{\mathrm{V}}$ at stable, minimum phase steady state (x_{1ss}=0.995, x_{2ss}=1.512, u_{ss}=0.3) and unstable, minimum phase steady state (x_{1ss}=1.530, x_{2ss}=0.176, u_{ss}=0.3). All state variables are assumed to be measured,

$u = D = \frac{F}{\mathrm{V}}$, $x_1 = X_B$ and $y = x_2 = S$. The values of model parameters for process are listed in Table 9.

Table 9 The parameter values of SISO biochemical reactor

Parameter	Value
D	0.1 m^3
S_F	4 kg m^{-3}
Y	0.4
μ_{max}	8.82×10^{-3} min^{-1}
K_1	0.12 m^3 kg^{-1}
K_m	4.55×10^{-1} kg m^{-3}

The manipulated input (u) is used as a continuation parameter to trace the steady state branches in constructing the bifurcation diagram as shown in Figure 66.

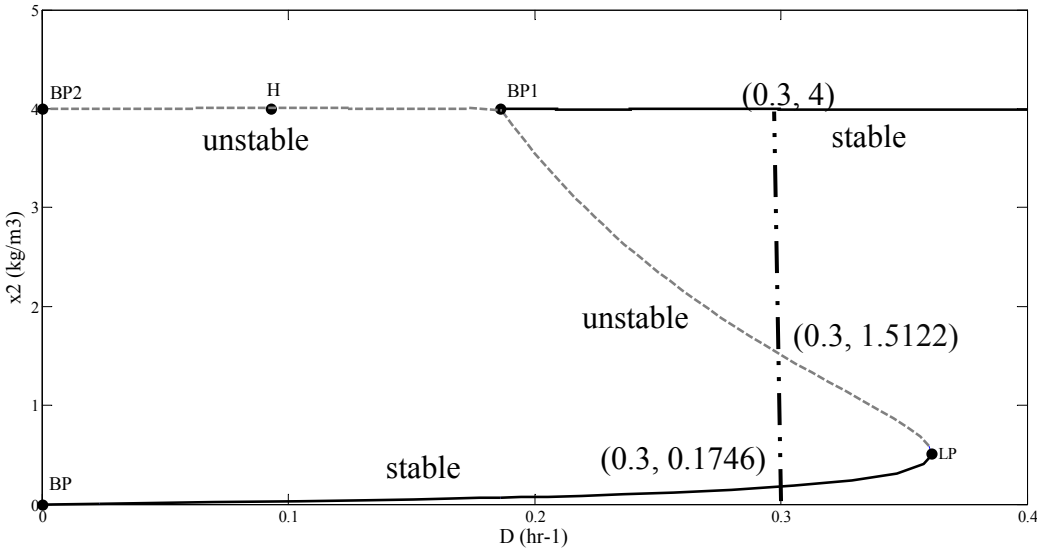

Figure 66 Bifurcation diagram of substrate concentration.

Controller tuning results under the proposed I/O linearizing method integrating with Lyapunov stability constraint

For a control of the output at stable, minimum phase steady state, we select the initial value of tuning parameter at ε=0.001 to ε=0.01, 0.1, 1, 10 and 20, respectively. The optimal range of tuning parameter is ε=1-10 because it cover the bifurcation diagram at stable, minimum phase behavior (low steady state). Then, we adjust the tuning parameter at ε=1, 2, 3, …, 10, respectively. The optimal range of tuning parameter is ε=4-5 due to the largest domain of solution. To investigate the closed-loop response of the controlled output, the biochemical reactor under the tuning parameter at ε=4.1, 4.2, 4.3, …, 5.0 is simulated. The simulation results show that the best value of tuning parameter under I/O linearization technique is ε=4.8 because the closed-loop response of the output is the fastest, no oscillation and overshoot. To clearly illustrate the domain of solution and the closed-loop response under the various tuning parameter, Figure 67 and Figure 68 show the domain of solution and the closed-loop response of the controlled output at ε=2.8, 3.8, 4.8, 5.8, and 6.8, respectively. In Figure 68, we found that the various tuning parameter affects seriously the output response. The output response is oscillation when the value of the tuning parameter is too small such as the output response at ε=2.8. On the other hand, the output response is sluggish when the value of the tuning parameter is too large such as the output response with ε=6.8. To guarantee the stability, the closed-loop response of the controlled output is plotted under domain of solution of I/O linearization method and the domain of stability of Lyapunov stability constraint. The tuning parameter under Lyapunov method is β=4.8 and

$$P = \begin{bmatrix} a_{11} & a_{12} \\ a_{21} & a_{22} \end{bmatrix} = \begin{bmatrix} 734.525 & 0.167 \\ 0.167 & 0.105 \end{bmatrix}$$

When the response time is infinity, the closed-loop response of the controlled output is stable. The setpoint trajectory under I/O linearization technique can track the output to the desired steady state without Lyapunov stability constraint. We observe from

Lyapunov stability constraint that is not active when the output is controlled to stable, minimum phase steady state as shown in Figure 70.

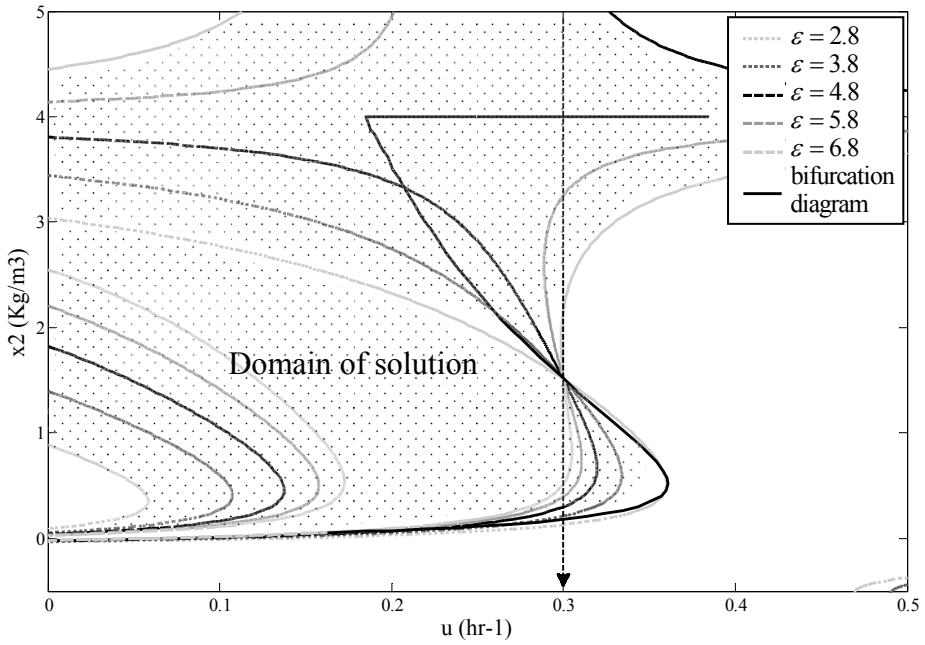

Figure 67 Domain of solution of controlled output for biochemical reactor with stable minimum phase and unstable minimum phase steady state by varying parameter (ε) under proposed method.

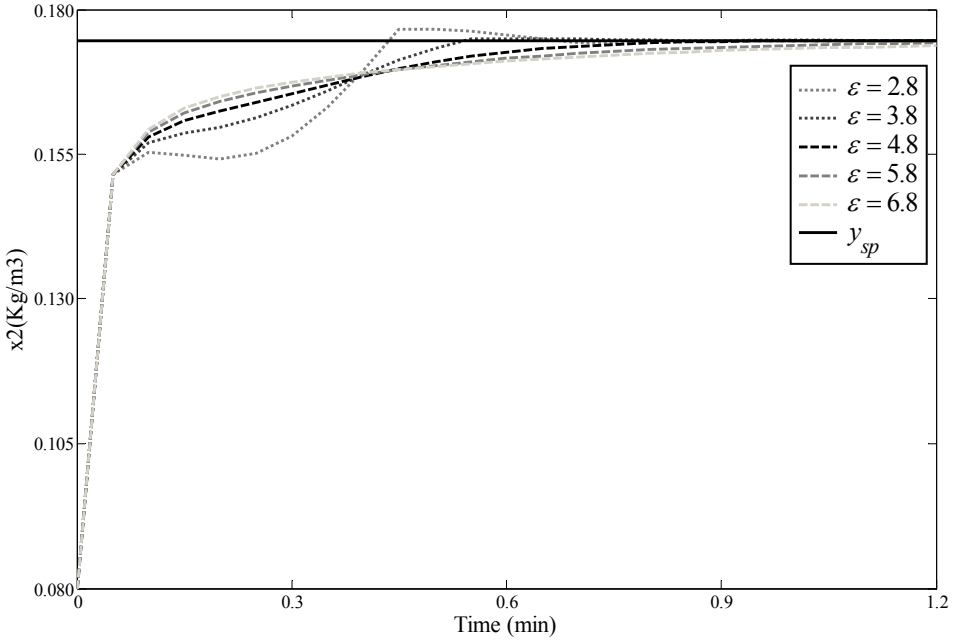

Figure 68 Closed-loop responses of controlled output for biochemical reactor with stable minimum phase steady state by varying parameter (ε) under proposed method.

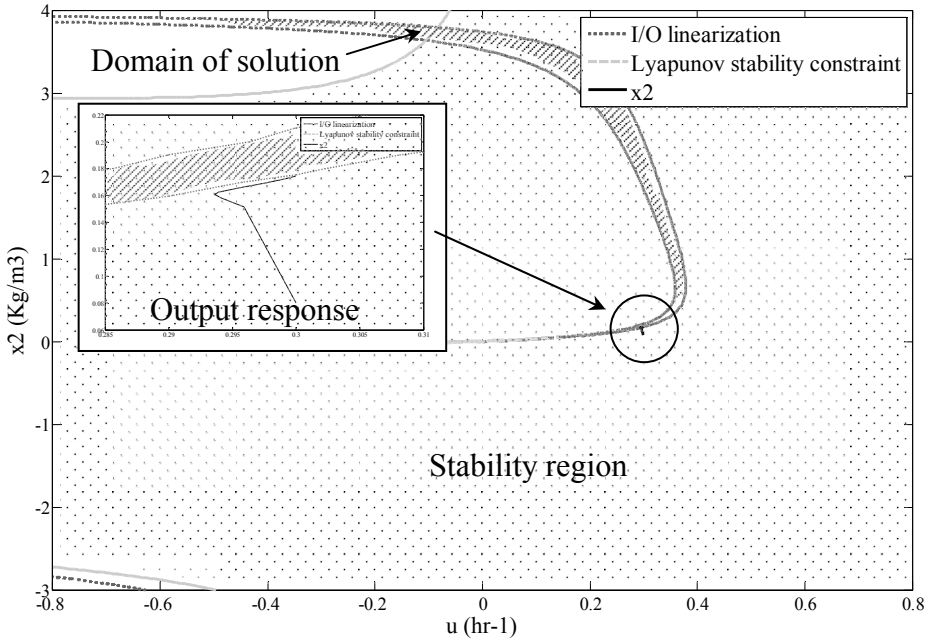

Figure 69 Domain of solution for biochemical reactor with stable minimum phase, under proposed method.

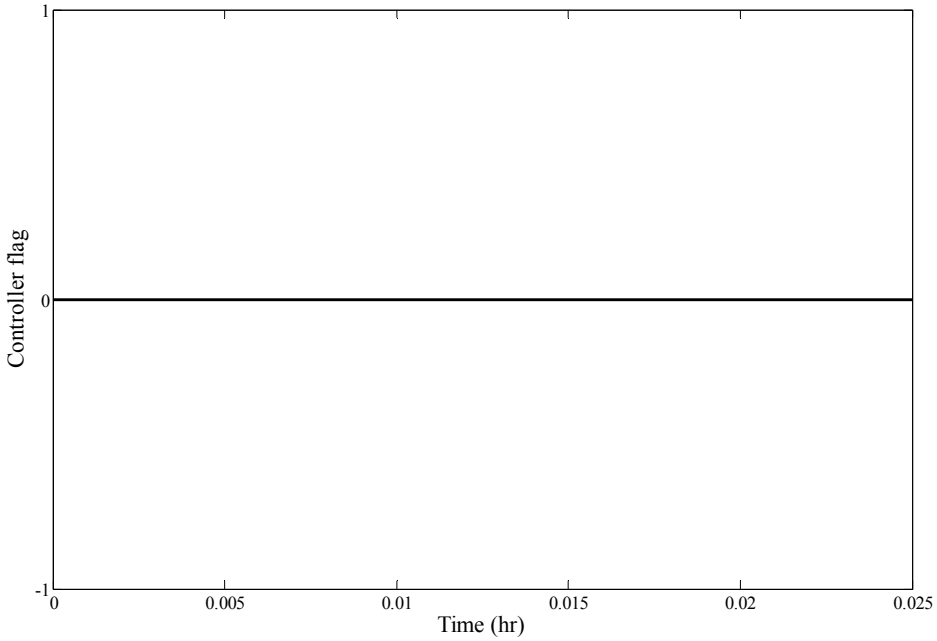

Figure 70 The corresponding controller flag for biochemical reactor with stable minimum phase steady state.

For a control of the output at unstable, minimum phase steady state, we select the initial value of tuning parameter at ε=0.001 to ε=0.01, 0.1, 1, 10 and 20, respectively. The optimal range of tuning parameter is ε=1-10 because it cover the bifurcation diagram at unstable, minimum phase behavior (middle steady state). Then, we adjust the tuning parameter at ε=1, 2, 3, …, 10, respectively. The optimal range of tuning parameter is ε=4-5 due to the largest domain of solution. To investigate the closed-loop response of the controlled output, the biochemical reactor under the tuning parameter at ε=4.1, 4.2, 4.3, …, 5.0 is simulated. The simulation results show that the best value of tuning parameter under I/O linearization technique is ε=4.8 because the closed-loop response of the output is the fastest, no oscillation and overshoot. To clearly illustrate the domain of solution and the closed-loop response under the various tuning parameter, Figure 71 and Figure 72 show the domain of solution and the closed-loop response of the controlled output at ε=2.8, 3.8, 4.8, 5.8, and 6.8, respectively. In Figure 72, we found that the various tuning parameter affects seriously the output response. The output response is oscillation when the value of the tuning parameter is too small such as the output response at ε=2.8. On the other hand,

the output response is sluggish when the value of the tuning parameter is too large such as the output response with ε=6.8. To guarantee the stability, the closed-loop response of the controlled output is plotted under domain of solution of I/O linearization method and the domain of stability of Lyapunov stability constraint. The tuning parameter under Lyapunov method is β=4.8 and

$$P = \begin{bmatrix} a_{11} & a_{12} \\ a_{21} & a_{22} \end{bmatrix} = \begin{bmatrix} 734.525 & 0.167 \\ 0.167 & 0.105 \end{bmatrix}$$

When the response time is infinity, the closed-loop response of the controlled output is stable. The setpoint trajectory under I/O linearization technique can track the output to the desired steady state with Lyapunov stability constraint. We observe from Lyapunov stability constraint that is active when the output is controlled to unstable, minimum phase steady state as shown in Figure 73.

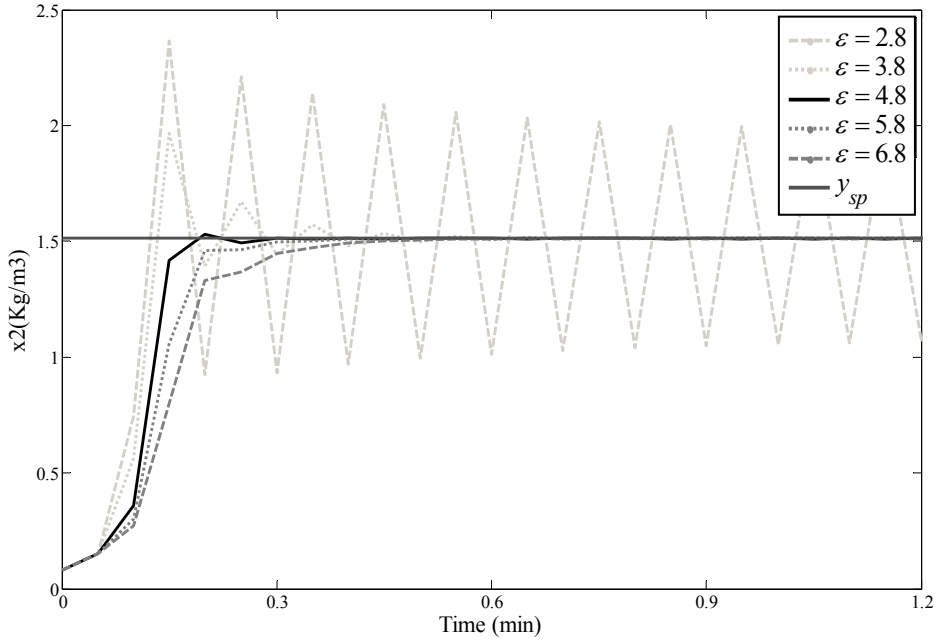

Figure 71 Closed-loop responses of controlled output for biochemical reactor with unstable minimum phase steady state by varying parameter (ε) under proposed method.

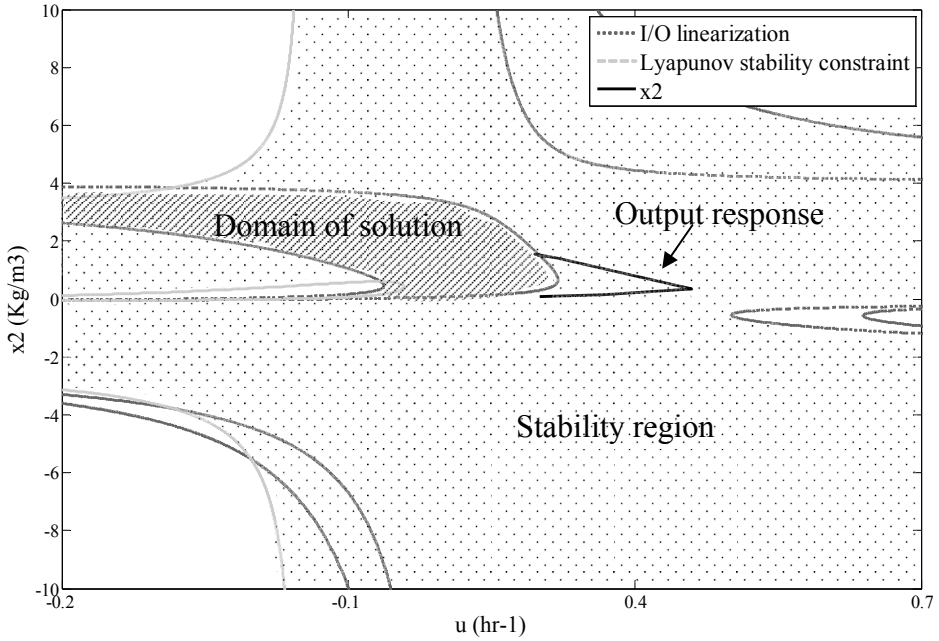

Figure 72 Domain of solution for biochemical reactor with unstable minimum phase under proposed method.

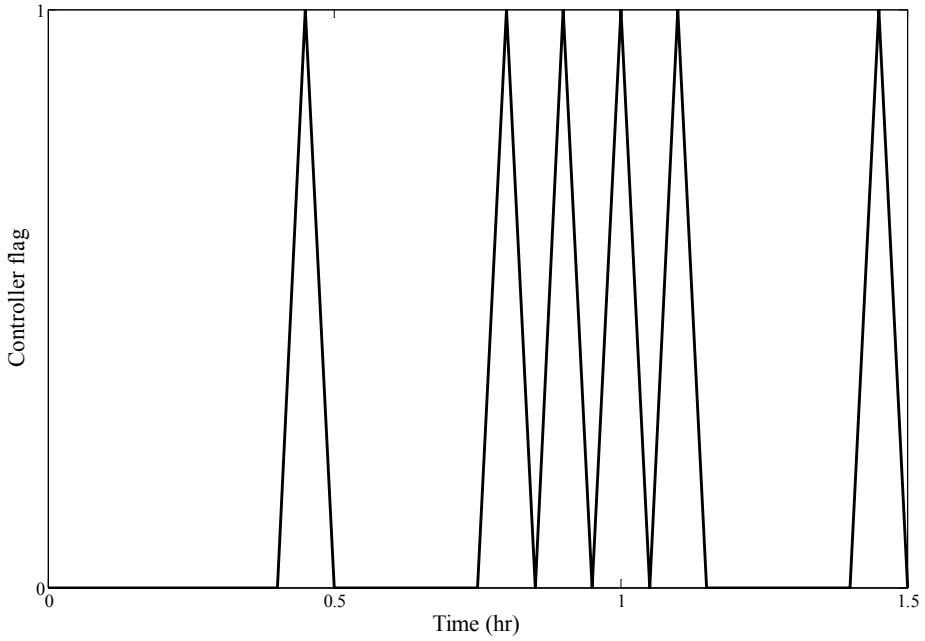

Figure 73 The corresponding controller flag for biochemical reactor with unstable minimum phase steady state.

CONCLUSION AND RECOMMENDATION

Conclusion

In this work, the new control method for a class of uncertain chemical processes with multiplicity behavior was presented. The method combines the advantages of I/O linearization and Lyapunov stability constraint to guarantee certain stability and performance specifications. The integral action was used to eliminate offset. The simplified procedure of tuning parameter selection to achieve the optimal response was also proposed by analyzing the stabilized domain of closed-loop system and bifurcation diagram. The tuning method with bifurcation analysis can reduce the difficulty in determining the optimal tuning parameters that adjust speed response leading to achieving the maximum profitability.

The proposed method was tested by simulating with several applications of chemical and biochemical processes. From the simulation results, the controller successfully operated the reactors at the desired multiple steady states. The effects of parametric uncertainty and unmeasured disturbances were compensated by control system to maintain the closed-loop stability. To compare control performance, a control method of uncertain chemical process with stable non-minimum phase behavior by Kolevennu (Kolevennu, 2000) was considered. The simulation results are clearly shown that our proposed method performs better than Kolevennu's method.

Recommendation

Even though the examples showed the proposed control method is successful in a control of uncertain chemical processes with multiplicity behavior. The domains of stability under Lyapunov stability constraint are only approximation without uncertainty when the state variables are constant at the steady states. Moreover, the technique of controller tuning can use only single-input single-output processes. Thus, the development of the controller tuning still needed to control the multi-input multi-output processes.

LITERATURE CITED

Al-Rabiah, A. and A. Ajbar. 2007. Study of the operability of a continuous bioreactor for the pre-fermentation of cheese culture. **Eng. Life Sci.** 7(6): 1–11.

Alamo, T., D.R. Ramez and E.F. Camacho. 2005. Efficient implementation of constrained min–max model predictive control with bounded uncertainties: a vertex rejection approach. **J. Proc. Cont.** 15: 149-158.

Bequette, B.W. 1998. **Process dynamics modeling, analysis, and simulation.** Prentice-Hall, Inc, New Jersey.

Casavola, A., D. Famularo and G. Franze. 2004. Robust constrained predictive control of uncertain norm-bounded linear systems. **Automatica.** 40: 1865-1876.

Cheng, X. and D. Jia. 2002. Robust stability constrained model predictive control, pp. 440-444. *In* **Proceeding of the American Control Conference.** Boston, Massachusetts.

Dubljevic, S. and P.D. Christofides. 2006. Predictive control of parabolic PDEs with boundary control actuation. **Chem. Eng. Sci**. 61: 6239-6248.

El-Farra, N.H. and P.D. Christofides. 1999. Robust optimal control of nonlinear systems, pp. 124-128. *In* **Proceedings of the American Control Conference,** San Diego, California.

_____. 2001. Integrating robustness, optimality and constraints in control of nonlinear processes. **Chem. Eng. Sci**. 56: 1841-1868.

Elisante, E., G.P. Rangaiah and S. Palanki. 2004. Robust controller synthesis for multivariable nonlinear systems with unmeasured disturbances. **Chem. Eng. Sci**. 59: 977-986.

Femat, R., J.A. Ramirez and M.R. Torres. 1999. Robust asymptotic linearization via uncertainty estimation: regulation of temperature in a fluidized bed reactor. **Comput. Chem. Eng.** 23: 697-708.

Feng, L., J. Wang and E. Poh. 2005. Off-line formulation of robust model predictive control based on several Lyapunov functions, pp. 1705-1710. *In* **International Conference on Control, Automation, Robotics and Vision Kunming 8th**, China.

Fu, S.H. and C. Cheng. 2008. On direct adaptive control design for nonlinear discrete-time uncertain system. **J. Frank. Inst.** 345: 119-135.

Galluzzo, M., B. Cosenza and A. Matharu. 2008. Control of a nonlinear continuous bioreactor with bifurcation by a type-2 fuzzy logic controller. **Comp. Chem. Eng.** 32: 2986-2993.

Gerhard, J., M. Monnigmann and W. Marquardt. 2004. Robust stable nonlinear control and design of a CSTR in a large operating range.

Gu, D.W., P.Hr. Petkov and M.M. Konstantinov. 2005. **Robust control design with MATLAB.** Springer, Germany.

Haddad, W.M and V. Chellaboina. 2008. **Nonlinear dynamic systems and control: a Lyapunov-based approach.** Princeton University Press, New Jersey.

Hahn, J., M. Monnigmann and W. Marquardt. 2004. A method for robustness analysis of controlled nonlinear systems. **Chem. Eng. Sci**. 59: 4325-4338.

_____ , _____ and _____. 2008. On the use of bifurcation analysis for robust controller tuning for nonlinear systems. **J. Proc. Cont.** 18: 408-420.

He, Y. and J. Han. 2007. A new nonlinear controller design method based on control Lyapunov function, pp. 1112-1116. *In* **Proceedings of the 2006 IEEE International Conference on Robotics and Biomimetics,** Kunming, China.

Jalali, A.A. and V. Nadimi. 2006. A Survey on Robust Model Predictive Control from 1999-2006. *In* **International Conference on Computational Intelligence for Modelling Control and Automation,and International Conference on Intelligent Agents,Web Technologies and Internet Commerce**.

Jovanovic, M.R. and B. Bamieh. 2005. Lyapunov-based distributed control of systems on lattices. **IEEE Trans. Auto. Contr.** 50: 422-433.

Kravaris, C. and S. Palanki. 1988. A Lyapunov approach for robust nonlinear state feedback synthesis. **IEEE Trans. Auto. Contr.** 33: 1188-1191.

_____ and J.C. Kantor. 1990. Geometric Methods for Nonlinear Process Control. 1. Background. **Ind. Eng. Chem. Res.** 29: 2295-2310.

Kolavennu, S., S. Palanki and J.C. Cockburn. 2000. Robust control of I/O linearizable systems via multi-model H_2 / H_∞ synthesis. **Chem. Eng. Sci**. 55: 1583-1589.

_____ , J.C. Cockburn and S. Palanki. 2001. Synthesis of robust controllers for nonsquare multivariable nonlinear systems, pp. 4032-4037. *In* **Proceedings of the American Control Conference,** Arlington.

Kothare, M.V., V.B. Balakrishnan and M. Morari. **1994.** Robust constrained model predictive control using linear matrix inequalities. **Amer. Contr. Conf.** 1: 440-444.

Kravaris, C. and D. Mousavere. 2007. ISE-optimal nonminimum-phase compensation for nonlinear processes. **J. Proc. Cont.** 17: 453–461.

Krothapally, M., J.C. Cockburnb and S. Palanki. 1998. Sliding mode control of I/O linearizable systems with uncertainty. **ISA Trans.** 37: 313-322.

Lin, Y. and E.D. Sontag. 1991. A universal formula for stabilization with bounded controls. **Syst. Cont. Let.** 16: 393-397.

Palanki, S., J.C. Cockburn and S.N. Kolavennu. 2003. Robust state feedback synthesis for control of non-square multivariable nonlinear systems. **J. Proc. Contr.** 13: 623-631.

Makila, P.M. 2000. On three puzzles in robust control. **IEEE Trans. Auto. Contr.** 45: 552-556.

Mhaskar, P., N.H. El-Farra and P.D. Christofides. 2005. Robust hybrid predictive control of nonlinear systems. **Automatica.** 41: 209-217.

Monnigmann, M. and W. Marquardt. 2002. Bifurcation placement of hopf points for stabilization of equilibria. *In* **IFAC 2002 World Congress**, Barcelona, Spain.

Munoz, D., D.R. Ramirez, E.F. Camacho and T. Alamo. 2005. Application of an explicit min-max MPC to a scaled laboratory process. **Contr. Eng. Pract.**

Panjapornpon, C. 2005. **Model-based controller design for general nonlinear processes.** Ph.D. Thesis, Drexel University.

_____ and M. Soroush. 2007. Shortest-prediction-horizon non-linear model-predictive control with guaranteed asymptotic stability. **J. Proc. Contr.** 80(19): 1533-1543.

Pannocchia, G. 2002. Robust offset-free model predictive control. *In* **IFAC 2002 World Congress**, Barcelona, Spain.

Qing, Y. and L. Shurong. 2006. Robust model predictive control for a class of nonlinear systems with uncertainty. **IEEE Conf. Ind. Elect. App.**

Ramaswamy**,** S., T.J. Cutright and H.K. Qammar**.** 2005. Control of a continuous bioreactor using model predictive control. **Proc. Bio. Ind.** 40: 2763–2770.

Russo, L.P. and B.W. Bequette. 1998. Operability of chemical reactors: multiplicity behavior of a jacketed styrene polymerization reactor. **Chem. Eng. Sci**. 53(1): 27-45.

Sampath, V., S. Palanki and J.C. Cockburn. 1998. Robust nonlinear control of polymethylmethacrylate production in a batch reactor. **Comp. Chem. Eng.** 22: 451-457.

Seborg, D.E., T.F. Edgar and D.A. Mellichamp. 2004. **Process dynamics and control.** 2nd ed. John Wiley & Sons, Inc.

Soroush, M. 1997. Nonlinear state-observer design with application to reactors. **Chem. Eng. Sci.** 52(3): 387.

_____ and C. Kravaris. 1992. A continuous-time formulation of nonlinear model predictive control. **Proc. of American Contr. Conf.** 2: 1561–1567.

Tsourdos, A., A.L. Blumely and B.A. White. 1999. Flight control design for a missile. an approximate feedback linearization approach, pp. 593-602. *In* **Proceedings of the Mediterranean Conference on Control and Automation (MED99) 7th,** Haifa, Israel.

Wan, Z. and M.V. Kothare. 2003. An efficient off-line formulation of robust model predictive control using linear matrix inequalities. **Automatica.** 39: 837-846.

Wang, D. and J.A. Romagnoli. 2003. Robust model predictive control design using a generalized objective function**. Comp. Chem. Eng.** 27: 965-982.

Wang, Y. and J.B. Rawlings. 2004a. A new robust model predictive control method I: Theory and computation. **J. Proc. Contr.** 14: 231–247.

_____. 2004b. A new robust model predictive control method. II: examples. **J. Proc. Contr.** 14: 249-262.

Witsenhausen, H.S. 1968. A minimax control problem for sampled linear systems. **IEEE Trans. Auto. Contr.** 13: 5-21.

Zhang, Y., G.Z. Abdelqader, M.Z. Michael, A. Henson and M.A. Hjortso. 2000. Bifurcation analysis and control of yeast cultures in continuous bioreactors, pp. 1742-1746. *In* **Proceedings of the American Control Conference**, Illinois, Chicago.

_____ , A.M. Zamamiri, M.A. Henson and M.A. Hjortso. 2002. Cell population models for bifurcation analysis and nonlinear control of continuous yeast bioreactors. **J. Proc. Cont.** 12: 721-734.

APPENDICES

APPENDIX A

Zero dynamics of styrene polymerization reactor

To describe the zero dynamics of styrene polymerization process, the nominal parameter values are

Beta=6, x4f=0; Pd=0.012.

The zero dynamic variables are given by

$$\zeta_1 = Z1,\ \zeta_2 = Z2,\ \zeta_4 = Z4,\ \zeta_6 = Z6,\ \zeta_7 = Z7$$

The zero dynamics of styrene polymerization process in Example 1.2.2 are briefly described, followed by

```
Z1=0.007736+(-0.00916128*Z4^2+0.043058*Z4*ysp-
    0.0505932*ysp^2)/(Beta^2*EXP((1.76301*ysp)/(1.+0.0927748*ysp))*Z2^2)+
    (-0.00916128*Z4^2+0.043058*Z4*ysp-0.0505932*ysp^2)/
    (Beta^2*EXP((5.95109*ysp)/(1.+0.0927748*ysp))*Pd*Z2^2)+
    (0.007736*Beta^2*EXP((5.95109*ysp)/(1.+0.0927748*ysp))*Pd*Z2^2+(-0.00916128-
    0.00916128*EXP((4.18808*ysp)/(1+0.0927748*ysp))*Pd)*Z4^2+(0.043058+0.043058*EXP((4.1
    8808*ysp)/(1+0.0927748*ysp))*Pd)*Z4*ysp+(-0.0505932-
    0.0505932*EXP((4.18808*ysp)/(1+0.0927748*ysp))*Pd)*ysp^2)/(Beta^2*EXP((1.76301*ysp)/(1.
    +0.0927748*ysp))*Z2^2)+((0.00916128*Z4^2-0.043058*Z4*ysp+0.0505932*ysp^2)*
    (Z4*(3.10228+2.1065499999999998*^-7*ysp)-4.950389999999999*^-
    7*ysp^2+32.4118*Beta*EXP(ysp/(1+0.0927748*ysp))*Z2*Sqrt[(0.00916128*Z4^2-
    0.043058*Z4*ysp+0.0505932*ysp^2)/(Beta^2*EXP((2.*ysp)/(1.+0.0927748*ysp))*Z2^2)]+
    ysp*(-7.29036+2.20086*^-6*Beta*EXP(ysp/(1+0.0927748*ysp))*Z2*Sqrt[(0.00916128*Z4^2-
    0.043058*Z4*ysp+0.0505932*ysp^2)/(Beta^2*EXP((2.*ysp)/(1.+0.0927748*ysp))*Z2^2)])))/
    (Beta^2*EXP((1.76301*ysp)/(1.+0.0927748*ysp))*Z2^2*(1.+0.0927748*ysp)^2)-
    (2.*(0.007736*Beta^2*EXP((5.95109*ysp)/(1.+0.0927748*ysp))*Pd*Z2^2+(-0.00916128-
    0.00916128*EXP((4.18808*ysp)/(1+0.0927748*ysp))*Pd)*Z4^2+(0.043058+0.043058*EXP((4.1
    8808*ysp)/(1+0.0927748*ysp))*Pd)*Z4*ysp+(-0.0505932-0.0505932*
    EXP((4.18808*ysp)/(1+0.0927748*ysp))*Pd)*ysp^2)*(Z4*(3.10228+2.1065499999999998*^-
    7*ysp)-4.950389999999999*^-7*ysp^2+32.4118*Beta*EXP(ysp/(1+0.0927748*ysp))*Z2*
    Sqrt[(0.00916128*Z4^2-0.043058*Z4*ysp+0.0505932*ysp^2)/(Beta^2*EXP((2.*ysp)/
    (1.+0.0927748*ysp))*Z2^2)]+ysp*(-7.29036+2.20086*^-6*Beta*
    EXP(ysp/(1+0.0927748*ysp))*Z2*Sqrt[(0.00916128*Z4^2-
    0.043058*Z4*ysp+0.0505932*ysp^2)/(Beta^2*EXP((2.*ysp)/(1.+0.0927748*ysp))*Z2^2)])))/…
```

```
Z2=0.4-Z2-7.73905*EXP(ysp/(1+0.0927748*ysp))*Z2*Sqrt[(0.00916128*Z4^2-
    0.043058*Z4*ysp+0.0505932*ysp^2)/(Beta^2*EXP((2.*ysp)/(1.+0.0927748*ysp))*Z2^2)]+
    (EXP(ysp/(1+0.0927748*ysp))*Z2*Sqrt[(0.00916128*Z4^2-
    0.043058*Z4*ysp+0.0505932*ysp^2)/
    (Beta^2*EXP((2.*ysp)/(1.+0.0927748*ysp))*Z2^2)]*(0.74074*Z4-1.74074*ysp+7.73905*Beta*
    EXP(ysp/(1+0.0927748*ysp))*Z2*Sqrt[(0.00916128*Z4^2-
    0.043058*Z4*ysp+0.0505932*ysp^2)/
    (Beta^2*EXP((2.*ysp)/(1.+0.0927748*ysp))*Z2^2)]))/(1.+0.0927748*ysp)^27.73905-
    (EXP(ysp/(1+0.0927748*ysp))*Z2*Sqrt[(0.00916128*Z4^2-
    0.043058*Z4*ysp+0.0505932*ysp^2)/
    (Beta^2*EXP((2.*ysp)/(1.+0.0927748*ysp))*Z2^2)]*(0.74074*Z4-1.74074*ysp+7.73905*Beta*
    EXP(ysp/(1+0.0927748*ysp))*Z2*Sqrt[(0.00916128*Z4^2-0.043058*Z4*ysp+
    0.0505932*ysp^2)/(Beta^2*EXP((2.*ysp)/(1.+0.0927748*ysp))*Z2^2)])^2)/
    (1.+0.0927748*ysp)^47.73905+7.73905*EXP(ysp/(1+0.0927748*ysp))*
    Sqrt[(0.00916128*Z4^2-0.043058*Z4*ysp+0.0505932*ysp^2)/
    (Beta^2*EXP((2.*ysp)/(1.+0.0927748*ysp))*Z2^2)]*(0.4+Z2*(-1.-
    7.73905*EXP(ysp/(1+0.0927748*ysp))*
    Sqrt[(0.00916128*Z4^2-0.043058*Z4*ysp+0.0505932*ysp^2)/(Beta^2*EXP((2.*ysp)/
    (1.+0.0927748*ysp))*Z2^2)]))-(EXP(ysp/(1+0.0927748*ysp))*
    Sqrt[(0.00916128*Z4^2-0.043058*Z4*ysp+0.0505932*ysp^2)/
    (Beta^2*EXP((2.*ysp)/(1.+0.0927748*ysp))*Z2^2)]*
    (0.74074*Z4-1.74074*ysp+7.73905*Beta*EXP(ysp/(1+0.0927748*ysp))*Z2*
    Sqrt[(0.00916128*Z4^2-0.043058*Z4*ysp+0.0505932*ysp^2)/
    (Beta^2*EXP((2.*ysp)/(1.+0.0927748*ysp))*Z2^2)])*(0.4+Z2*(-1.-
    7.73905*EXP(ysp/(1+0.0927748*ysp))*
    Sqrt[(0.00916128*Z4^2-0.043058*Z4*ysp+0.0505932*ysp^2)/(Beta^2*EXP((2.*ysp)/
    (1.+0.0927748*ysp))*Z2^2)])))/(1.+0.0927748*ysp)^215.4781+
    (3.86953*EXP((4.95109*ysp)/(1+0.0927748*ysp))*Z2*(Pd*(0.007736+(-
    0.00916128*Z4^2+0.043058*Z4*ysp-0.0505932*ysp^2)/(Beta^2*EXP((1.76301*ysp)/
    (1.+0.0927748*ysp))*Z2^2)+(-0.00916128*Z4^2+0.043058*Z4*ysp-0.0505932*ysp^2)/
    (Beta^2*EXP((5.95109*ysp)/(1.+0.0927748*ysp))*Pd*Z2^2))+((0.00916128*Z4^2-
    0.043058*Z4*ysp+
    0.0505932*ysp^2)*(Z4*(2.92673-3.07754*^-7*ysp)+7.23222*^-7*ysp^2+30.5777*Beta*
    EXP(ysp/(1+0.0927748*ysp))*Z2*Sqrt[(0.00916128*Z4^2-0.043058*Z4*ysp+
    0.0505932*ysp^2)/(Beta^2*EXP((2.*ysp)/(1.+0.0927748*ysp))*Z2^2)]+
    ysp*(-6.87782-3.2153299999999995*^-6*Beta*EXP(ysp/(1+0.0927748*ysp))*Z2*
    Sqrt[(0.00916128*Z4^2-0.043058*Z4*ysp+0.0505932*ysp^2)/(Beta^2*EXP((2.*ysp)/(1.+
    0.0927748*ysp))*Z2^2)])))/(Beta^2*EXP((5.95109*ysp)/(1.+0.0927748*ysp))*Z2^2*…
```

```
Z4=-0.27597*Z4+0.27597*ysp+(1.35*(Z4f-Z4)*(1.49386*Z4-3.2346*ysp+
    13.4717*Beta*EXP(ysp/(1.+0.0927748*ysp))*Z2*Sqrt[(0.00916128*Z4^2-
    0.043058*Z4*ysp+0.0505932*ysp^2)/(Beta^2*EXP((2.*ysp)/(1.+0.0927748*ysp))*Z2^2)]-
    (Beta*EXP(ysp/(1.+0.0927748*ysp))*Z2*Sqrt[(0.00916128*Z4^2-0.043058*Z4*ysp+
    0.0505932*ysp^2)/(Beta^2*EXP((2.*ysp)/(1.+0.0927748*ysp))*Z2^2)]*(0.74074*Z4-
    1.74074*ysp+7.73905*Beta*EXP(ysp/(1.+0.0927748*ysp))*Z2*Sqrt[(0.00916128*Z4^2-
    0.043058*Z4*ysp+0.0505932*ysp^2)/(Beta^2*EXP((2.*ysp)/(1.+0.0927748*ysp))*Z2^2)]))/(1.+
    0.0927748*ysp)^27.73905-.73905*Beta*EXP(ysp/(1.+0.0927748*ysp))*Sqrt[(0.00916128*Z4^2-
    0.043058*Z4*ysp+0.0505932*ysp^2)/(Beta^2*EXP((2.*ysp)/(1.+0.0927748*ysp))*Z2^2)]*
    (0.4+Z2*(-1.-7.73905*EXP(ysp/(1.+0.0927748*ysp))*Sqrt[(0.00916128*Z4^2-
    0.043058*Z4*ysp+0.0505932*ysp^2)/(Beta^2*EXP((2.*ysp)/(1.+0.092778*ysp))*Z2^2)]))-
    (3.86953*Beta*EXP(ysp/(1.+0.0927748*ysp))*Z2*(EXP((3.95109*ysp)/(1.+0.0927748*ysp))*Pd
    *(0.007736+(-0.00916128*Z4^2+0.043058*Z4*ysp-
    0.0505932*ysp^2)/(Beta^2*EXP((1.76301*ysp)/(1.+0.0927748*ysp))*Z2^2)+(-
    0.00916128*Z4^2+0043058*Z4*ysp-0.0505932*ysp^2)/
    (Beta^2*EXP((5.95109*ysp)/(1.+0.0927748*ysp))*Pd*Z2^2))+((0.00916128*Z4^2-
    0.043058*Z4*ysp+0.0505932*ysp^2)*(Z4*(2.92673-3.07754*^-7*ysp)+7.23222*^-
    7*ysp^2+30.5777*Beta*EXP(ysp/(1.+0.0927748*ysp))*Z2*Sqrt[(0.00916128*Z4^2-
    0.043058*Z4*ysp+0.0505932*ysp^2)/(Beta^2*EXP((2.*ysp)/(1.+0.0927748*ysp))*Z2^2)]+
    ysp*(-6.87782-3.2153299999999995*^-6*Beta*EXP(ysp/(1.+0.0927748*ysp))*Z2*
    Sqrt[(0.00916128*Z4^2-0.043058*Z4*ysp+0.0505932*ysp^2)/(Beta^2*EXP((2.*ysp)/(1.+
    0.0927748*ysp))*Z2^2)])))/(Beta^2*EXP((2.*ysp)/(1.+0.0927748*ysp))*Z2^2*
    (1.+0.0927748*ysp)^2)))/Sqrt[(0.00916128*Z4^2-0.043058*Z4*ysp+0.0505932*ysp^2)/
    (Beta^2*EXP((2.*ysp)/(1.+0.0927748*ysp))*Z2^2)]))/(Z4f-1.*Z4)

Z6=-Z6+(0.599984*EXP((4.18808/(1+0.0927748*x3)-5.95109/(1.+0.0927748*ysp))*
    ysp)*(0.00916128*Z4^2-0.043058*Z4*ysp+0.0505932*ysp^2))/(Beta^2*Z2^2)-
    0.599984*EXP((4.18808*ysp)/(1+0.0927748*x3))*Pd*(0.007736+(-
    0.00916128*Z4^2+0.043058*Z4*ysp-
    0.0505932*ysp^2)/(Beta^2*EXP((1.76301*ysp)/(1.+0.0927748*ysp))*Z2^2)+
    (-0.00916128*Z4^2+0.043058*Z4*ysp-0.0505932*ysp^2)/
    (Beta^2*EXP((5.95109*ysp)/(1.+0.0927748*ysp))*Pd*Z2^2))-
    (2.51278*EXP((4.18808/(1+0.0927748*x3)-
    5.95109/(1.+0.0927748*ysp))*ysp)*(0.00916128*Z4^2-0.043058*Z4*ysp+
    0.0505932*ysp^2)*(0.74074*Z4-1.74074*ysp+7.73905*Beta*EXP(ysp/(1+0.0927748*ysp))*Z2*
    Sqrt[(0.00916128*Z4^2-0.043058*Z4*ysp+0.0505932*ysp^2)/
    (Beta^2*EXP((2.*ysp)/(1.+0.0927748*ysp))*Z2^2)]))/(Beta^2*(1.+0.0927748*x3)*Z2^2)+
    (5.02556*EXP((4.18808/(1+0.0927748*x3)-5.95109/(1.+0.0927748*ysp))*
```

ysp)*(0.007736*Beta^2*EXP((5.95109*ysp)/(1.+0.0927748*ysp))*Pd*Z2^2+
(-0.00916128-0.00916128*EXP((4.18808*ysp)/(1+0.0927748*ysp))*
Pd)*Z4^2+(0.043058+0.043058*EXP((4.18808*ysp)/(1+0.0927748*ysp))*Pd)*
Z4*ysp+(-0.0505932-0.0505932*EXP((4.18808*ysp)/(1+0.0927748*ysp))*Pd)*ysp^2)*
(0.74074*Z4-1.74074*ysp+7.73905*Beta*EXP(ysp/(1+0.0927748*ysp))*Z2*
Sqrt[(0.00916128*Z4^2-0.043058*Z4*ysp+0.0505932*ysp^2)/
(Beta^2*EXP((2.*ysp)/(1.+0.0927748*ysp))*Z2^2)]))/(Beta^2*(1.+0.0927748*x3)*Z2^2)+
(10.5237*EXP((4.18808/(1+0.0927748*x3)-5.95109/(1.+0.0927748*ysp))*
ysp)*(0.00916128*Z4^2-0.043058*Z4*ysp+0.0505932*ysp^2)*(0.74074*Z4-1.74074*ysp+
7.73905*Beta*EXP(ysp/(1+0.0927748*ysp))*Z2*Sqrt[(0.00916128*Z4^2-0.043058*Z4*ysp+
0.0505932*ysp^2)/(Beta^2*EXP((2.*ysp)/(1.+0.0927748*ysp))*Z2^2)])^2)/
(Beta^2*(1.+0.0927748*x3)^2*Z2^2)+0.599984*EXP((4.18808*ysp)/(1+0.0927748*x3))*Pd*
(-0.007736+(0.00916128*Z4^2-
0.043058*Z4*ysp+0.0505932*ysp^2)/(Beta^2*EXP((1.76301*ysp)/
(1.+0.0927748*ysp))*Z2^2)+(0.00916128*Z4^2-0.043058*Z4*ysp+0.0505932*ysp^2)/
(Beta^2*EXP((5.95109*ysp)/(1.+0.0927748*ysp))*Pd*Z2^2)+
(-0.007736*Beta^2*EXP((5.95109*ysp)/(1.+0.0927748*ysp))*Pd*
Z2^2+(0.00916128+0.00916128*EXP((4.18808*ysp)/(1+0.0927748*ysp))*Pd)*Z4^2+
(-0.043058-0.043058*EXP((4.18808*ysp)/(1+0.0927748*ysp))*
Pd)*Z4*ysp+(0.0505932+0.0505932*EXP((4.18808*ysp)/(1+0.0927748*ysp))*
Pd)*ysp^2)/(Beta^2*EXP((1.76301*ysp)/(1.+0.0927748*ysp))*Z2^2)-
(1.*(0.00916128*Z4^2-0.043058*Z4*ysp+0.0505932*ysp^2)*
(Z4*(3.10228+2.1065499999999998*^-7*ysp)-4.950389999999999*^-7*ysp^2+32.4118*Beta*
EXP(ysp/(1+0.0927748*ysp))*Z2*Sqrt[(0.00916128*Z4^2-0.043058*Z4*ysp+
0.0505932*ysp^2)/(Beta^2*EXP((2.*ysp)/(1.+0.0927748*ysp))*Z2^2)]+
ysp*(-7.29036+2.20086*^-6*Beta*EXP(ysp/(1+0.0927748*ysp))*Z2*
Sqrt[(0.00916128*Z4^2-
0.043058*Z4*ysp+0.0505932*ysp^2)/(Beta^2*EXP((2.*ysp)/(1.+0.0927748*
ysp))*Z2^2)])))/(Beta^2*EXP((1.76301*ysp)/(1.+0.0927748*ysp))*Z2^2*
(1.+0.0927748*ysp)^2))+(2.51278*EXP((4.18808/(1+0.0927748*x3)-
5.95109/(1.+0.0927748*ysp))*
ysp)*(0.00916128*Z4^2-0.043058*Z4*ysp+0.0505932*ysp^2)*(-1.28944*Z4+3.03018*ysp-
13.4717*Beta*EXP(ysp/(1+0.0927748*ysp))*Z2*Sqrt[(0.00916128*Z4^2-
0.043058*Z4*ysp+0.0505932*ysp^2)/(Beta^2*EXP((2.*ysp)/(1.+0.0927748*ysp))*Z2^2)]+
(Beta*EXP(ysp/(1+0.0927748*ysp))*Z2*Sqrt[(0.00916128*Z4^2-0.043058*Z4*ysp+
0.0505932*ysp^2)/(Beta^2*EXP((2.*ysp)/(1.+0.0927748*ysp))*Z2^2)]*(0.74074*Z4-
1.74074*ysp+7.73905*Beta*EXP(ysp/(1+0.0927748*ysp))*…

```
Z7=-Z7+(7.73905*(0.00916128*Z4^2-0.043058*Z4*ysp+0.0505932*ysp^2)^2)/
    (Beta^4*EXP((3.*ysp)/(1.+0.0927748*ysp))*Z2^3)-(15.4781*(0.00916128*Z4^2-
    0.043058*Z4*ysp+0.0505932*ysp^2)*(0.007736*Beta^2*EXP((5.95109*ysp)/(1.+0.0927748*ys
    p))*Pd*Z2^2+(-0.00916128-0.00916128*EXP((4.18808*ysp)/(1+0.0927748*ysp))*Pd)*Z4^2+
    (0.043058+0.043058*EXP((4.18808*ysp)/(1+0.0927748*ysp))*Pd)*
    Z4*ysp+(-0.0505932-0.0505932*EXP((4.18808*ysp)/(1+0.0927748*ysp))*Pd)*ysp^2))/
    (Beta^4*EXP((3.*ysp)/(1.+0.0927748*ysp))*Z2^3)+(15.4781*(0.007736*Beta^2*EXP((5.95109*
    ysp)/(1.+0.0927748*ysp))*Pd*Z2^2+(-0.00916128-
    0.00916128*EXP((4.18808*ysp)/(1+0.0927748*ysp))*Pd)*Z4^2+
    (0.043058+0.043058*EXP((4.18808*ysp)/(1+0.0927748*ysp))*Pd)*
    Z4*ysp+(-0.0505932-0.0505932*EXP((4.18808*ysp)/(1+0.0927748*ysp))*Pd)*ysp^2)^2)/
    (Beta^4*EXP((3.*ysp)/(1.+0.0927748*ysp))*Z2^3)-(7.73905*(0.00916128*Z4^2-
    0.043058*Z4*ysp+0.0505932*ysp^2)^2*(0.4+Z2*(-1.-7.73905*EXP(ysp/(1+0.0927748*ysp))*
    Sqrt[(0.00916128*Z4^2-0.043058*Z4*ysp+0.0505932*ysp^2)/(Beta^2*EXP((2.*ysp)/
    (1.+0.0927748*ysp))*Z2^2)])))/(Beta^4*EXP((3.*ysp)/(1.+0.0927748*ysp))*Z2^4)+
    (30.9562*(0.00916128*Z4^2-0.043058*Z4*ysp+0.0505932*ysp^2)*
    (0.007736*Beta^2*EXP((5.95109*ysp)/(1.+0.0927748*ysp))*Pd*
    Z2^2+(-0.00916128-0.00916128*EXP((4.18808*ysp)/(1+0.0927748*ysp))*Pd)*Z4^2+
    (0.043058+0.043058*EXP((4.18808*ysp)/(1+0.0927748*ysp))*Pd)*Z4*ysp+(-0.0505932-
    0.0505932*EXP((4.18808*ysp)/(1+0.0927748*ysp))*Pd)*ysp^2)*(0.4+Z2*(-1.-
    7.73905*EXP(ysp/(1+0.0927748*ysp))*
    Sqrt[(0.00916128*Z4^2-0.043058*Z4*ysp+0.0505932*ysp^2)/(Beta^2*EXP((2.*ysp)/
    (1.+0.0927748*ysp))*Z2^2)])))/(Beta^4*EXP((3.*ysp)/(1.+0.0927748*ysp))*Z2^4)-
    (7.73905*(0.00916128*Z4^2-0.043058*Z4*ysp+0.0505932*ysp^2)^
    2*(Z4*(6.5942-2.29155*^-8*ysp)+5.3851500000000004*^-8*
    ysp^2+68.8944*Beta*EXP(ysp/(1+0.0927748*ysp))*Z2*
    Sqrt[(0.00916128*Z4^2-0.043058*Z4*ysp+0.0505932*ysp^2)/
    (Beta^2*EXP((2.*ysp)/(1.+0.0927748*ysp))*Z2^2)]+ysp*(-15.4964-2.39415*^-
    7*Beta*EXP(ysp/(1+0.0927748*ysp))*Z2*Sqrt[(0.00916128*Z4^2-
    0.043058*Z4*ysp+0.0505932*ysp^2)/(Beta^2*EXP((2.*ysp)/
    (1.+0.0927748*ysp))*Z2^2)])))/(Beta^4*EXP((3.*ysp)/(1.+0.0927748*ysp))*Z2^3*
    (1.+0.0927748*ysp)^2)+(30.9562*(0.00916128*Z4^2-0.043058*Z4*ysp+0.0505932*ysp^2)*
    (0.007736*Beta^2*EXP((5.95109*ysp)/(1.+0.0927748*ysp))*Pd*Z2^2+(-0.00916128-
    0.00916128*EXP((4.18808*ysp)/(1+0.0927748*ysp))*Pd)*Z4^2+
    (0.043058+0.043058*EXP((4.18808*ysp)/(1+0.0927748*ysp))*Pd)*
    Z4*ysp+(-0.0505932-0.0505932*EXP((4.18808*ysp)/(1+0.0927748*ysp))*Pd)*ysp^2)*…
```

APPENDIX B

Bifurcation analysis with MATCONT continuation toolbox for MATLAB

To illustrate determination of bifurcation diagram, the mass balances in continuous bioreactor process are considered (Al-Rabiah and Ajbar, 2007):

$$\begin{aligned}
\frac{dX}{dT} &= D\left(\frac{aX_f}{1+a} - X\right) + \frac{\mu_0[H^+]X}{K_1 + [H^+] + \dfrac{[H^+]^2}{K_2}} \\
\frac{dS}{dT} &= D\left(\frac{S_f}{1+a} - S\right) + \frac{\sigma_0[H^+]X}{K_3 + [H^+] + \dfrac{[H^+]^2}{K_4}} \\
\frac{d[H^+]}{dT} &= D\left(\frac{aP_f}{1+a} - P\right) + \frac{\pi_0[H^+]X}{K_5 + [H^+] + \dfrac{[H^+]^2}{K_6}} \\
\frac{dX}{dT} &= D\left(\frac{[H^+]_1}{1+a} + \frac{a[H^+]_2}{1+a} - [H^+]\right) + \frac{\nu_0 X}{K_5 + [H^+] + \dfrac{[H^+]^2}{K_6}}
\end{aligned} \tag{46}$$

where X , S , $[H^+]$, and P are the concentrations of cells, the concentrations of lactose, hydrogen ion concentrations in the bioreactor and the concentrations of lactic acid, respectively. It is desired to maintain hydrogen ion concentrations ($y = [H^+]$) by manipulating the ratio of seed to substrate feed rate ($u = a$). The values of model parameters for process (46) are listed in Table B1.

Appendix Table B1 Nominal values of model parameters of a continuous bioreactor process.

Parameter	Value	Parameter	Value
K_1 (g/L)	4×10^{-7}	σ_0 (g/L)	1.02
K_2 (g/L)	6.85×10^{-6}	S_f (g/L)	80
K_3 (g/L)	4.88×10^{-8}	X_f (g/L)	5.5
K_4 (g/L)	4.2×10^{-6}	P_f (g/L)	5.9

Appendix Table B1 (Continued)

Parameter	Value	Parameter	Value
K_5 (g/L)	1.5×10^{-6}	pH_1	6.7
K_6 (g/L)	3.91×10^{-6}	pH_2	5.5
μ_0 (h^{-1})	0.51	D (h^{-1})	0.35
ν_0 (h^{-1})	3.35×10^{-7}	a	0.03
π_0 (h^{-1})	3.35		

Procedures of determination of multiplicity diagrams with MATCONT are shown in Appendix Figure A1.

On behavior analysis of stable and unstable, the message Limit point will appear in the status field of the MATCONT window. The appeared one eigenvalue in Numeric has positive real part. Then the curve of equilibria has a turning point. On one side the equilibria are stable on the other unstable. For the used function for solving and analyzing differential equations, the symbolic toolbox of MATLAB is used to compute derivatives of order up to five of the object function as shown in Appendix Figure C2.

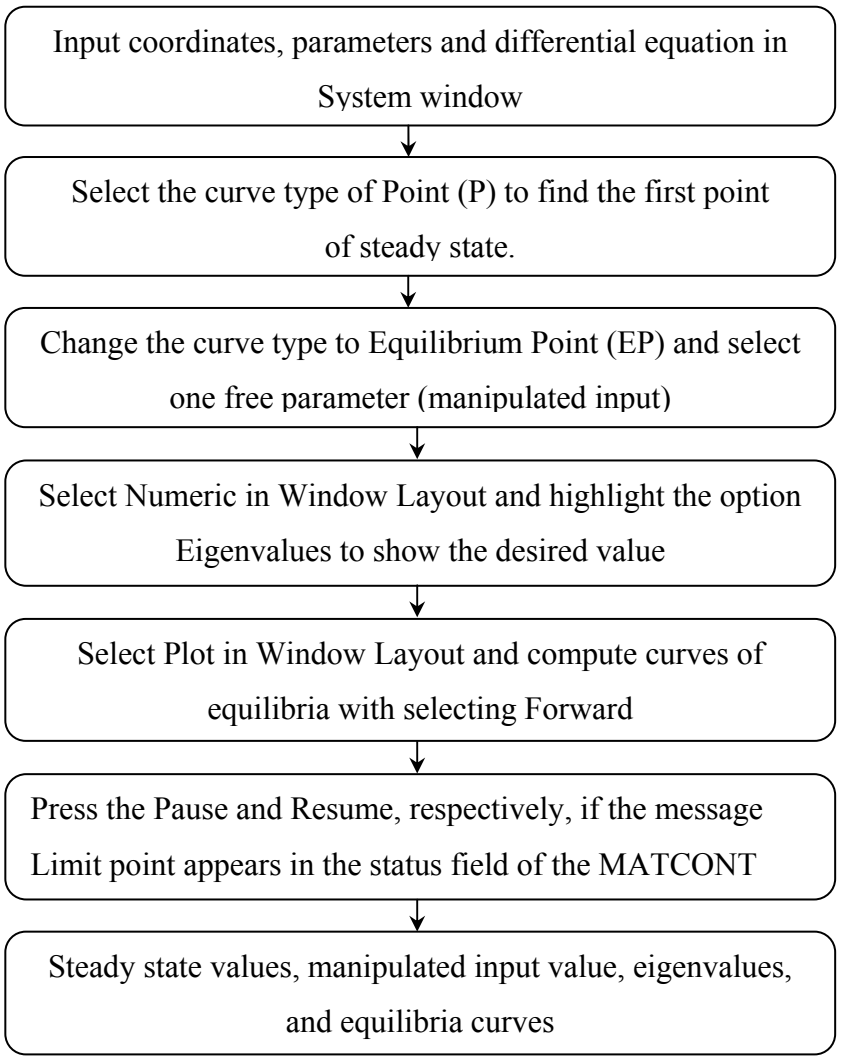

Appendix Figure B1 Procedures of determination of multiplicity diagrams with MATCONT continuation toolbox.

```
function out = JReal
out{1} = @init;
out{2} = @fun_eval;
out{3} = @jacobian;
out{4} = @jacobianp;
out{5} = @hessians;
out{6} = @hessiansp;
out{7} = [];
out{8} = [];
out{9} = [];

% --------------------------------------------------------------------
function dydt = fun_eval(t,kmrgd,um)
dydt=[10*um*(1-kmrgd(1))- 500000000*exp(-27/kmrgd(2))*kmrgd(1);
78000000*exp(-27/kmrgd(2))*kmrgd(1)+10*um*(1-kmrgd(2))-0.02519/300;];

% --------------------------------------------------------------------
function [tspan,y0,options] = init
handles = feval(JReal);
y0=[0,0];
options = odeset('Jacobian',handles(3),'JacobianP',handles(4),'Hessians',handles(5),'HessiansP',handles(6));
tspan = [0 10];

% --------------------------------------------------------------------
function jac = jacobian(t,kmrgd,um)
jac=[[-10*um-500000000*exp(-27/kmrgd(2)),-13500000000/kmrgd(2)^2*exp(-27/kmrgd(2))*kmrgd(1)];[78000000*exp(-27/kmrgd(2)),2106000000/kmrgd(2)^2*exp
% --------------------------------------------------------------------
function jacp = jacobianp(t,kmrgd,um)
jacp=[[10-10*kmrgd(1)];[10-10*kmrgd(2)]];
% --------------------------------------------------------------------
function hess = hessians(t,kmrgd,um)
hess1=[[0,-13500000000/kmrgd(2)^2*exp(-27/kmrgd(2))];[0,2106000000/kmrgd(2)^2*exp(-27/kmrgd(2))]];
hess2=[[-13500000000/kmrgd(2)^2*exp(-27/kmrgd(2)),27000000000/kmrgd(2)^3*exp(-27/kmrgd(2))*kmrgd(1)-364500000000/kmrgd(2)^4*exp(-27/kmrgd(2))*kmrg
hess(:,:,1) =hess1;
```

Appendix Figure B2 The code viewer window showing in m-file of MATLAB.

The results show in Appendix Figure C3 that this process has three steady states, (4.6841, 68.9610, 20.1815, 2.2866e-6), (1.6724, 73.7680, 5.4031, 0.8093e-6), (0.5307, 76.3897, 1.1948, 3.8816e-7). The first and third point of steady state is stable because the eigenvalues of Jacobian matrix of process is negative. The second point of steady state is unstable because the eigenvalues of Jacobian matrix of process is positive.

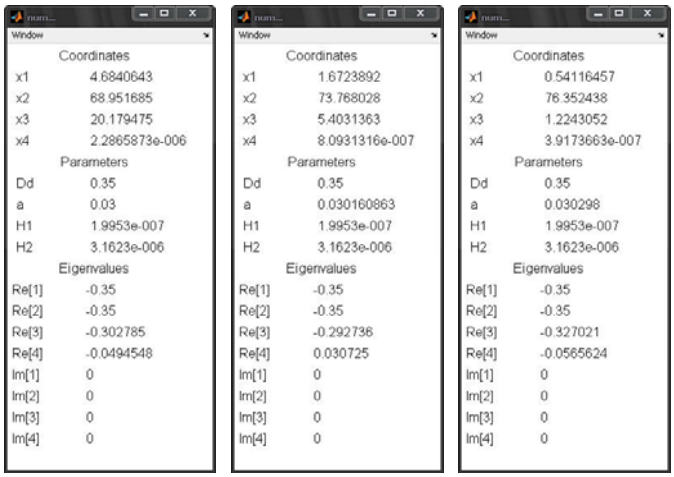

Appendix Figure B3 Value of three steady states, manipulated input and eigenvalue of a continuous bioreactor process.

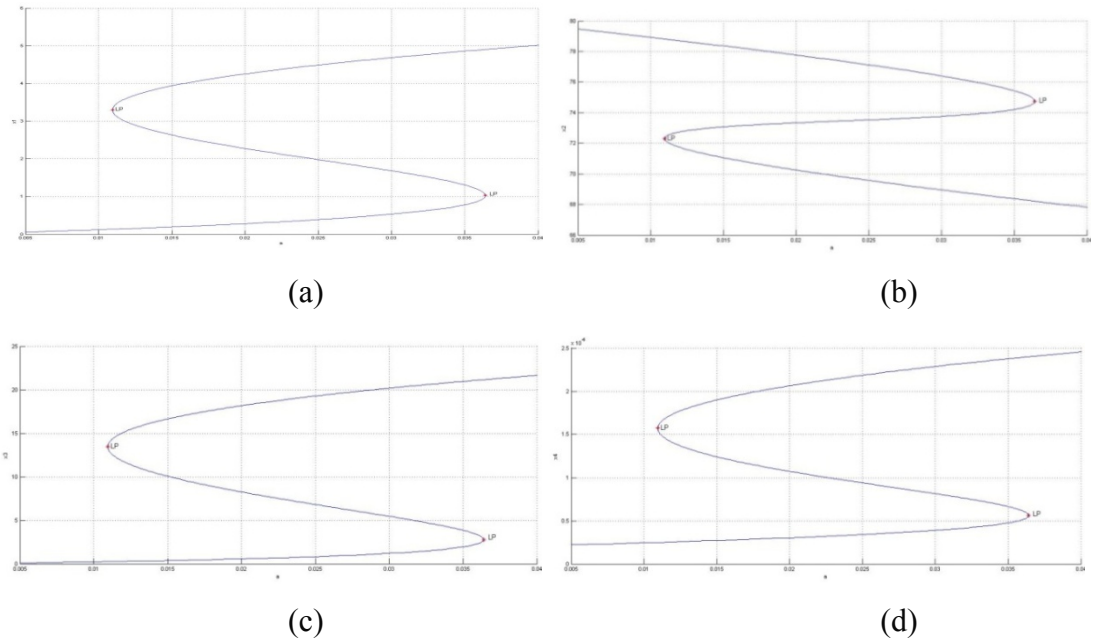

(a) (b)

(c) (d)

Appendix Figure B4 Steady state multiplicity behavior of (a) the concentrations of cells (X), (b) the concentrations of lactose (S), (c) hydrogen ion concentrations in the bioreactor ($[H^+]$) and, (d) the concentrations of lactic acid (P).

CURRICULUM VIATE

NAME : Ms. Solada Naksiri

BIRTH DATE : April 12, 1985

BIRTH PLACE : Nakhon Pathom, Thailand

EDUCATION :

YEAR	**INSTITUTION**	**DEGREE/DIPLOMA**
2003-2007	Srinakharinwirot University	B. Eng. (Chemical Engineering)